Supplementary Information (SI) for Chemical Science.
This journal is © The Royal Society of Chemistry 2025

# Supplementary Information

## Triple-Helical Aggregates of Copper(I) Cyclic Trinuclear Complexes for Circularly Polarized Luminescence

Guo-Quan Huang,[#a] Hu Yang,[#a] Ri-Qin Xia,[a] Kun Wu,[a] Yong-Liang Huang,[b] De-Bo Hao,[a] Shun-Bo Li,[a] Weigang Lu,*[a] Ji Zheng,*[a] Xiao-Ping Zhou*[a] and Dan Li*[a]

[a]College of Chemistry and Materials Science, Guangdong Provincial Key Laboratory of Supramolecular Coordination Chemistry, Jinan University, Guangzhou, Guangdong 510632, P. R. China

[b]Department of Chemistry, Shantou University Medical College, Shantou, Guangdong 515041, P. R. China.

[#]G.-Q. Huang and H. Yang contributed equally to this work.

**Contents**

## 1. General procedure

Infrared spectra were recorded using KBr disks on a Thermo Scientific Fourier transform infrared spectroscopy (FT-IR) Nicolet iS10 spectrometer, covering the range of 4000~400 $cm^{-1}$, the abbreviations used for the IR bands are: w = weak, m = medium, b = broad, s = strong, vs = very strong. $^{1}H$ and $^{13}C$ NMR spectra were obtained by using a Bruker Biospin Advance spectrometer (400 MHz). Elemental analyses were carried out with an Elementar vario MICRO CUBE equipment. Thermogravimetric analysis (TGA) curves were recorded by using TGA Q50 V20.6 with a heating rate of 10 °C/min from 40 to 800 °C in a nitrogen atmosphere. Powder X-ray diffraction (PXRD) experiments were performed on an Rigaku miniflex600 (Cu Kα, λ = 1.5418 Å) in the step of 0.02° under the conditions 40 kV and 40 mA. Scanning electron microscopy (SEM) analyses were performed on a COXEM EM 30AX PLUS microscope. Photoluminescence spectra and emission decay times at room temperature were acquired using the FLS-1000, while temperature-dependent photoluminescence spectra and emission decay times were acquired using the FLS-1000 equipped with an Oxford OptistatDN2 optical cryostat. Absolute quantum yields (QYs) were recorded by Hamamatsu C11347-11 absolute PL quantum yield spectrometer. Solid-state UV-vis absorption and circular dichroism (CD) spectra of **R-1/S-1**, **R-2/S-2** were thoroughly mixed with KBr through grinding and pressed into disks, and recorded by Bio-Logic MOS-500 multifunctional circular dichroism spectrometer. The circularly polarized luminescence (CPL) spectra of crystalline and non-crystalline samples were recorded by JASCO CPL-300 with scanning rate of 50 $nm \cdot min^{-1}$. The $g_{lum}$ values were transferred from CPL spectra using the Spectra Manager software of JASCO.

## 2. Experimental section

All reagents and materials were obtained from Bidepharm, *J&K* Scientific and GHTECH *et al.*, and used as received without further purification.

### 2.1 Preparation of R-$HL_1$/S-$HL_1$ and R-$HL_2$/S-$HL_2$

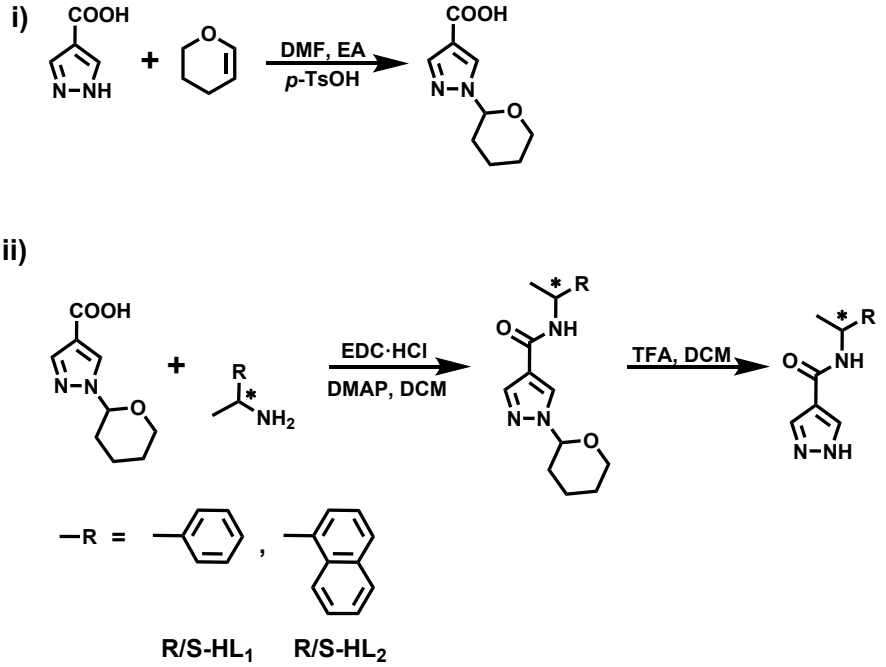


**Scheme S1** The Synthesis of R-$HL_1$/S-$HL_1$ and R-$HL_2$/S-$HL_2$.

**Synthesis of 1-(tetrahydro-2H-pyran-2-yl)-1H-pyrazole-4-carboxylic acid**

This complex was synthesized according to the previously reported methods.[1]

**Synthesis of (R/S)-*N*-(1-phenylethyl)-1*H*-pyrazole-4-carboxamide (R-$HL_1$/S-$HL_1$)**

A solution of 1-(tetrahydro-2H-pyran-2-yl)-1H-pyrazole-4-carboxylic acid (10 mmol, 1.96 g) in dichloromethane (DCM) (200 mL) was prepared. To this, 4-dimethylaminopyridine (DMAP) (2 mmol, 0.25 g), 1-(3-dimethylaminopropyl)-3-ethylcarbodiimide hydrochloride (EDC·HCl) (25 mmol, 4.70 g), and (R/S)-1-phenylethan-1-amine (10 mmol, 1.3 mL) were added at room temperature. The reaction mixture was then refluxed for 12 hours, with progress monitored by TLC. Upon completion, 200 mL of water was added to the mixture. The solution was extracted with

DCM, and the organic layer was washed with brine (100 mL), dried over anhydrous sodium sulfate, and concentrated under reduced pressure using a rotary evaporator. The resulting yellow crude product was used directly in the next step without further purification.

The crude product obtained in the previous step was dissolved in 100 mL of DCM, followed by the addition of 20 mL of trifluoroacetic acid (TFA). The reaction mixture was stirred at room temperature for 24 hours. Upon completion, monitored by TLC, the solvent was removed under reduced pressure using a rotary evaporator, yielding a dark brown gel. The crude product was then purified by column chromatography, initially using a mixture of petroleum ether (PE) and ethyl acetate (EA) (PE:EA = 1:1), followed by pure EA, to yield R-$HL_1$/S-$HL_1$ as a white solid with a yield of 0.65 g (30%). The corresponding crystals were obtained by volatilization of methanol solution of R-$HL_1$/S-$HL_1$.

**Synthesis of (R/S)-*N*-(1-(naphthalen-1-yl)ethyl)-1*H*-pyrazole-4-carboxamide (R-$HL_2$/S-$HL_2$)**

The synthesis steps for R-$HL_2$/S-$HL_2$ were identical to those for R-$HL_1$/S-$HL_1$, with the exception that (R/S)-1-phenylethan-1-amine (10 mmol, 1.3 mL) was replaced by (R/S)-1-(naphthalen-1-yl)ethan-1-amine (10 mmol, 1.6 mL). R-$HL_2$/S-$HL_2$ was obtained as a colourless solid with a yield of 0.56 g (21%). The corresponding crystals were obtained by volatilization of methanol solution of R-$HL_2$/S-$HL_2$.

## 2.2. Preparation of R-1/S-1 and R-2/S-2

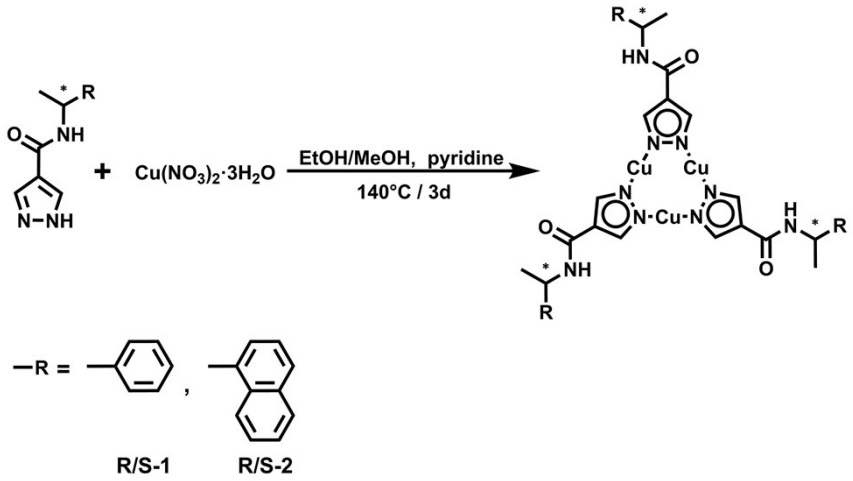


**Scheme S2** The Synthesis of **R-1/S-1** and **R-2/S-2**.

### Synthesis of R-1/S-1

After mixing $Cu(NO_3)_2 \cdot 3H_2O$ (0.01 mmol, 2.4 mg), R-$HL_1$/S-$HL_1$ (0.015 mmol, 3.2 mg) and 10 $\mu$L pyridine in 2 mL of EtOH in 8-mm-inside-diameter Pyrex tube, the tube was sealed and then heated to 140 ℃ for 72 h in a programmable oven, followed by the slow cooling down to room temperature with the rate of 3 ℃/h. Colourless needle crystals were collected and air-dried. Yield: 1.0 mg (35% based on $Cu(NO_3)_2 \cdot 3H_2O$) for **R-1**, 0.9 mg (31% based on $Cu(NO_3)_2 \cdot 3H_2O$) for **S-1**. Elemental analyses of **R-1** ($C_{36}H_{36}Cu_3N_9O_3$, %): calculated: C, 51.89; H, 4.67; N, 14.59; found: C, 51.50; H, 4.79; N, 14.94. Elemental analyses of **S-1** ($C_{36}H_{36}Cu_3N_9O_3$, %): calculated: C, 51.89; H, 4.67; N, 14.59; found: C, 51.54; H, 4.62; N, 14.93. FT-IR data (KBr, $cm^{-1}$) of **R-1**: 553 (s), 603 (w), 630 (w), 698 (w), 762 (s), 841 (m), 865 (m), 913 (w), 1018 (m), 1054 (s), 1094 (w), 1109 (w), 1127 (w), 1184 (m), 1210 (m), 1253 (vs), 1375 (m), 1402 (m), 1446 (s), 1494 (s), 1557 (vs), 1633 (vs), 2870 (w), 2933 (w), 2973 (m), 3031 (m), 3060 (w), 3087 (w), 3114 (w), 3308 (b), 3420 (b). FT-IR data (KBr, $cm^{-1}$) of **S-1**: 552 (s), 603 (w), 629 (w), 700 (w), 749 (s), 841 (m), 864 (m), 913 (w), 1019 (m), 1052 (s), 1098 (w), 1126 (w), 1189 (w), 1207 (w), 1253 (vs), 1374 (w), 1399 (m), 1448 (s), 1492 (s), 1557 (vs), 1635 (vs), 2869 (w), 2926 (w), 2970 (m), 3031 (m), 3065 (w), 3085 (w), 3105 (w), 3269 (b), 3424 (b).

**Synthesis of R-2/S-2**

After mixing $Cu(NO_3)_2 \cdot 3H_2O$ (0.01 mmol, 2.4 mg), R-$HL_2$/S-$HL_2$ (0.015 mmol, 4.0 mg) and 10 $\mu$L pyridine in 3 mL of MeOH in 8-mm-inside-diameter Pyrex tube, the tube was sealed and then heated to 140 ℃ for 72 h in a programmable oven, followed by the slow cooling down to room temperature with the rate of 3 ℃/h. Colourless needle crystals were collected and air-dried. Yield: 1.6 mg (48% based on $Cu(NO_3)_2 \cdot 3H_2O$) for **R-2**, 1.8 mg (54% based on $Cu(NO_3)_2 \cdot 3H_2O$) for **S-2**. Elemental analyses for **R-2** ($C_{48}H_{42}Cu_3N_9O_3$, %): calculated: C, 58.62; H, 4.30; N, 12.82; found: C, 57.60; H, 4.81; N, 12.94. Elemental analyses for **S-2** ($C_{48}H_{42}Cu_3N_9O_3$, %): calculated: C, 58.62; H, 4.30; N, 12.82; found: C, 58.53; H, 4.23; N, 12.81. FT-IR data (KBr, $cm^{-1}$) of **R-2**: 439 (w), 467 (w), 509 (w), 554 (w), 575 (w), 613 (w), 636 (m), 646 (w), 651 (w), 675 (w), 707 (m), 717 (w), 733 (m), 739 (m), 774 (vs), 803 (s), 825 (w), 865 (w), 912 (w), 985 (w), 1014 (w), 1054 (s), 1089 (w), 1123 (w), 1174 (w), 1192 (w), 1249 (vs), 1334 (w), 1380 (w), 1403 (m), 1443 (m), 1512 (s), 1558 (vs), 1632 (vs), 2867 (w), 2936 (w), 2976 (w), 3056 (m), 3113 (w), 3307 (b), 3433 (b), 3622 (m), 3640 (w). FT-IR data (KBr, $cm^{-1}$) of **S-2**: 424 (w), 449 (w), 474 (w), 509 (w), 545 (w), 576 (w), 607 (w), 637 (m), 667 (w), 703 (m), 739 (w), 776 (vs), 806 (s), 824 (m), 861 (m), 914 (w), 995 (w), 1018 (w), 1061 (s), 1085 (w), 1116 (w), 1170 (w), 1200 (m), 1243 (vs), 1333 (w), 1376 (w), 1400 (m), 1454 (m), 1515 (s), 1558 (vs), 1631 (vs), 2863 (w), 2934 (w), 2982 (w), 3055 (m), 3122 (w), 3322 (b), 3412 (b), 3630 (w).

**Film fabrication**

PMMA (2.5 g) was dissolved in dichloromethane (50 mL) under magnetic stirring at room temperature until complete dissolution, yielding a PMMA matrix solution with a concentration of 50 mg/mL. Subsequently, 1 mL aliquots of the matrix solution were transferred into centrifuge tubes, followed by the addition of crystalline powders of **S-1**/**R-2**/**S-2** (0.5 mg) into individual aliquots to fabricate flexible polymer films via solvent evaporation, resulting in **S-1**@PMMA, **R-2**@PMMA, and **S-2**@PMMA, respectively.

## 3. $^{1}H$ / $^{13}C$ NMR spectra

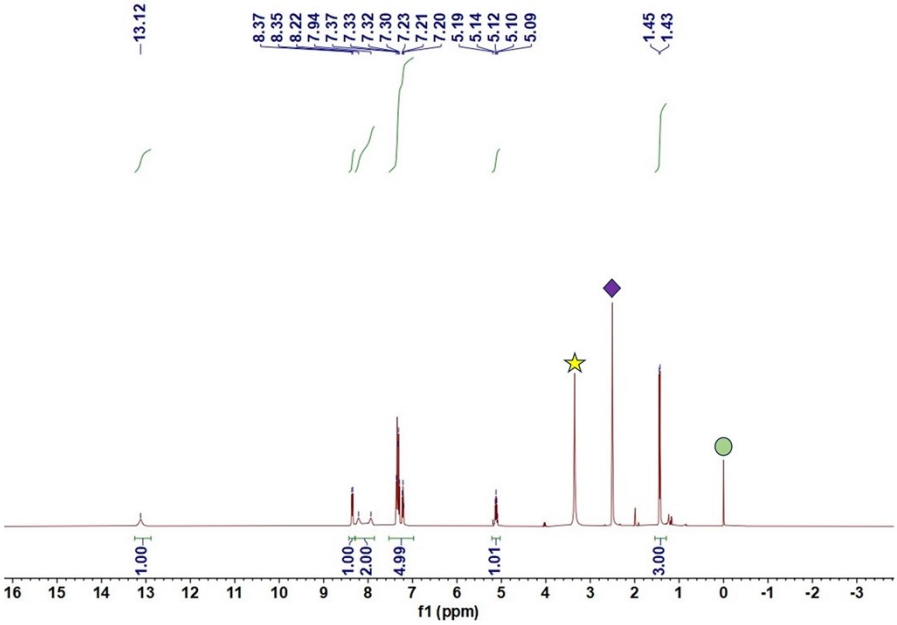


**Fig. S1** $^{1}H$ NMR (400 MHz, DMSO–$d_6$) spectrum of R-$HL_1$. The star, square and circle shapes denote the solvent residual signals of $H_2O$, DMSO and TMS, respectively.

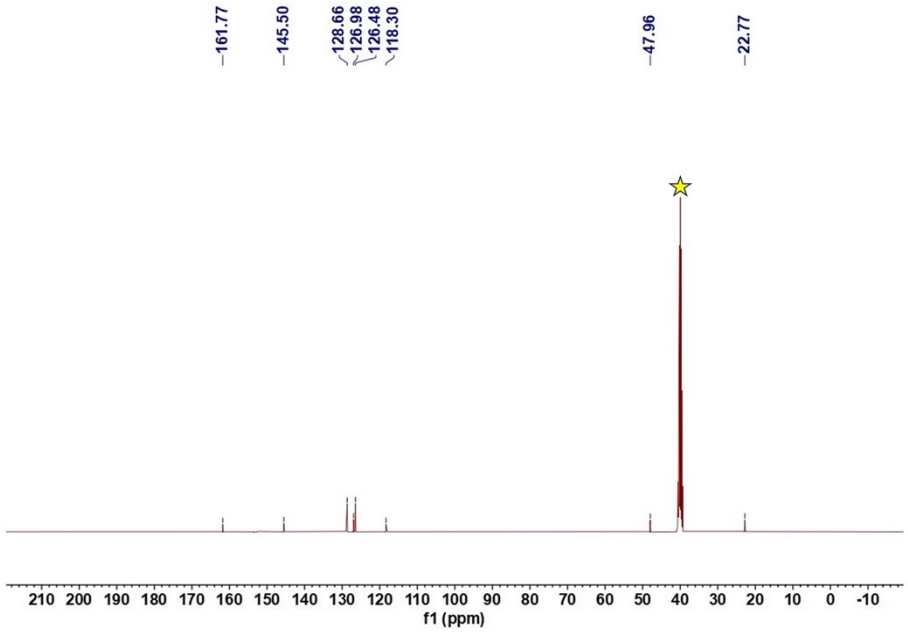


**Fig. S2** $^{13}C$ NMR (100 MHz, DMSO–$d_6$) spectrum of R-$HL_1$. The star shape denotes the solvent residual signals of DMSO.

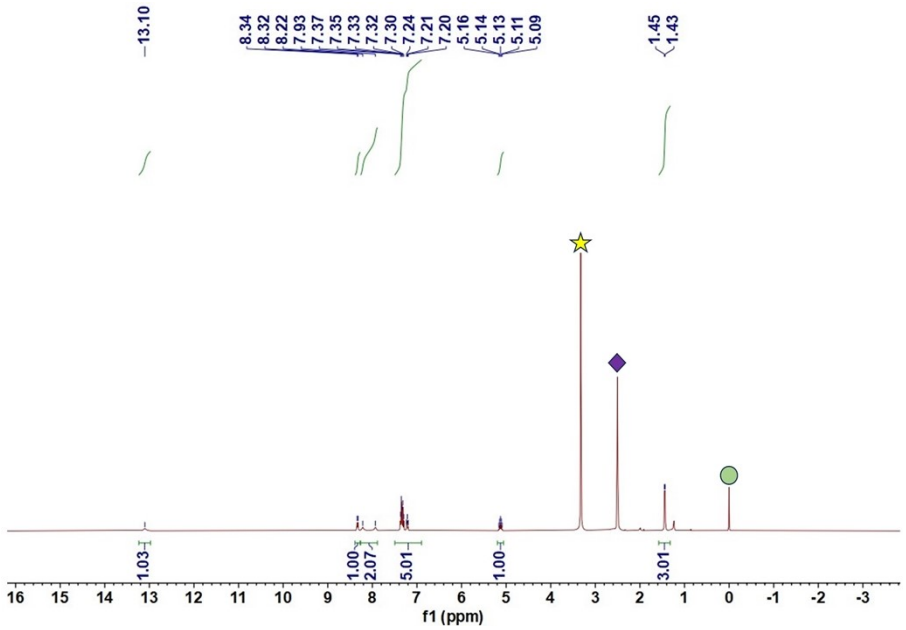


**Fig. S3** $^{1}$H NMR (400 MHz, DMSO–$d_6$) spectrum of S-$HL_1$. The star, square and circle shapes denote the solvent residual signals of $H_2O$, DMSO and TMS, respectively.

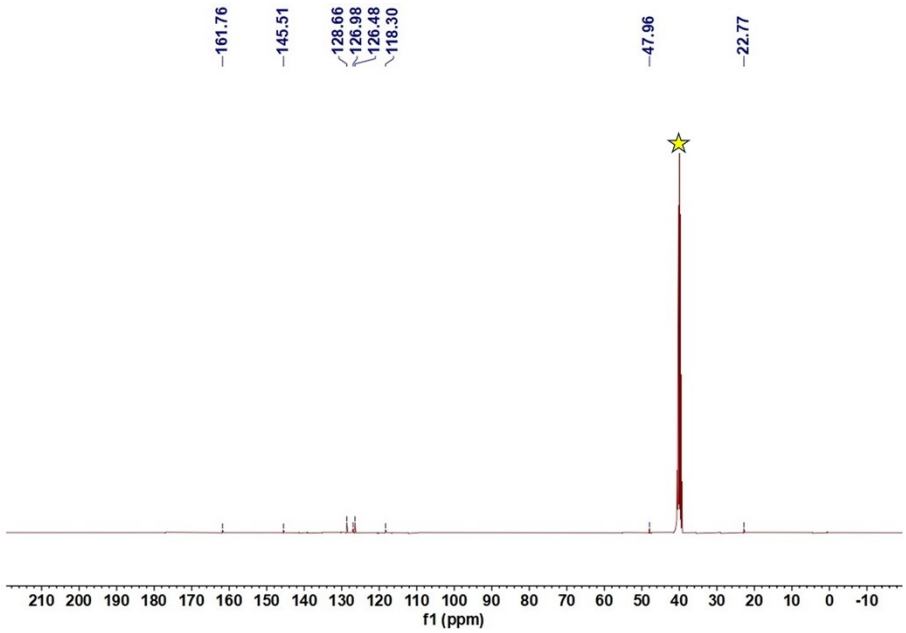


**Fig. S4** $^{13}$C NMR (100 MHz, DMSO–$d_6$) spectrum of S-$HL_1$. The star shape denotes the solvent residual signals of DMSO.

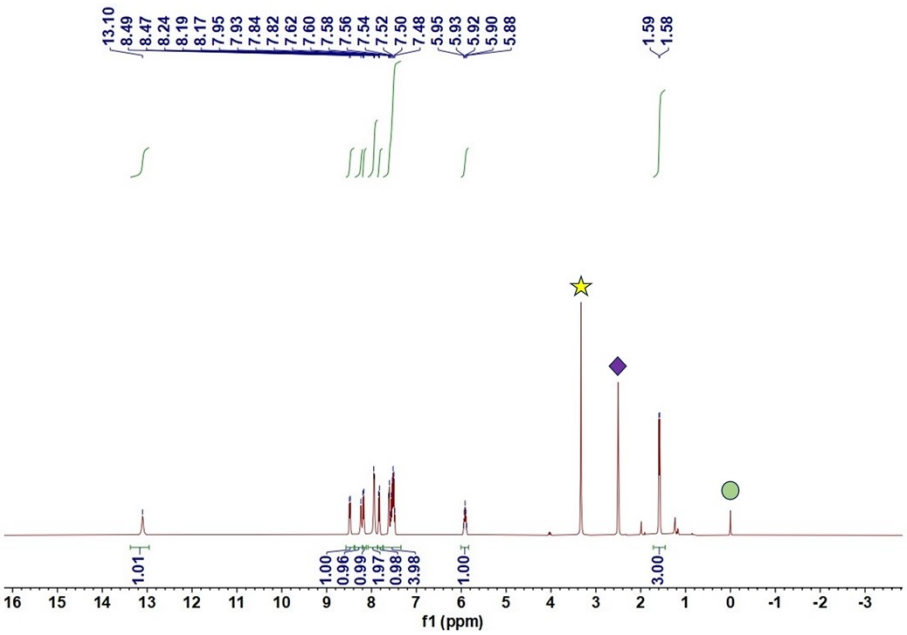


**Fig. S5** $^{1}$H NMR (400 MHz, DMSO–$d_6$) spectrum of R-$HL_2$. The star, square and circle shapes denote the solvent residual signals of $H_2O$, DMSO and TMS, respectively.

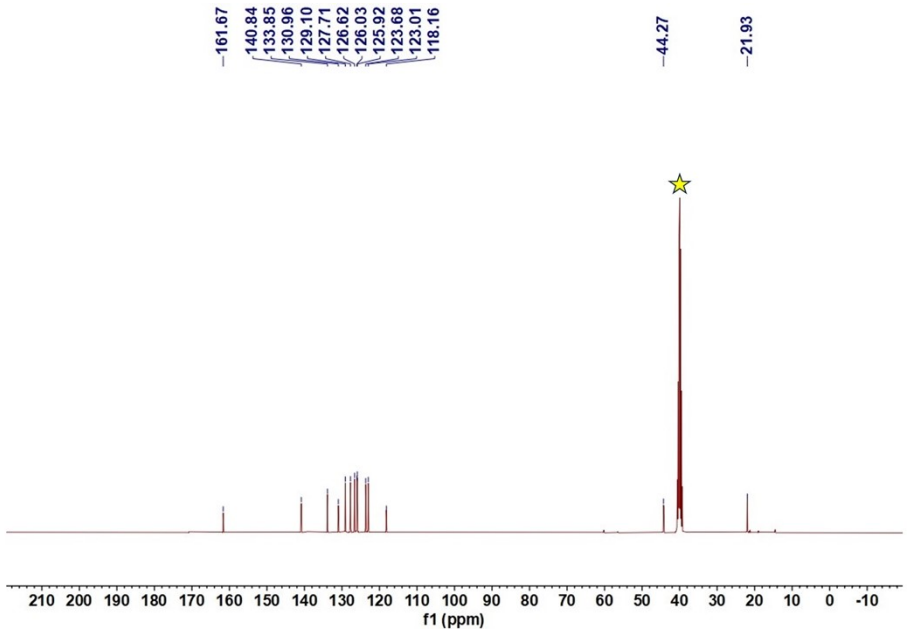


**Fig. S6** $^{13}$C NMR (100 MHz, DMSO–$d_6$) spectrum of R-$HL_2$. The star shape denotes the solvent residual signals of DMSO.

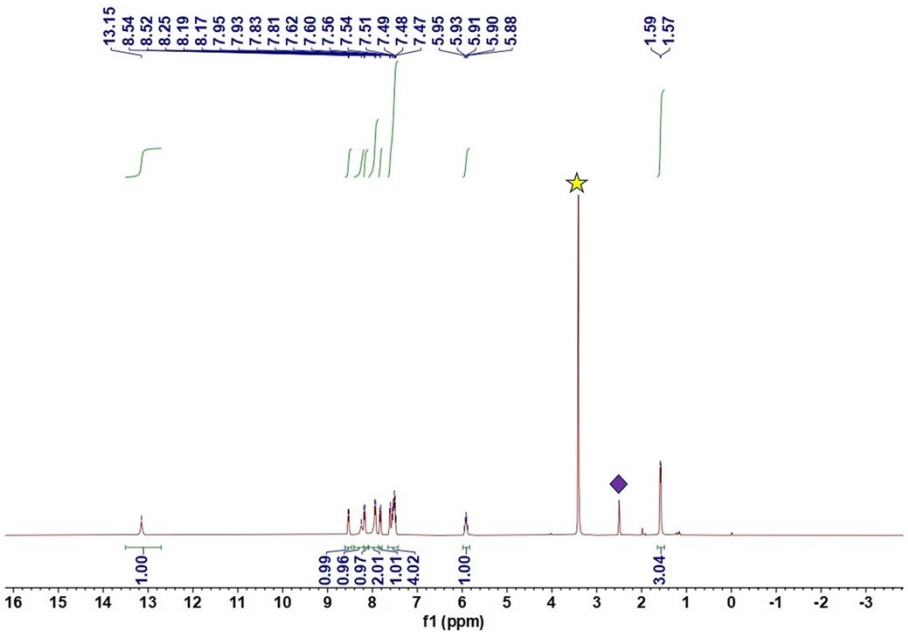


**Fig. S7** $^{1}$H NMR (400 MHz, DMSO–$d_6$) spectrum of S-$HL_2$. The star and square shapes denote the solvent residual signals of $H_2O$ and DMSO, respectively.

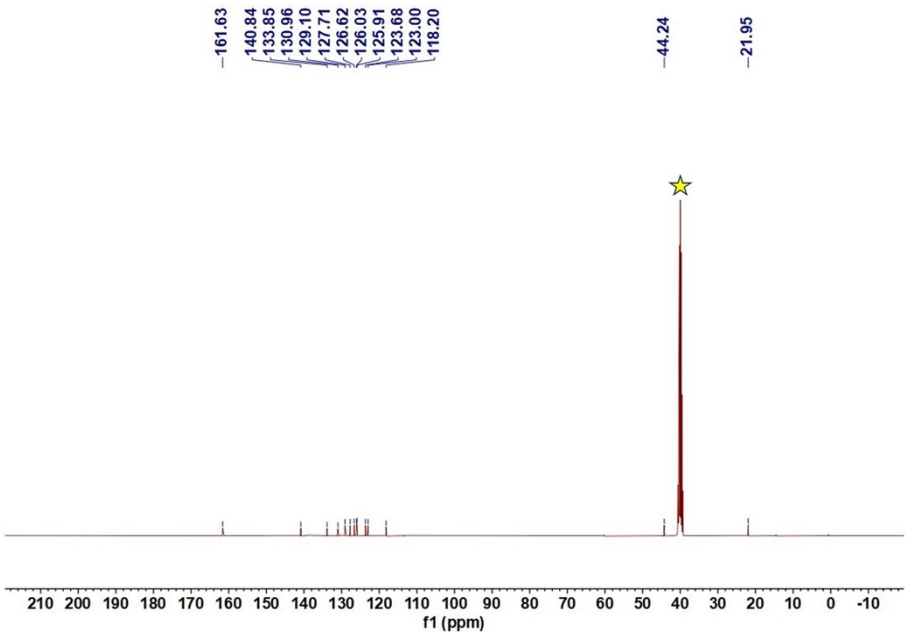


**Fig. S8** $^{13}$C NMR (100 MHz, DMSO–$d_6$) spectrum of S-$HL_2$. The star shape denotes the solvent residual signals of DMSO.

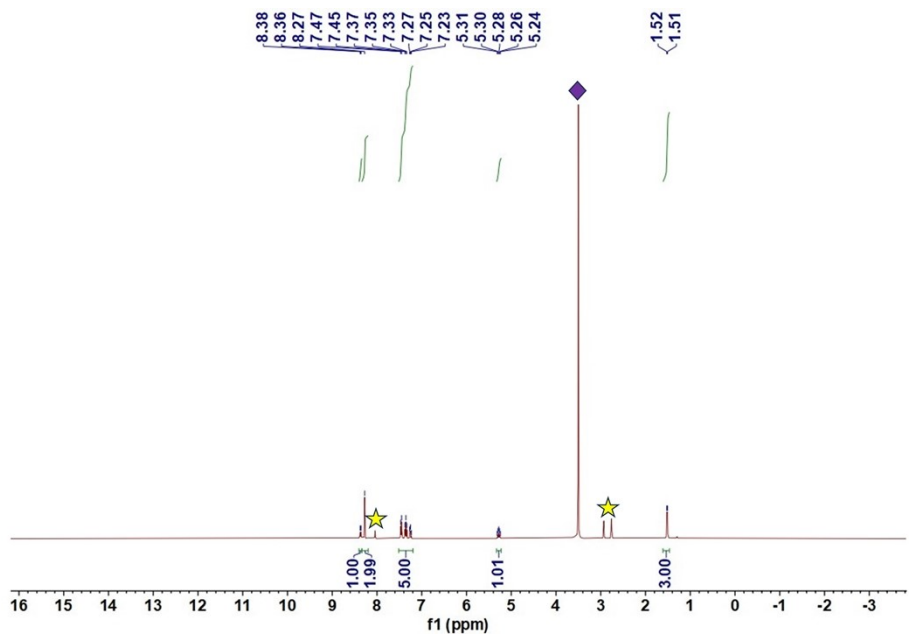


**Fig. S9** $^{1}$H NMR (400 MHz, DMF–$d_7$) spectrum of **R-1**. The star and square shapes denote the solvent residual signals of DMF and $H_2O$, respectively.

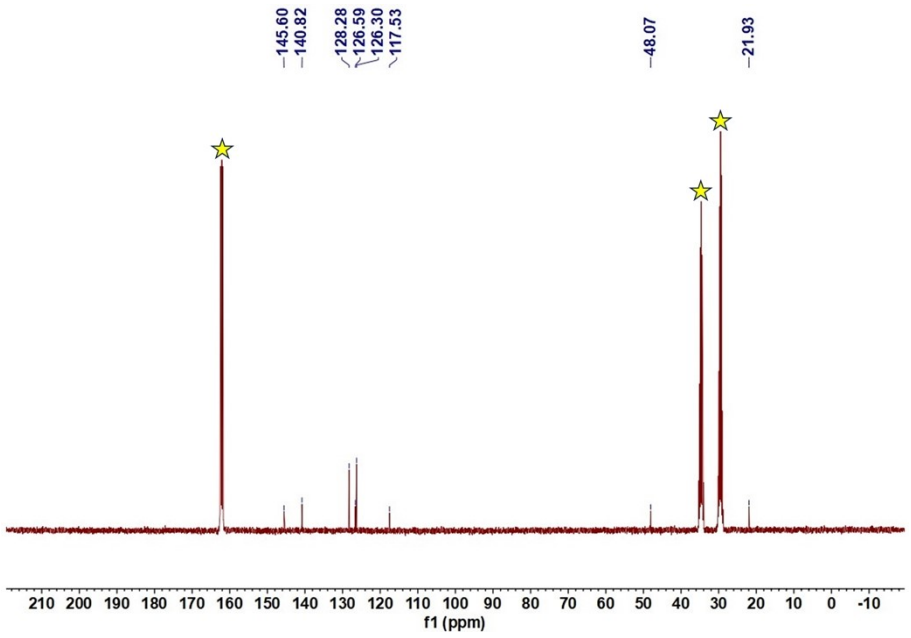


**Fig. S10** $^{13}$C NMR (100 MHz, DMF–$d_7$) spectrum of **R-1**. The star shape denotes the solvent residual signals of DMF.

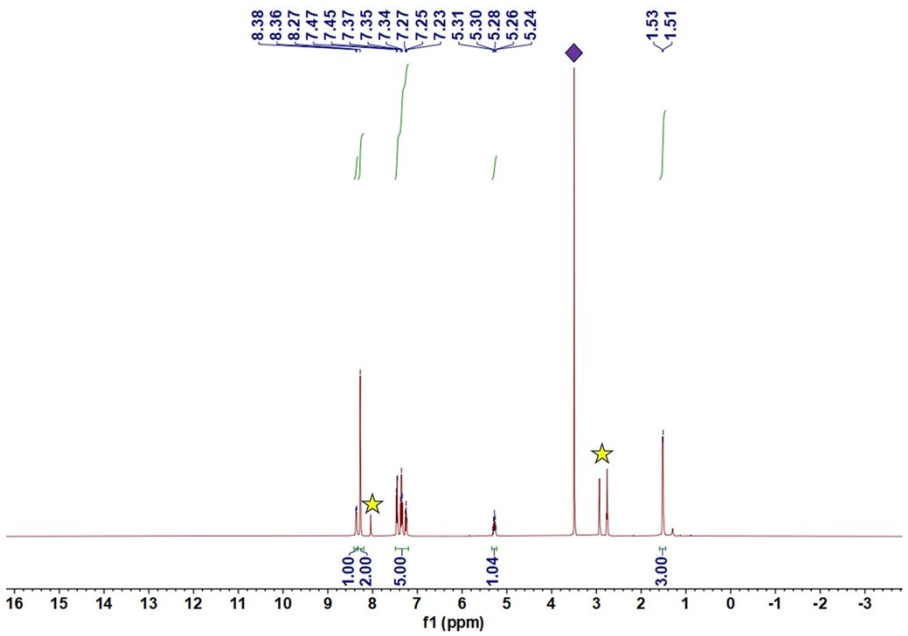


**Fig. S11** $^{1}$H NMR (400 MHz, DMF–$d_7$) spectrum of **S-1**. The star and square shapes denote the solvent residual signals of DMF and $H_2O$, respectively.

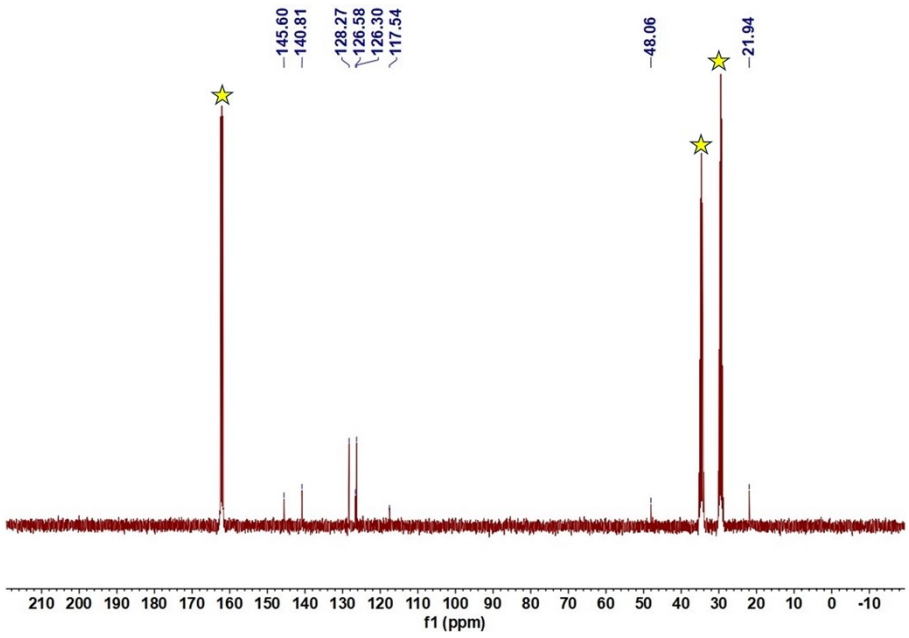


**Fig. S12** $^{13}$C NMR (100 MHz, DMF–$d_7$) spectrum of **S-1**. The star shape denotes the solvent residual signals of DMF.

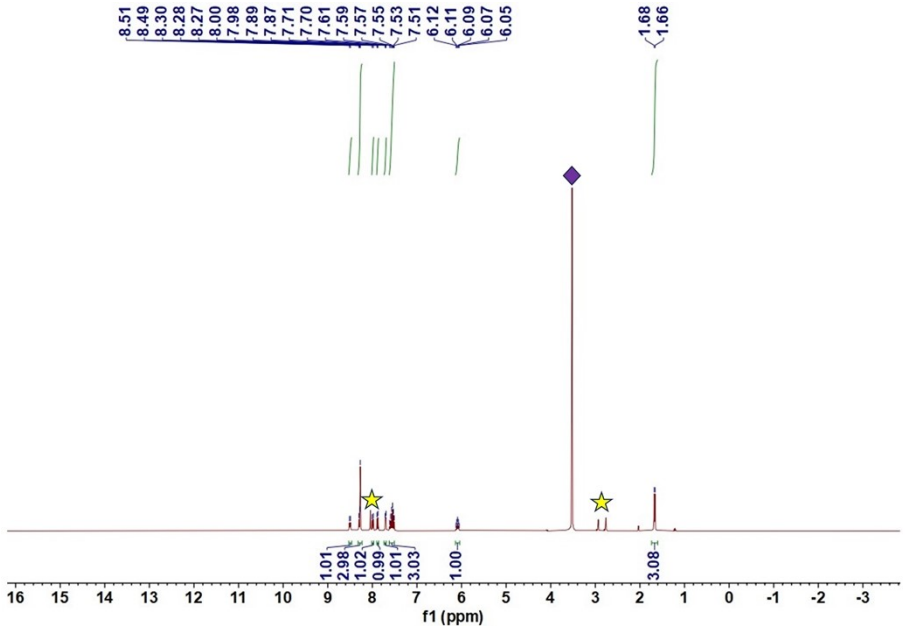


**Fig. S13** $^{1}$H NMR (400 MHz, DMF–$d_7$) spectrum of **R-2**. The star and square shapes denote the solvent residual signals of DMF and $H_2O$, respectively.

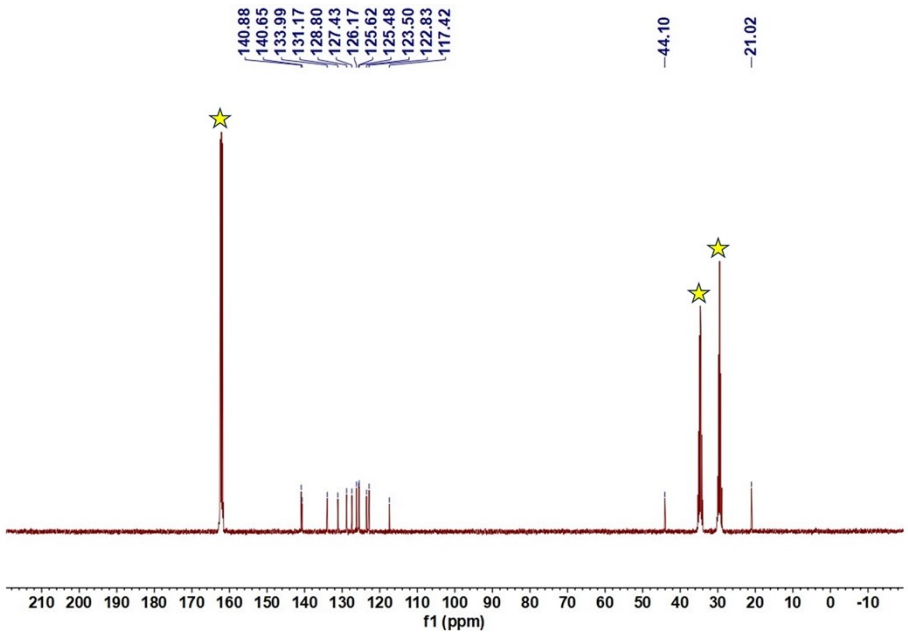


**Fig. S14** $^{13}$C NMR (100 MHz, DMF–$d_7$) spectrum of **R-2**. The star shape denotes the solvent residual signals of DMF.

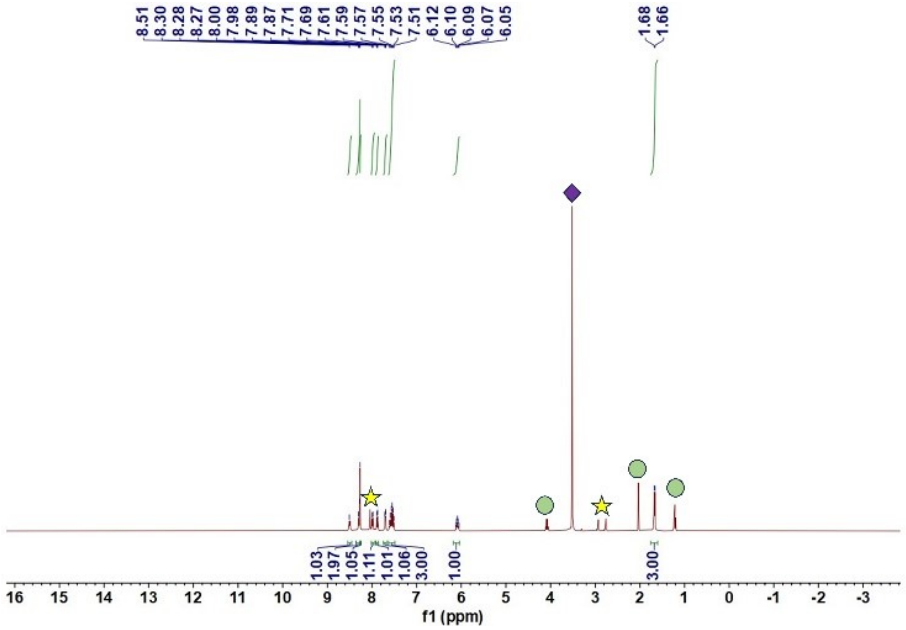


**Fig. S15** $^{1}$H NMR (400 MHz, DMF–$d_7$) spectrum of **S-2**. The star, circle and square shapes denote the solvent residual signals of DMF, ethyl acetate and $H_2O$, respectively.

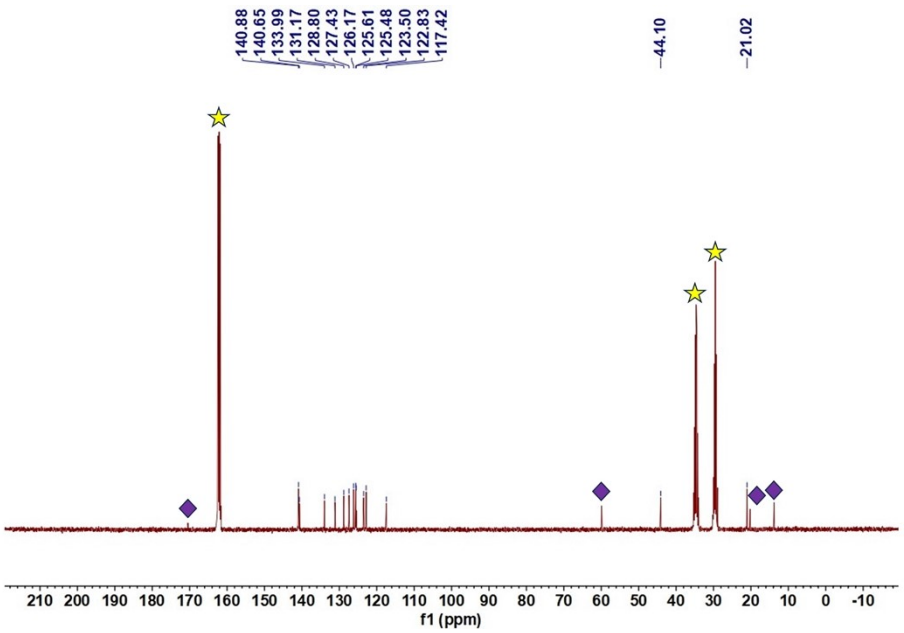


**Fig. S16** $^{13}$C NMR (100 MHz, DMF–$d_7$) spectrum of **S-2**. The square and star shapes denote the solvent residual signals of ethyl acetate and DMF, respectively.

## 4. PXRD patterns

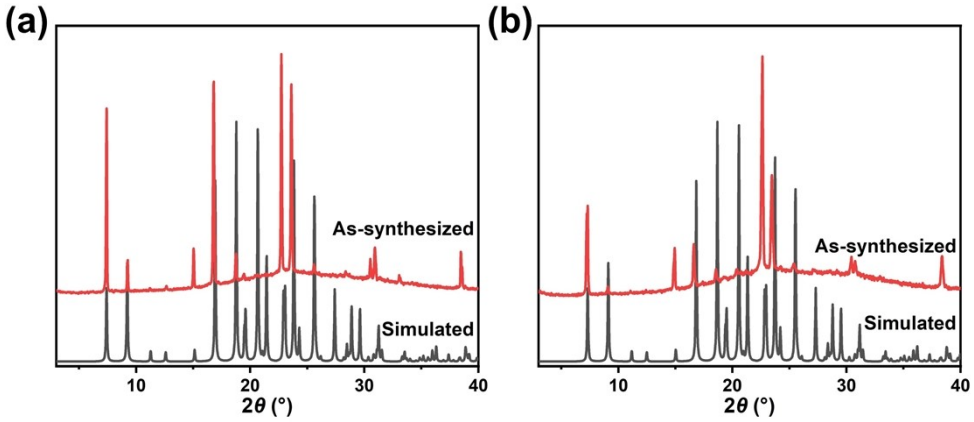


**Fig. S17** PXRD patterns of crystalline (a) R-$HL_1$ and (b) S-$HL_1$.

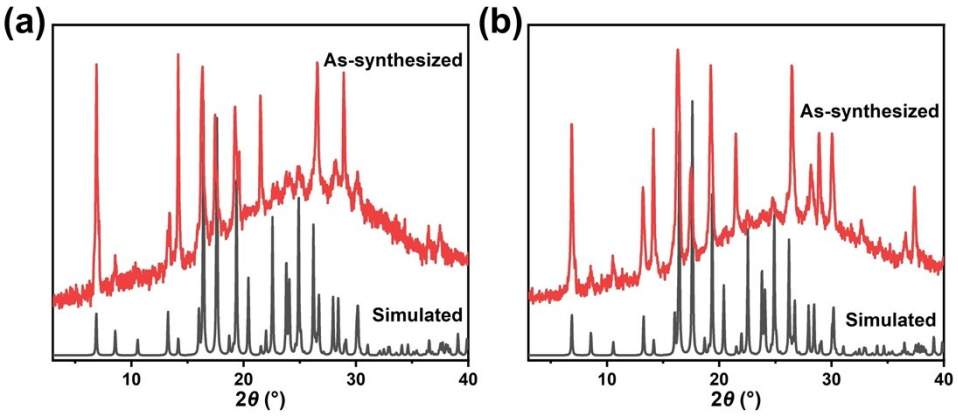


**Fig. S18** PXRD patterns of crystalline (a) R-$HL_2$ and (b) S-$HL_2$.

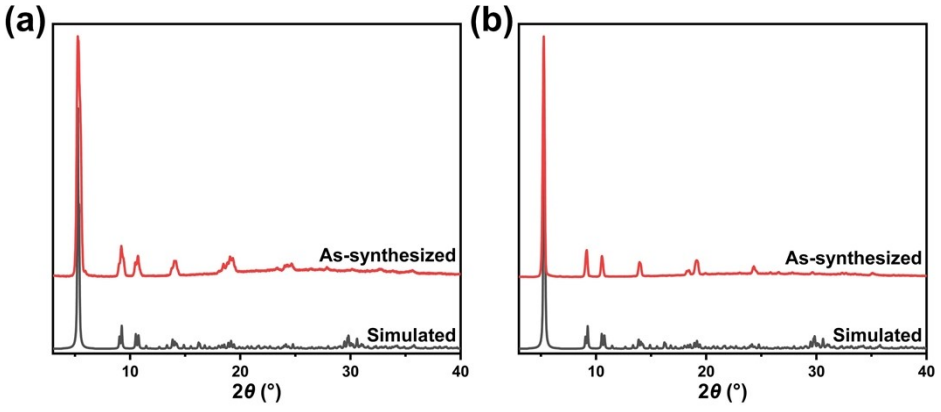


**Fig. S19** PXRD patterns of (a) **R-1** and (b) **S-1**.

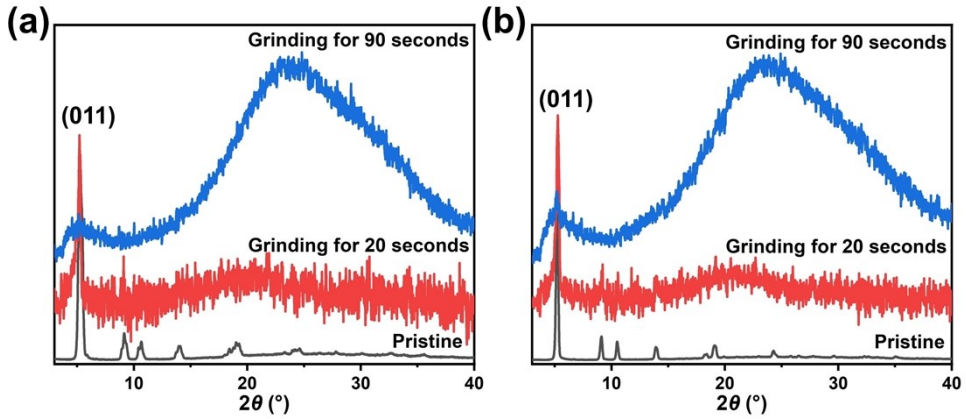


**Fig. S20** PXRD patterns of (a) **R-1** and (b) **S-1** before grinding, after grinding for 20 seconds (red line) with low-crystallinity and further grinding for 70 seconds (bule line) with non-crystallinity. The low-crystallinity and non-crystallinity of **R-1**/**S-1** in powder state suggest the possible decomposition of their helical structures along the *a*-axis.

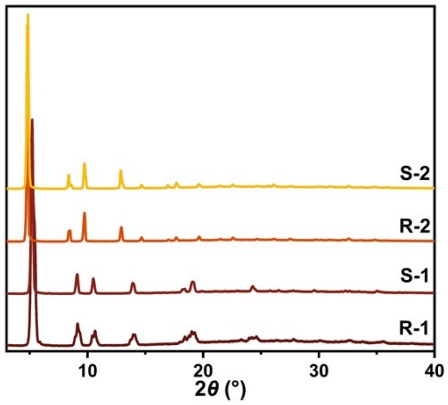


**Fig. S21** PXRD patterns of **R-1**/**S-1** and **R-2**/**S-2**.

## 5. Thermal stabilities

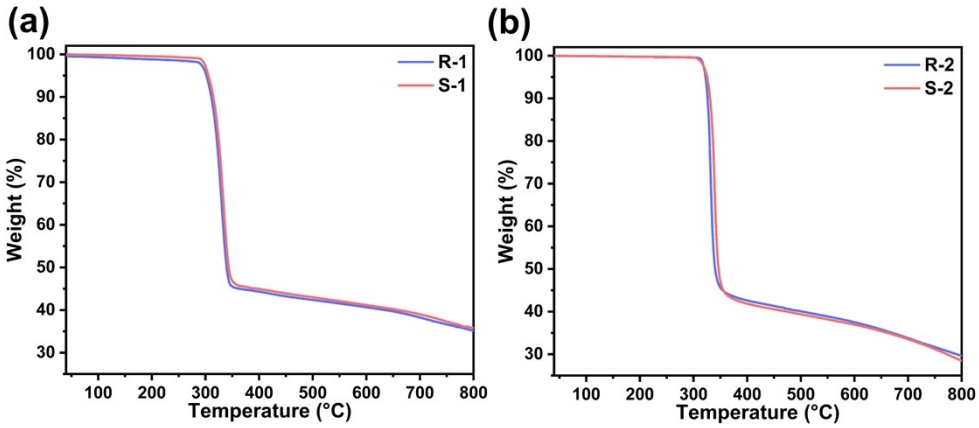


**Fig. S22** TGA curves of (a) **R-1/S-1** and (b) **R-2/S-2**.

## 6. Structural Determination

Single crystal structures of R-$HL_1$/S-$HL_1$, R-$HL_2$/S-$HL_2$ and **R-1/S-1** were determined by single-crystal X-ray diffraction (SCXRD) at 100 K using an XtaLAB PRO MM007-DW diffractometer system, equipped with an RA-Micro7HF-MR-DW(Cu/Mo) X-ray generator and HyPix-6000HE Hybrid Photon Counting (HPC) X-ray detector (Rigaku, Japan, Cu Kα, graphite monochromator, λ = 1.54 Å). The structures were solved by direct methods and refined by full-matrix least-squares refinements based on $F^2$. Anisotropic thermal parameters were applied to all non-hydrogen atoms, with hydrogen atoms placed in calculated positions and refined using isotropic thermal parameters, riding on their parent atoms. All calculations were performed using the SHELXTL system of computer programs.[2] Some reflections of all the complexes were omitted owing to poor agreement. Crystallographic data and structure refinement parameters are summarized in Tables S1–S3.

## 6.1 Structural Determination of R-$HL_1$/S-$HL_1$

**Table S1** Crystallographic data and refinement parameters of R-$HL_1$/S-$HL_1$.

| Item | R-$HL_1$ | S-$HL_1$ |
|---|---|---|
| CCDC number | 2378497 | 2378498 |
| Temperature (K) | 100.01(16) | 100.00(10) |
| Empirical formula | $C_{12}H_{13}N_3O$ | $C_{12}H_{13}N_3O$ |
| Formula weight | 215.25 | 215.25 |
| Crystal system | monoclinic | monoclinic |
| Space group | $P2_1$ | $P2_1$ |
| a (Å) | 9.3639(3) | 9.3663(2) |
| b (Å) | 5.08840(10) | 5.08920(10) |
| c (Å) | 11.5646(3) | 11.5614(2) |
| β (°) | 96.300(3) | 96.3050(10) |
| Volume (Å$^3$) | 547.69(3) | 547.764(19) |
| Z | 2 | 2 |
| $\rho_{calc}$ (g/cm$^3$) | 1.305 | 1.305 |
| F(000) | 228.0 | 228.0 |
| 2θ range for data collection (°) | 7.692 to 156.906 | 7.694 to 156.408 |
| Index ranges | −11 ≤ h ≤ 11, −6 ≤ k ≤ 6, −14 ≤ l ≤ 14 | −11 ≤ h ≤ 11, −6 ≤ k ≤ 6, −14 ≤ l ≤ 14 |
| Reflections collected | 9080 | 10392 |
| Independent reflections | 2284 [$R_{int}$ = 0.0430, $R_{sigma}$ = 0.0336] | 2278 [$R_{int}$ = 0.0323, $R_{sigma}$ = 0.0253] |
| Data/restraints/ parameters | 2284/1/146 | 2278/1/146 |
| Goodness-of-fit on $F^2$ | 1.145 | 1.112 |
| Completeness (%) | 99.9 | 99.2 |
| [a]Final R indexes [I>=2σ (I)] | $R_1$ = 0.0356 | $R_1$ = 0.0427 |
| [b]Final R indexes [all data] | $wR_2$ = 0.1011 | $wR_2$ = 0.0943 |
| Largest diff. peak/hole (e Å$^{-3}$) | 0.15/−0.22 | 0.19/−0.19 |
| Flack parameter | −0.15(18) | 0.08(14) |

[a]$R_1 = \sum||F_o|-|F_c||/\sum|F_o|$. [b]$wR_2 = \{[\sum w(F_o^2-F_c^2)^2]/\sum[w(F_o^2)]\}^{1/2}$; $w = 1/[\sigma^2(F_o^2)+(aP)^2+bP]$, where $P = [\max(F_o^2, 0) + 2F_c^2]/3$ for all data.

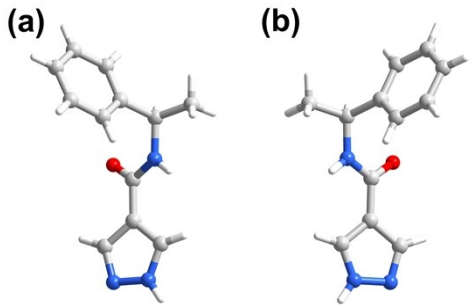


**Fig. S23** Molecular structures of (a) R-$HL_1$ and (b) S-$HL_1$. Colour codes: grey, C; blue, N; red, O; white, H.

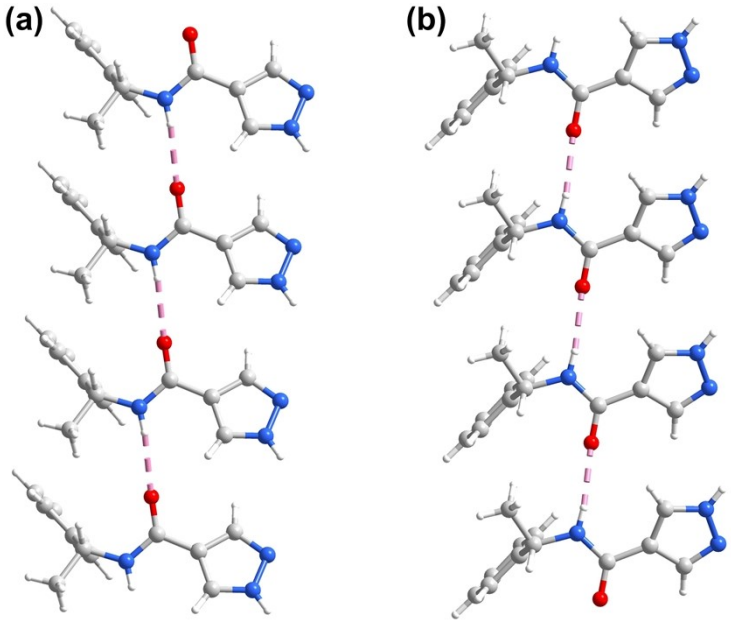


**Fig. S24** Packing modes of (a) R-$HL_1$ and (b) S-$HL_1$. Dashed lines showing hydrogen-bonding interactions between the adjacent molecules. Colour codes: grey, C; blue, N; red, O; white, H.

## 6.2 Structural Determination of R-$HL_2$/S-$HL_2$

**Table S2** Crystallographic data and refinement parameters of R-$HL_2$/S-$HL_2$.

| Item | R-$HL_2$ | S-$HL_2$ |
|---|---|---|
| CCDC number | 2378499 | 2378500 |
| Temperature (K) | 99.99(10) | 99.98(10) |
| Empirical formula | $C_{16}H_{15}N_3O$ | $C_{16}H_{15}N_3O$ |
| Formula weight | 265.31 | 265.31 |
| Crystal system | orthorhombic | orthorhombic |
| Space group | $P2_12_12_1$ | $P2_12_12_1$ |
| a (Å) | 5.02106(10) | 5.02560(10) |
| b (Å) | 10.7938(2) | 10.7811(4) |
| c (Å) | 24.2999(6) | 24.3162(7) |
| Volume (Å$^3$) | 1316.96(5) | 1317.49(7) |
| Z | 4 | 4 |
| $\rho_{calc}$ (g/cm$^3$) | 1.338 | 1.338 |
| F(000) | 560.0 | 560.0 |
| 2θ range for data collection (°) | 7.276 to 155.66 | 7.27 to 156.196 |
| Index ranges | $-3 \le h \le 6$, $-13 \le k \le 13$, $-30 \le l \le 30$ | $-6 \le h \le 6$, $-13 \le k \le 9$, $-30 \le l \le 30$ |
| Reflections collected | 5484 | 7298 |
| Independent reflections | 2528 [$R_{int}$ = 0.0405, $R_{sigma}$ = 0.0542] | 2714 [$R_{int}$ = 0.0520, $R_{sigma}$ = 0.0615] |
| Data/restraints/ parameters | 2528/0/170 | 2714/0/182 |
| Goodness-of-fit on $F^2$ | 1.102 | 1.064 |
| Completeness (%) | 99.4 | 99.8 |
| [a]Final R indexes [I>=2σ (I)] | $R_1$ = 0.0585 | $R_1$ = 0.0486 |
| [b]Final R indexes [all data] | $wR_2$ = 0.1668 | $wR_2$ = 0.1410 |
| Largest diff. peak/hole (e Å$^{-3}$) | 0.48/−0.55 | 0.44/−0.33 |
| Flack parameter | −0.2(2) | −0.2(2) |

[a]$R_1 = \sum||F_o|-|F_c||/\sum|F_o|$. [b]$wR_2 = \{[\sum w(F_o^2-F_c^2)^2]/\sum[w(F_o^2)]\}^{1/2}$; $w = 1/[\sigma^2(F_o^2)+(aP)^2+bP]$, where $P = [\max(F_o^2, 0) + 2F_c^2]/3$ for all data.

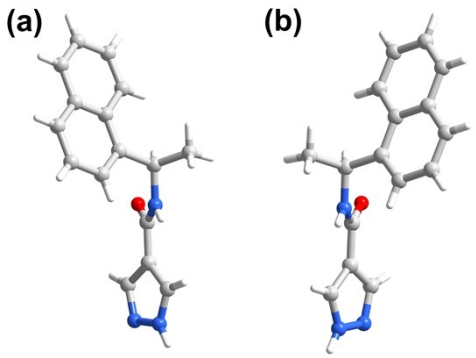


**Fig. S25** Molecular structures of (a) R-$HL_2$ and (b) S-$HL_2$. Colour codes: grey, C; blue, N; red, O; white, H.

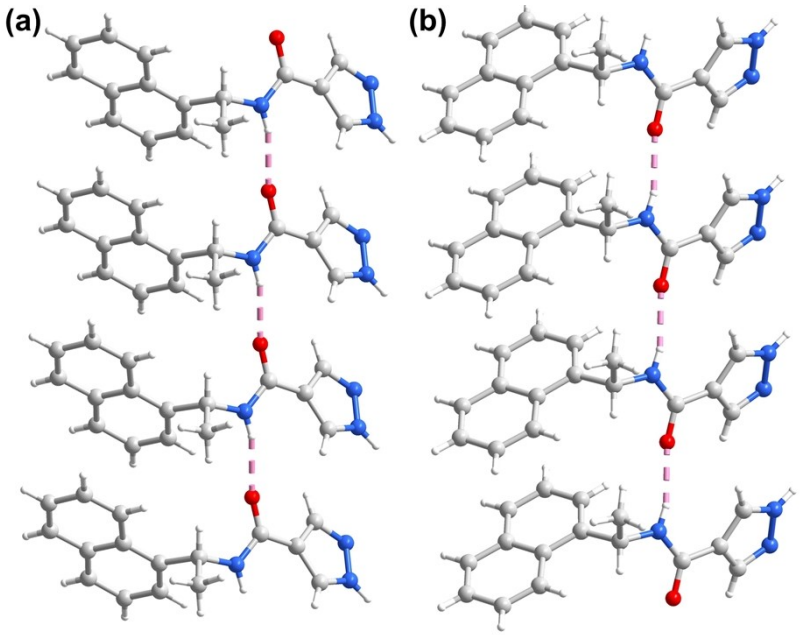


**Fig. S26** Packing modes of (a) R-$HL_2$ and (b) S-$HL_2$. Dashed lines showing hydrogen-bonding interactions the between adjacent molecules. Colour codes: grey, C; blue, N; red, O; white, H.

### 6.3 Structural Determination of R-1/S-1

**Table S3** Crystallographic data and refinement parameters of **R-1/S-1**.

| Item | **R-1** | **S-1** |
|---|---|---|
| CCDC number | 2378501 | 2378502 |
| Temperature (K) | 100.0(2) | 100.1(4) |
| Empirical formula | $C_{112}H_{119}Cu_9N_{27}O_{11}$ | $C_{112}H_{120}Cu_9N_{27}O_{11}$ |
| Formula weight | 2591.19 | 2592.20 |
| Crystal system | monoclinic | monoclinic |
| Space group | $P2_1$ | $P2_1$ |
| a (Å) | 9.09800(10) | 9.0903(2) |
| b (Å) | 19.5551(3) | 19.5430(4) |
| c (Å) | 33.1683(5) | 33.1835(9) |
| β (°) | 97.6660(10) | 97.787(2) |
| Volume (Å$^3$) | 5848.31(14) | 5840.7(2) |
| Z | 2 | 2 |
| $\rho_{calc}$ (g/cm$^3$) | 1.471 | 1.474 |
| F(000) | 2658.0 | 2660.0 |
| 2θ range for data collection (°) | 7.026 to 157.844 | 7.026 to 156.262 |
| Index ranges | −10 ≤ h ≤ 11,<br>−24 ≤ k ≤ 24,<br>−42 ≤ l ≤ 30 | −11 ≤ h ≤ 11,<br>−22 ≤ k ≤ 24,<br>−38 ≤ l ≤ 42 |
| Reflections collected | 60856 | 50804 |
| Independent reflections | 22685<br>[$R_{int}$ = 0.1268,<br>$R_{sigma}$ = 0.0755] | 20099<br>[$R_{int}$ = 0.0970,<br>$R_{sigma}$ = 0.0754] |
| Data/restraints/ parameters | 22685/1/1257 | 20099/2794/1558 |
| Goodness-of-fit on F$^2$ | 1.039 | 1.041 |
| Completeness (%) | 99.6 | 99.3 |
| [a]Final R indexes [I>=2σ (I)] | $R_1$ = 0.0845 | $R_1$ = 0.1093 |
| [b]Final R indexes [all data] | $wR_2$ = 0.2024 | $wR_2$ = 0.2828 |
| Largest diff. peak/hole (e Å$^{-3}$) | 1.06/−0.98 | 1.52/−1.02 |
| Flack parameter | 0.05(4) | 0.10(7) |

[a]$R_1 = \sum||F_o|-|F_c||/\sum|F_o|$. [b]$wR_2 = \{[\sum w(F_o^2-F_c^2)^2]/\sum[w(F_o^2)]\}^{1/2}$; $w = 1/[\sigma^2(F_o^2)+(aP)^2+bP]$, where $P = [\max(F_o^2, 0) + 2F_c^2]/3$ for all data.

**Table S4** Bond lengths (Å) and angles (°) in the single crystals of **R-1/S-1**.

| | | | |
|---|---|---|---|
| **R-1** | | | |
| Cu(1)–N(2) | 1.821(4) | Cu(1)–N(15) | 1.822(4) |
| Cu(2)–N(3) | 1.821(4) | Cu(2)–N(27) | 1.829(4) |
| Cu(3)–N(9) | 1.801(5) | Cu(3)–N(19) | 1.808(4) |
| Cu(4)–N(17) | 1.843(4) | Cu(4)–N(23) | 1.832(4) |
| Cu(5)–N(7) | 1.827(4) | Cu(5)–N(25) | 1.821(4) |
| Cu(6)–N(13) | 1.833(4) | Cu(6)–N(20) | 1.833(4) |
| Cu(7)–N(18) | 1.817(5) | Cu(7)–N(22) | 1.817(4) |
| Cu(8)–N(11) | 1.815(4) | Cu(8)–N(24) | 1.821(4) |
| Cu(9)–N(5) | 1.833(4) | Cu(9)–N(21) | 1.827(5) |
| N(2)–Cu(1)–N(15) | 176.2(3) | N(3)–Cu(2)–N(27) | 175.1(3) |
| N(9)–Cu(3)–N(19) | 174.1(3) | N(17)–Cu(4)–N(23) | 175.3(3) |
| N(7)–Cu(5)–N(25) | 176.5(3) | N(13)–Cu(6)–N(20) | 176.8(3) |
| N(18)–Cu(7)–N(22) | 178.2(3) | N(11)–Cu(8)–N(24) | 175.1(3) |
| N(5)–Cu(9)–N(21) | 177.1(3) | | |
| **S-1** | | | |
| Cu(1)–N(17) | 1.826(4) | Cu(1)–N(23) | 1.822(4) |
| Cu(2)–N(12) | 1.820(4) | Cu(2)–N(26) | 1.817(4) |
| Cu(3)–N(3) | 1.821(4) | Cu(3)–N(22) | 1.819(4) |
| Cu(4)–N(5) | 1.813(4) | Cu(4)–N(24) | 1.818(4) |
| Cu(5)–N(2) | 1.820(4) | Cu(5)–N(11) | 1.816(4) |
| Cu(6)–N(16) | 1.818(4) | Cu(6)–N(21) | 1.822(4) |
| Cu(7)–N(8) | 1.815(4) | Cu(7)–N(25) | 1.814(4) |
| Cu(8)–N(18) | 1.818(4) | Cu(8)–N(20) | 1.820(4) |
| Cu(9)–N(10) | 1.820(4) | Cu(9)–N(27) | 1.820(4) |
| N(17)–Cu(1)–N(23) | 175.5(5) | N(12)–Cu(2)–N(26) | 178.9(5) |
| N(3)–Cu(3)–N(22) | 177.0(5) | N(5)–Cu(4)–N(24) | 174.5(5) |
| N(2)–Cu(5)–N(11) | 175.9(5) | N(16)–Cu(6)–N(21) | 176.4(5) |
| N(8)–Cu(7)–N(25) | 174.4(5) | N(18)–Cu(8)–N(20) | 176.3(5) |
| N(10)–Cu(9)–N(27) | 174.4(5) | | |

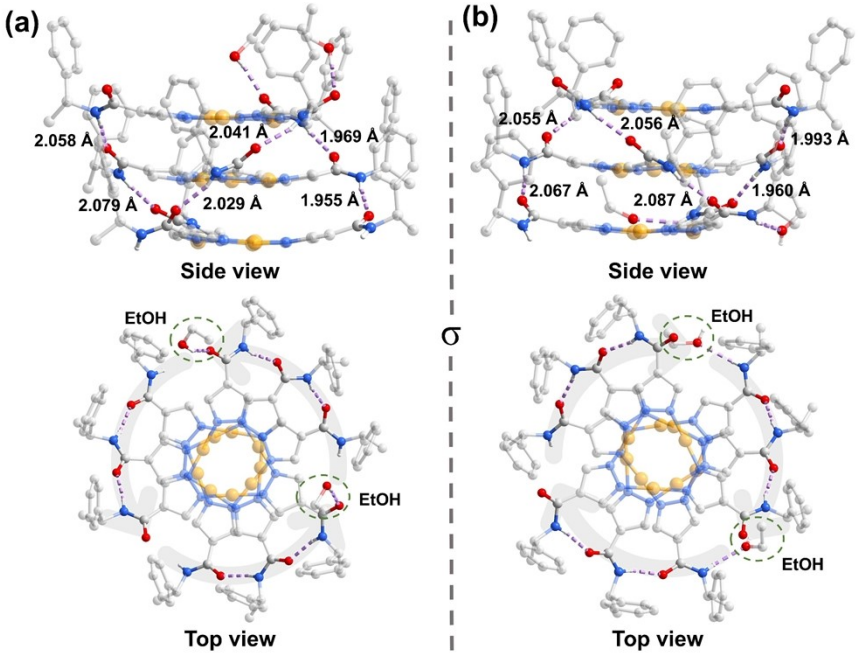


**Fig. S27** Asymmetric units of (a) **R-1** and (b) **S-1**, which are both built up of three Cu(I) CTC molecules and two EtOH molecules. The pink dashed lines highlight hydrogen bonding interactions. Colour codes: orange, Cu; grey, C; blue, N; red, O; white, H. For clarity, some H atoms have been omitted. Ethanol molecules also participate in the formation of hydrogen-bonding networks between the adjacent asymmetric units, see Figure S31.

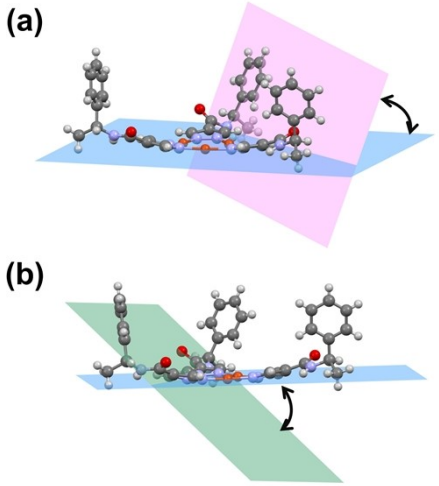


**Fig. S28** Schematic diagram of dihedral angles between (a) the pyrazolate planes and phenyl rings, (b) the pyrazolate planes and amide groups in **R-1**.

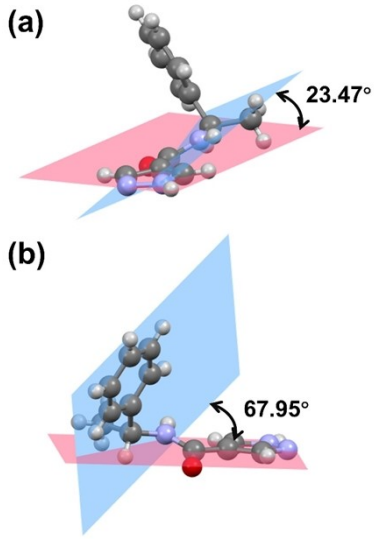


**Fig. S29** Dihedral angles between the (a) amide group and pyrazole planes, (b) phenyl ring and pyrazole planes in R-$HL_1$.

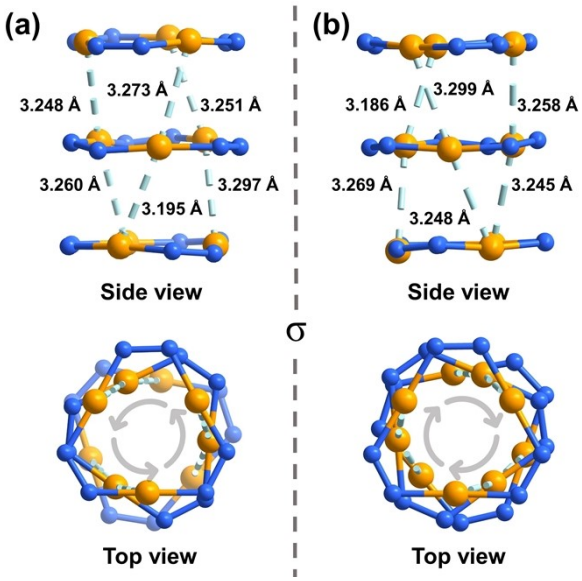


**Fig. S30** Stacking modes of $Cu_3N_6$ units in the asymmetric units of (a) **R-1** and (b) **S-1**. The blue dashed lines highlight intermolecular Cu···Cu interactions. Colour codes: orange, Cu; blue, N.

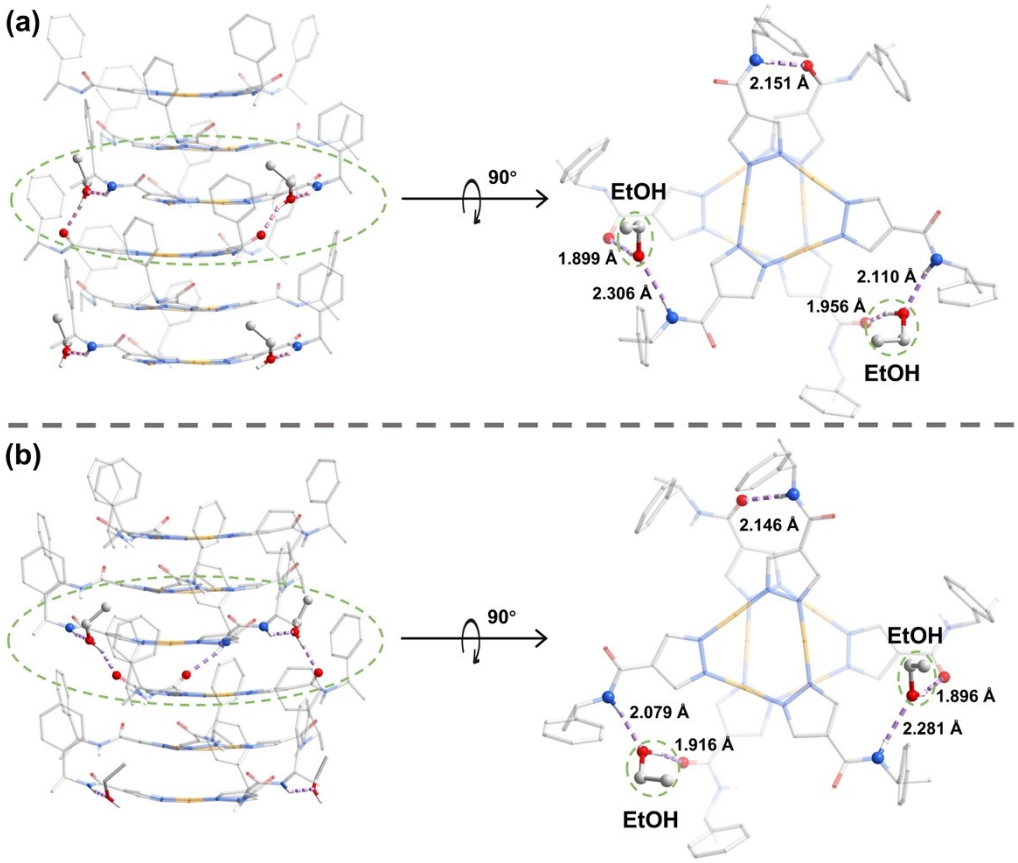


**Fig. S31** The hydrogen-bonding network between the adjacent $[Cu_3(R\text{-}L_1)_3]_3 \cdot (EtOH)_2$ units in (a) **R-1** and (b) **S-1**. In addition to hydrogen bonds formed by adjacent amide groups, the hydroxyl groups from ethanol molecules also participate in the hydrogen-bonding network. These hydroxyl groups act as both hydrogen bond donors and acceptors, forming hydrogen bonds through the N–H and C=O groups of adjacent amide groups. The pink dashed lines highlight hydrogen bonding interactions. Colour codes: orange, Cu; grey, C; blue, N; red, O; white, H. For clarity, some H atoms have been omitted.

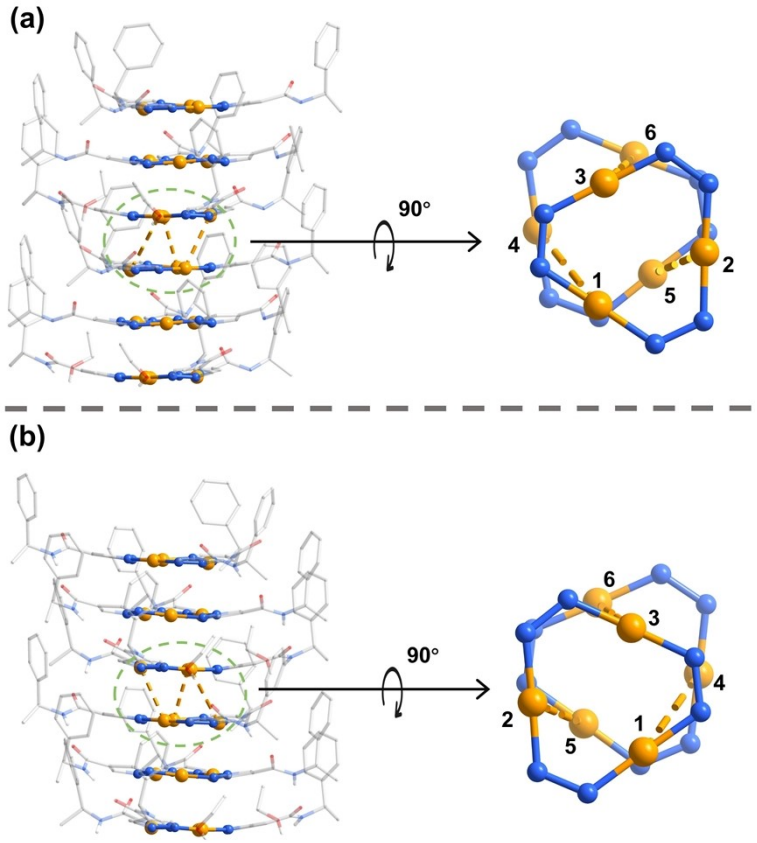


**Fig. S32** The metallophilic network between the adjacent $[Cu_3(R\text{-}L_1)_3]_3 \cdot (EtOH)_2$ units in (a) **R-1** and (b) **S-1**. The orange dashed lines highlight intermolecular Cu···Cu interactions. Intermolecular Cu···Cu distances (Å), **R-1**: 1–4 = 4.056, 2–5 = 3.297, 3–6 = 3.079; **S-1**: 1–4 = 4.053, 2–5 = 3.301, 3–6 = 3.074. Colour codes: orange, Cu; grey, C; blue, N; red, O; white, H. For clarity, some H atoms have been omitted.

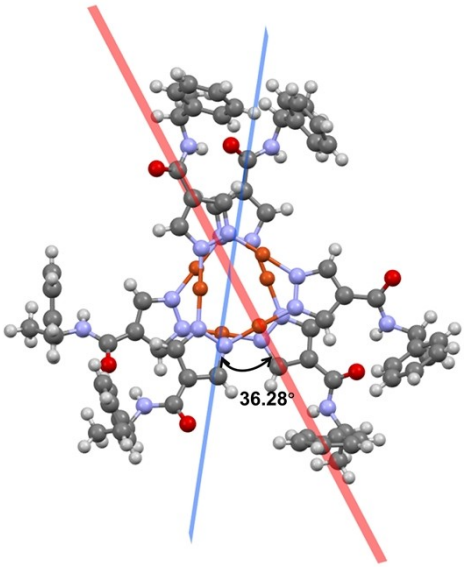


**Fig. S33** The twist angle between adjacent Cu(I) CTCs in **R-1**. Colour codes: orange, Cu; dark grey, C; purple, N; red, O; light grey, H.

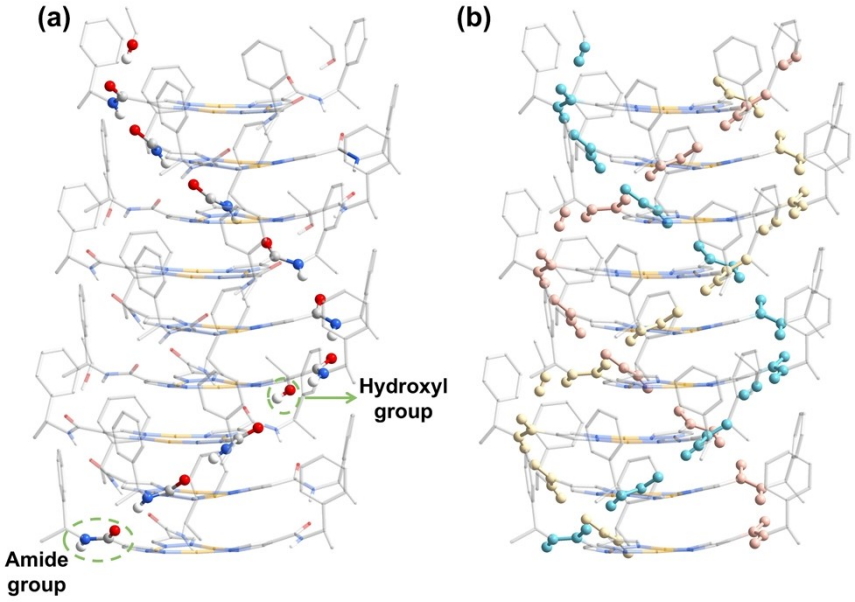


**Fig. S34** (a) A full turn of a hydrogen-bonded helical chain in **R-1** formed by nine amide groups and two hydroxyl groups. (b) Full turns of triple-helical hydrogen-bonding networks of the peripheral ligands in **R-1**. The entire triple-helical network is formed by the intertwining of three hydrogen-bonded helical chains. Colour codes for Figure S34a: orange, Cu; grey, C; blue, N; red, O; white, H. In Figure S34b, each helical chain is depicted in the same colour to emphasize the triple-helical assembly. For clarity, some hydrogen atoms have been omitted.

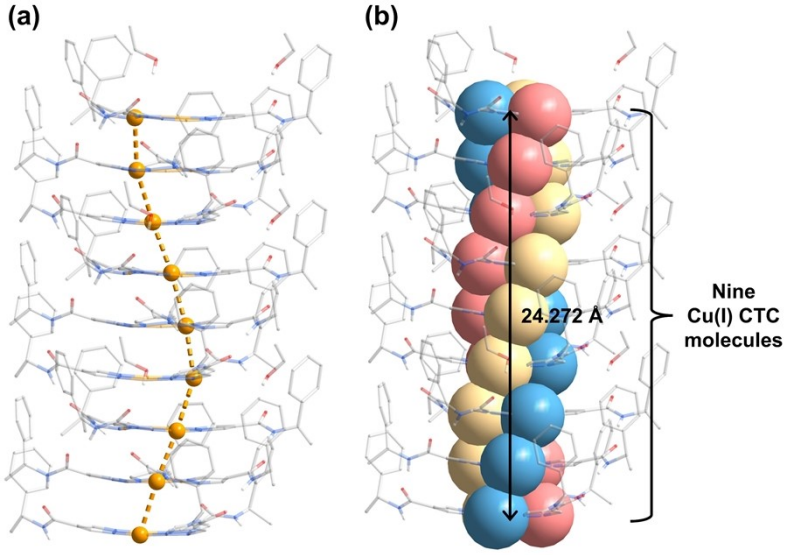


**Fig. S35** (a) A full turn of a metallophilically bonded helical chain in **R-1** formed by nine $Cu^{+}$ ions. (b) Full turns of triple-helical metallophilic networks of $Cu_3N_6$ units in **R-1**. The complete triple-helical network is formed by the intertwining of three metallophilically bonded helical chains. Colour codes for Figure S35a: orange, Cu; grey, C; blue, N; red, O; white, H. In Figure S35b, to emphasize the triple-helical assembly, each helical chain is depicted in the same colour. For clarity, some H atoms have been omitted.

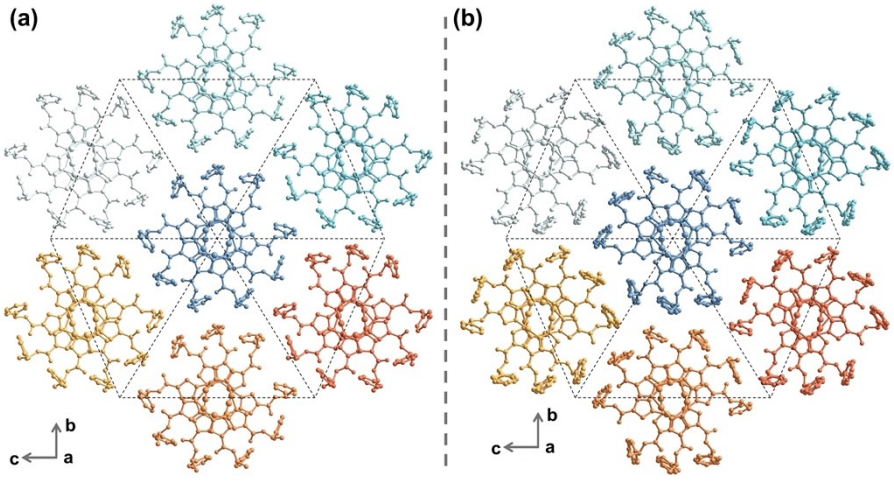


**Fig. S36** Pseudo-hexagonal packing of the triple helices along the *a*-axis in (a) **R-1** and (b) **S-1**.

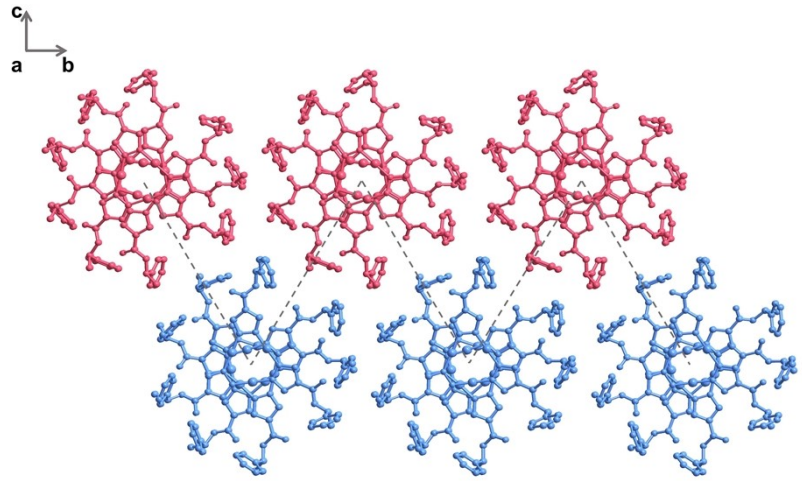


**Fig. S37** Crystal packing of **R-1** in the $P2_1$ space group, showing the arrangement of molecules along the $2_1$ axis parallel to the *b*-axis.

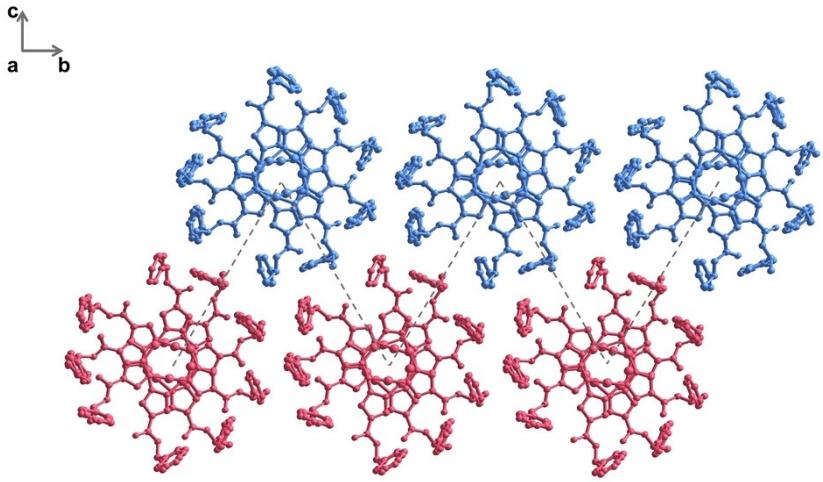


**Fig. S38** Crystal packing of **S-1** in the $P2_1$ space group, showing the arrangement of molecules along the $2_1$ axis parallel to the *b*-axis.

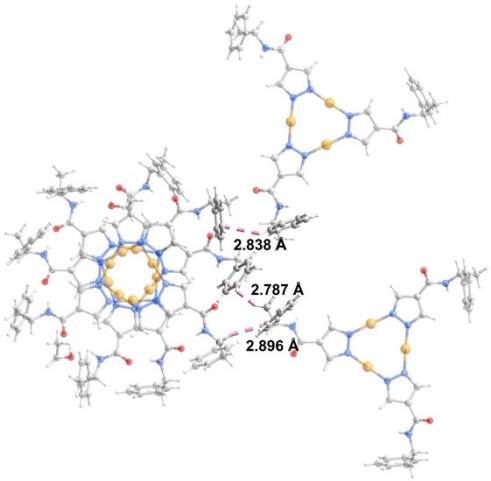


**Fig. S39** The pink dashed lines highlight C–H···π interactions in **R-1**. Colour codes: orange, Cu; grey, C; blue, N; red, O; white, H.

## 7. SEM images

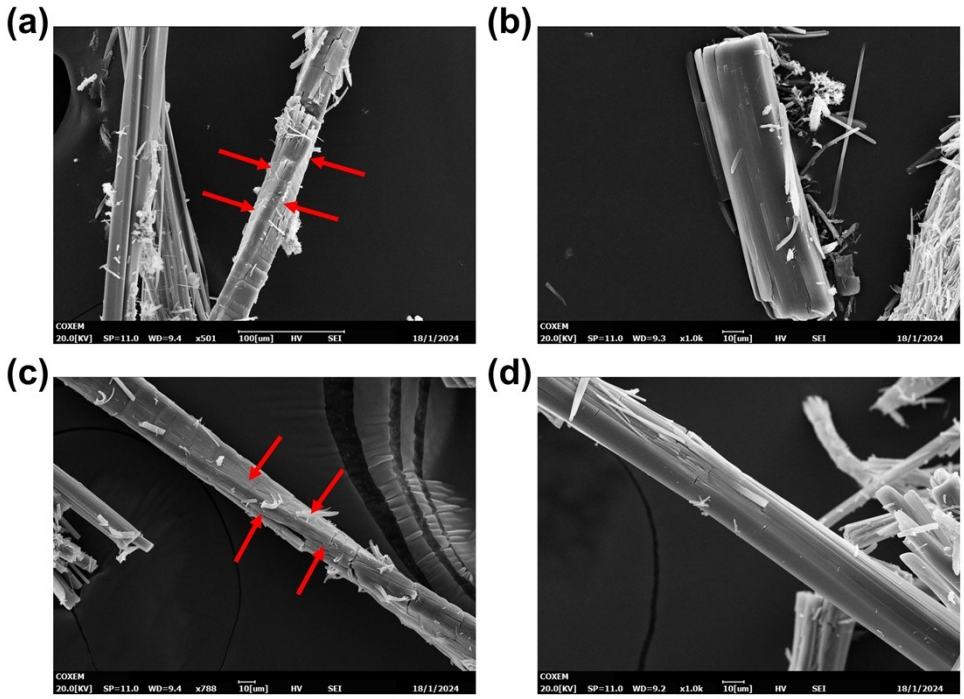


**Fig. S40** SEM images of (a, b) **R-1** and (c, d) **S-1.** In Figures a, c, the crystal of **R/S-1** show hierarchical chirality on the macroscopic scale. The chiral geometry may arise from the intrinsic crystal face position and their extrinsic differential growth, while uniform growth results in 'recessive chirality'.[3]

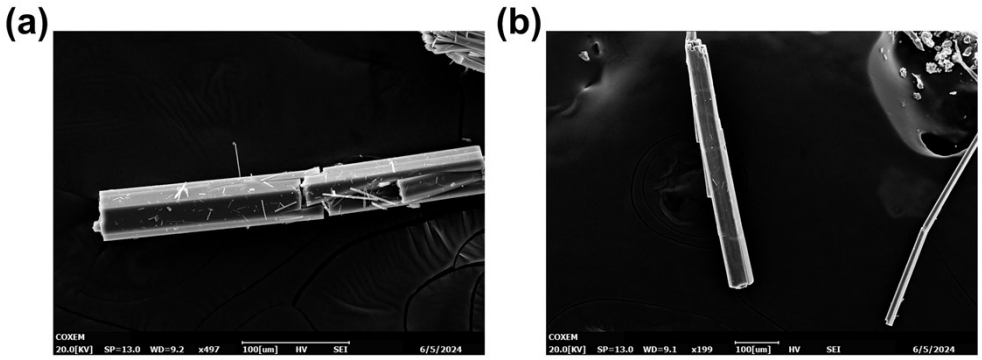


**Fig. S41** SEM images of (a) **R-2** and (b) **S-2**.

## 8. Photophysical Investigation

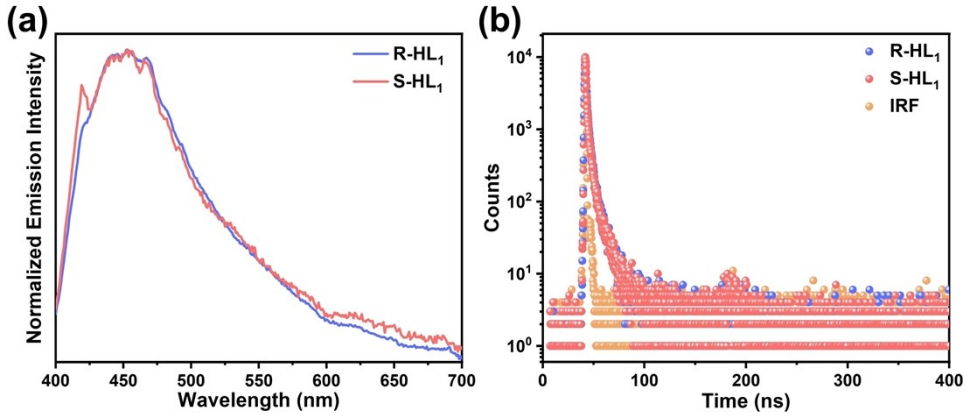


**Fig. S42** (a) Normalized emission spectra of R-$HL_1$/S-$HL_1$ when excited at 370 nm. (b) Emission decay profiles of R-$HL_1$/S-$HL_1$ ($\tau_{ave}$ = 0.27 ns for R-$HL_1$, $\tau_{ave}$ = 0.28 ns for S-$HL_1$). IRF: instrument response function.

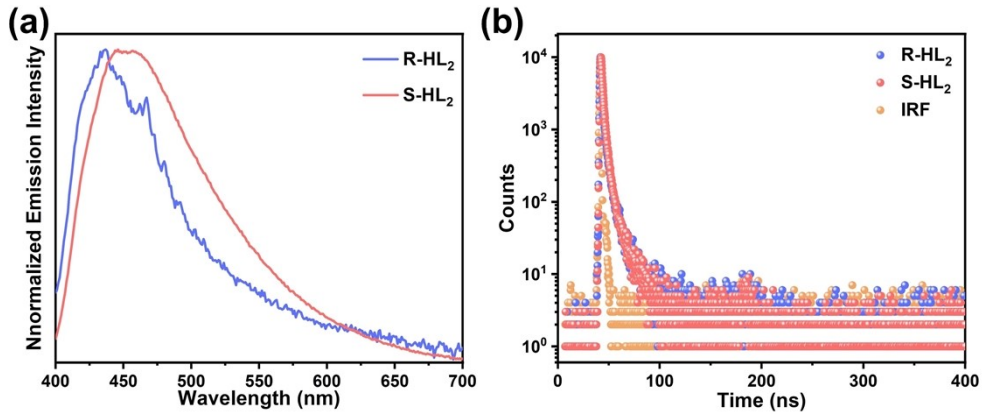


**Fig. S43** (a) Normalized emission spectra of R-$HL_2$/S-$HL_2$ when excited at 370 nm. (b) Emission decay profiles of R-$HL_2$/S-$HL_2$ ($\tau_{ave}$ = 0.53 ns for R-$HL_2$, $\tau_{ave}$ = 1.41 ns for S-$HL_2$). IRF: instrument response function.

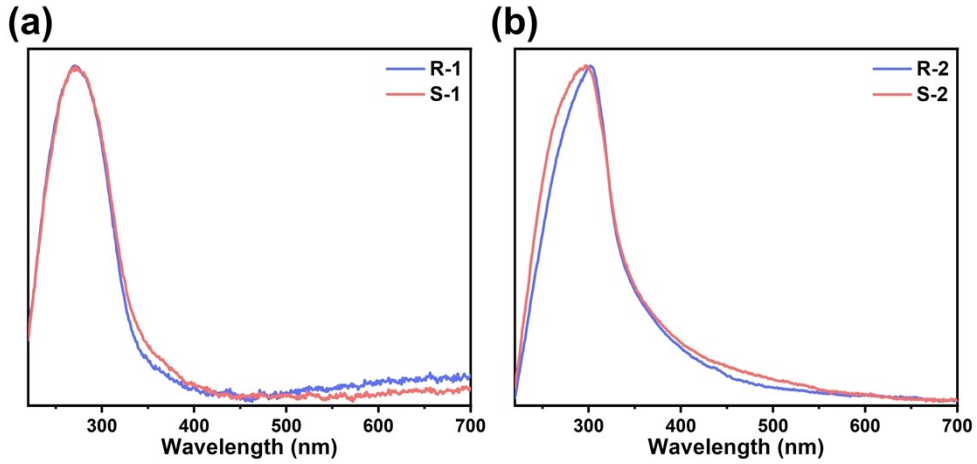


**Fig. S44** The normalized steady-state UV-vis absorption spectra of (a) **R-1**/**S-1** and (b) **R-2**/**S-2** in air at room temperature.

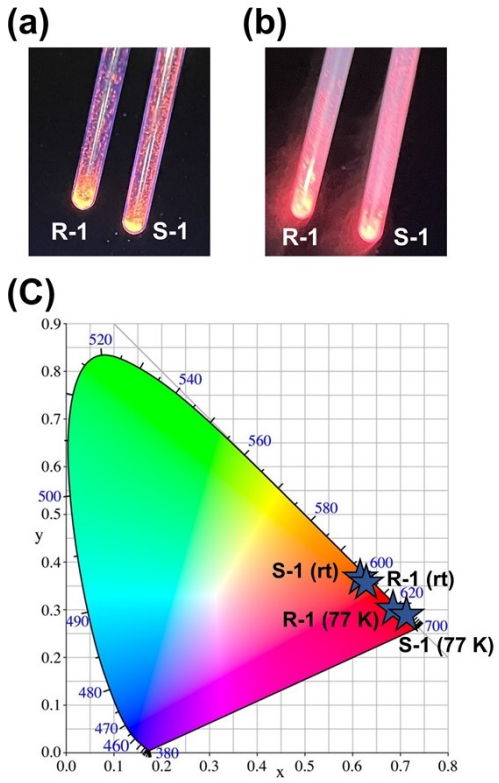


**Fig. S45** The photographs of **R-1** and **S-1** in NMR tubes under the UV-light excitation of 310 nm at (a) room temperature (rt) and (b) 77 K. (c) CIE chromaticity diagram of **R-1** and **S-1** under λ = 310 nm excitation wavelength at 77 K and rt.

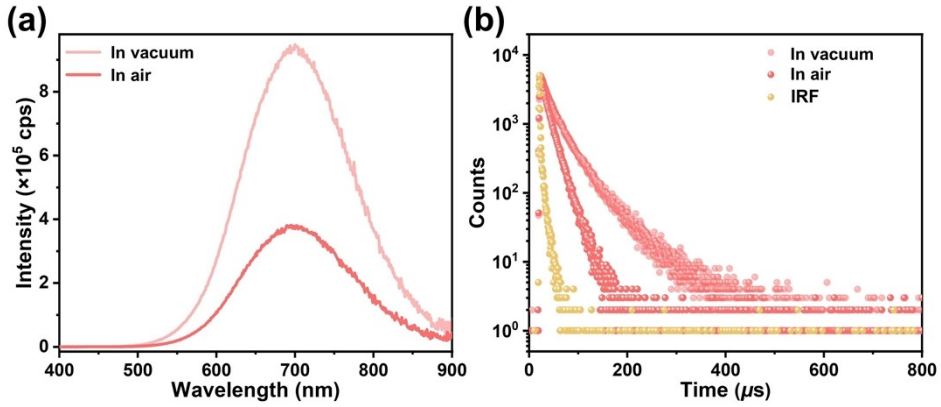


**Fig. S46** Comparison of (a) emission spectra and (b) lifetime decay curves of **S-1** in vacuum and air at room temperature. IRF: instrument response function.

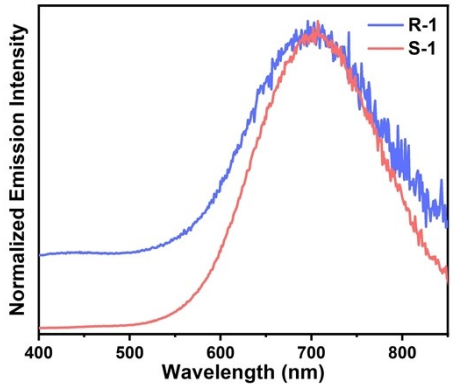


**Fig. S47** The normalized emission spectra of **R-1** and **S-1** when excited at 370 nm in air at room temperature.

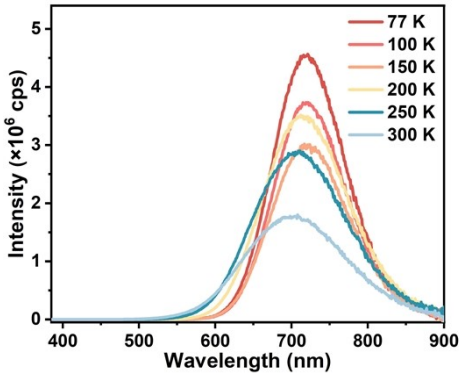


**Fig. S48** Temperature-dependent emission spectra ($\lambda_{ex}$ = 310 nm) of **R-1** in vacuum.

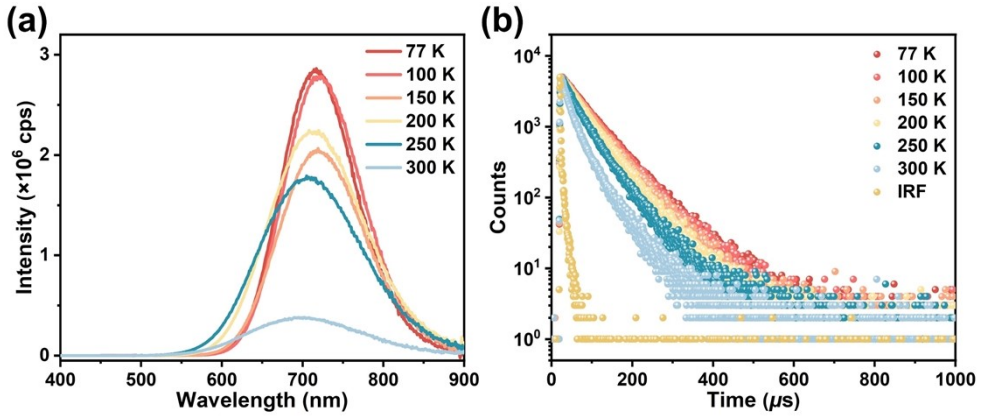


**Fig. S49** Temperature-dependent (a) emission spectra ($\lambda_{ex}$ = 310 nm) and (b) lifetime decay curves of **S-1** in vacuum. IRF: instrument response function.

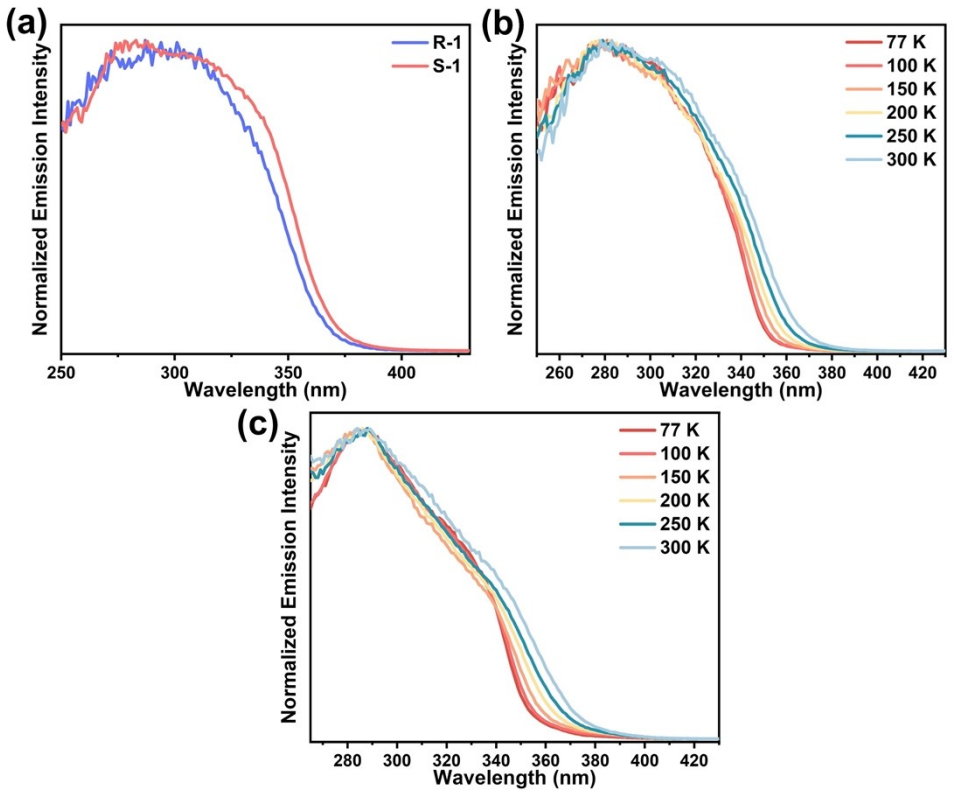


**Fig. S50** (a) The normalized excitation spectra of **R-1** and **S-1** in air at room temperature. Temperature-dependent normalized excitation spectra of (b) **R-1** and (c) **S-1** in vacuum.

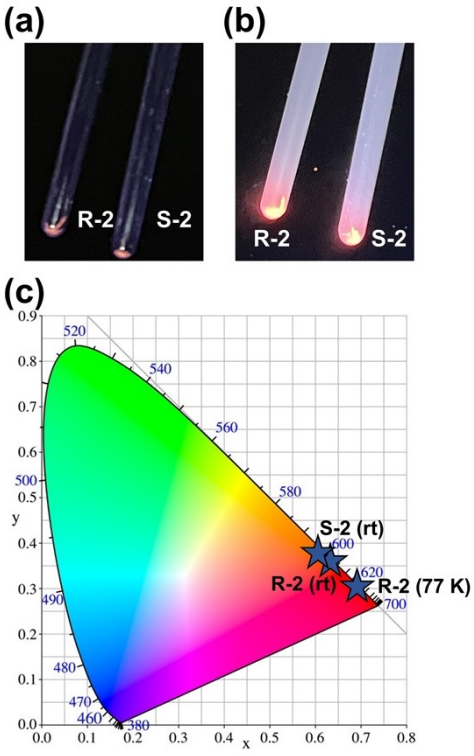


**Fig. S51** The photographs of **R-2** and **S-2** in NMR tubes under the UV-light excitation of 310 nm at (a) room temperature (rt) and (b) 77 K. (c) CIE chromaticity diagram of **R-2** and **S-2** under λ = 310 nm excitation wavelength at 77 K and rt.

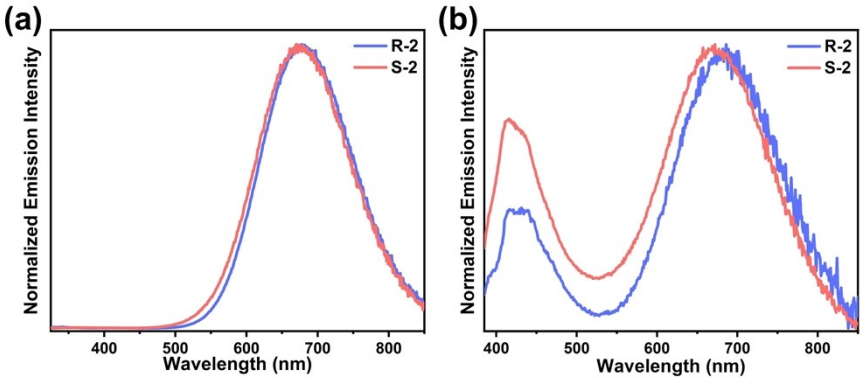


**Fig. S52** The normalized emission spectra of **R-2** and **S-2** when excited at (a) 310 nm and (b) 370 nm in air at room temperature.

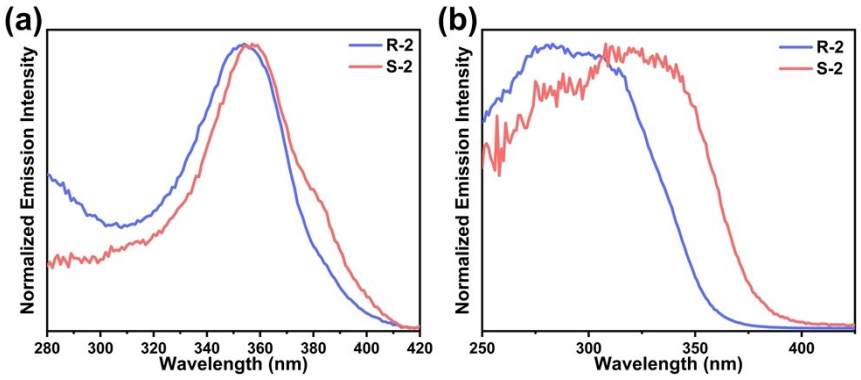


**Fig. S53** The excitation spectra of (a) high-energy emission and (b) low-energy emission of **R-2** and **S-2** in air at room temperature.

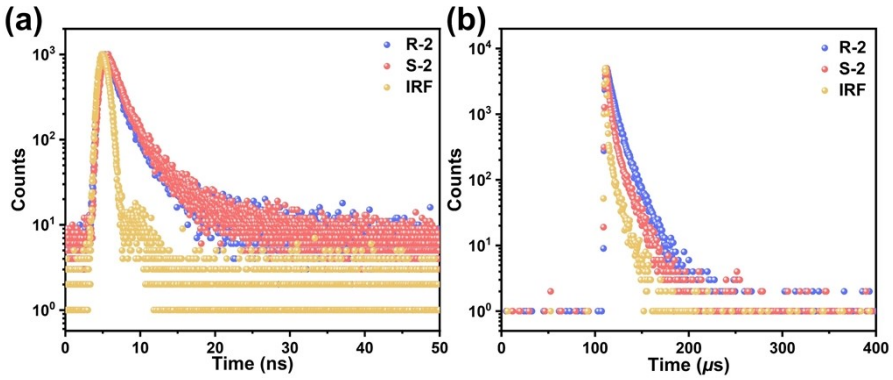


**Fig. S54** Emission decay profiles of (a) high-energy emission and (b) low-energy emission of **R-2** and **S-2** in air at room temperature. IRF: instrument response function.

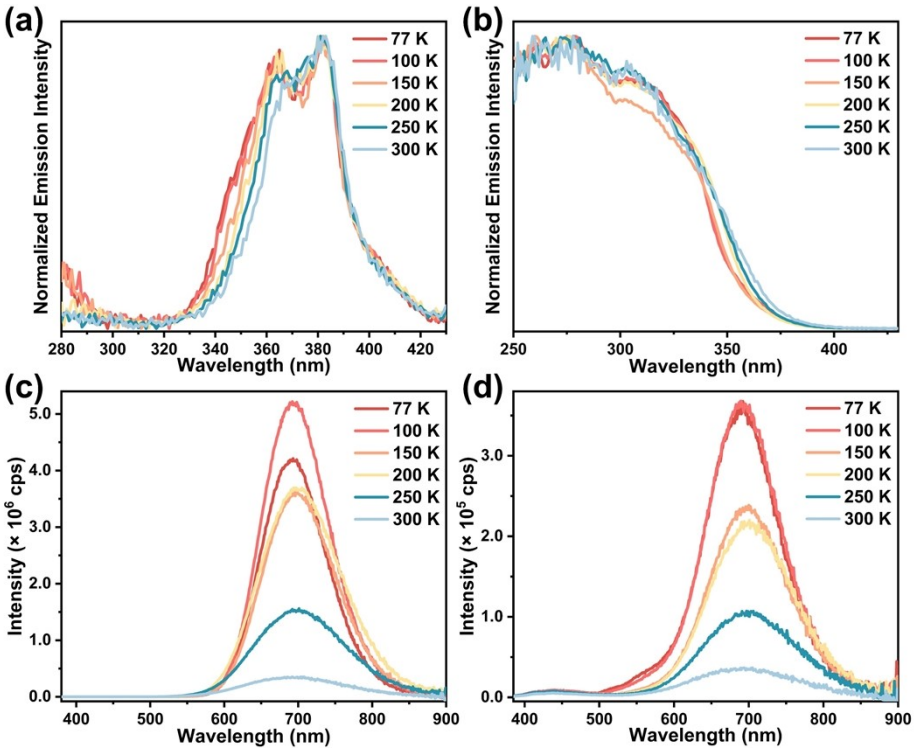


**Fig. S55** Temperature-dependent normalized excitation spectra of (a) high-energy emission and (b) low-energy emission of **R-2** in vacuum. Temperature-dependent emission spectra of **R-2** when excited at (c) 310 nm and (d) 370 nm in vacuum.

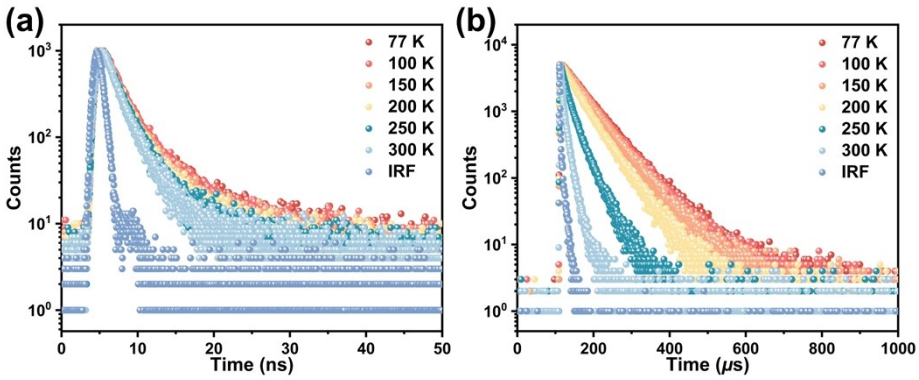


**Fig. S56** Temperature-dependent emission decay profiles of (a) high-energy emission and (b) low-energy emission of **R-2** in vacuum. IRF: instrument response function.

**Table S5** The summary of photophysical data of **R-1**, **S-1**, **R-2** and **S-2** in air at room temperature.

| | $\lambda_{Abs}$ (nm) | $\lambda_{Ex}$ (nm) | $\lambda_{Em}$ (nm) | $\tau_{ave}$ | $\Phi$ (%) |
|---|---|---|---|---|---|
| **R-1** | 272 | 294 | 699 | 12.27 $\mu$s | 21.7 |
| **S-1** | 271 | 290 | 700 | 14.23 $\mu$s | 26.6 |
| **R-2** | 302 | 354 | 426 | 2.27 ns | 13.2 |
| | | 300 | 680 | 6.24 $\mu$s | |
| **S-2** | 298 | 358 | 424 | 2.36 ns | 12.9 |
| | | 314 | 677 | 3.67 $\mu$s | |

**Table S6** The summary of photophysical data of **R-1** at different temperatures between 77 K and 300 K in vacuum.

| T (K) | $\lambda_{Ex}$ (nm) | $\lambda_{Em}$ (nm) | $\tau_{ave}$ ($\mu$s) |
|---|---|---|---|
| 77 | 287 | 719 | 63.82 |
| 100 | 290 | 718 | 64.25 |
| 150 | 287 | 722 | 59.46 |
| 200 | 288 | 716 | 55.21 |
| 250 | 288 | 708 | 48.30 |
| 300 | 291 | 702 | 41.04 |

**Table S7** The summary of photophysical data of **S-1** at different temperatures between 77 K and 300 K in vacuum.

| T (K) | $\lambda_{Ex}$ (nm) | $\lambda_{Em}$ (nm) | $\tau_{ave}$ ($\mu$s) |
|---|---|---|---|
| 77 | 288 | 717 | 62.32 |
| 100 | 288 | 718 | 60.48 |
| 150 | 288 | 717 | 57.42 |
| 200 | 289 | 714 | 56.03 |
| 250 | 289 | 706 | 45.42 |
| 300 | 290 | 700 | 37.12 |

**Table S8** The summary of photophysical data of **R-2** at different temperatures between 77 K and 300 K in vacuum.

| T (K) | $\lambda_{Ex}$ (nm) | $\lambda_{Em}$ (nm) | $\tau_{ave}$ |
|---|---|---|---|
| 77 | 381 | 440 | 3.07 ns |
| | 281 | 694 | 61.63 $\mu$s |
| 100 | 382 | 439 | 2.90 ns |
| | 280 | 694 | 59.65 $\mu$s |
| 150 | 382 | 440 | 2.70 ns |
| | 276 | 696 | 56.18 $\mu$s |
| 200 | 381 | 441 | 2.46 ns |
| | 278 | 700 | 46.29 $\mu$s |
| 250 | 381 | 440 | 2.25 ns |
| | 281 | 697 | 25.80 $\mu$s |
| 300 | 382 | 440 | 2.00 ns |
| | 280 | 696 | 7.92 $\mu$s |

**Table S9** The luminescence lifetimes of **R-1**, **S-1**, **R-2** and **S-2** in air at room temperature.

| | Lifetime 1 ($\tau_1$) | Lifetime 2 ($\tau_2$) | $\tau_1$% | $\tau_2$% |
|---|---|---|---|---|
| **R-1** | 3.39 $\mu$s | 15.16 $\mu$s | 24.57 | 75.43 |
| **S-1** | 4.73 $\mu$s | 17.74 $\mu$s | 26.94 | 73.06 |
| **R-2** | 1.17 ns | 5.24 ns | 72.94 | 27.06 |
| | 3.70 $\mu$s | 10.14 $\mu$s | 60.51 | 39.49 |
| **S-2** | 1.27 ns | 5.30 ns | 72.82 | 27.18 |
| | 2.42 $\mu$s | 10.67 $\mu$s | 84.78 | 15.22 |

**Table S10** The luminescence lifetimes of **R-1** at different temperatures between 77 K and 300 K in vacuum.

| T (K) | Lifetime 1 ($\tau_1$/$\mu$s) | Lifetime 2 ($\tau_2$/$\mu$s) | $\tau_1$% | $\tau_2$% |
|---|---|---|---|---|
| 77 | 17.62 | 69.12 | 10.30 | 89.70 |
| 100 | 23.94 | 69.29 | 11.11 | 88.89 |
| 150 | 18.44 | 63.97 | 9.89 | 90.11 |
| 200 | 17.80 | 60.25 | 11.86 | 88.14 |
| 250 | 15.15 | 55.45 | 17.74 | 82.26 |
| 300 | 10.88 | 51.26 | 25.30 | 74.70 |

**Table S11** The luminescence lifetimes of **S-1** at different temperatures between 77 K and 300 K in vacuum.

| T (K) | Lifetime 1 ($\tau_1$/$\mu$s) | Lifetime 2 ($\tau_2$/$\mu$s) | $\tau_1$% | $\tau_2$% |
|---|---|---|---|---|
| 77 | 19.07 | 66.53 | 8.88 | 91.12 |
| 100 | 14.54 | 64.51 | 8.07 | 91.93 |
| 150 | 13.60 | 60.43 | 6.42 | 93.58 |
| 200 | 12.01 | 56.03 | 6.63 | 93.37 |
| 250 | 18.14 | 53.97 | 23.87 | 76.13 |
| 300 | 13.28 | 56.74 | 45.14 | 54.86 |

**Table S12** The luminescence lifetimes of high-energy emission of **R-2** at different temperatures between 77 K and 300 K in vacuum.

| T (K) | Lifetime 1 ($\tau_1$/ns) | Lifetime 2 ($\tau_2$/ns) | $\tau_1$% | $\tau_2$% |
|---|---|---|---|---|
| 77 | 1.69 | 6.88 | 73.39 | 26.61 |
| 100 | 1.67 | 6.35 | 73.68 | 26.32 |
| 150 | 1.59 | 5.88 | 74.24 | 25.76 |
| 200 | 1.54 | 5.35 | 75.78 | 24.22 |
| 250 | 1.48 | 5.07 | 78.87 | 21.13 |
| 300 | 1.36 | 4.33 | 78.14 | 21.86 |

**Table S13** The luminescence lifetimes of low-energy emission of **R-2** at different temperatures between 77 K and 300 K in vacuum.

| T (K) | Lifetime 1 ($\tau_1$/$\mu$s) | Lifetime 2 ($\tau_2$/$\mu$s) | $\tau_1$% | $\tau_2$% |
|---|---|---|---|---|
| 77 | 47.04 | 75.83 | 49.31 | 50.69 |
| 100 | 45.39 | 71.62 | 45.64 | 54.36 |
| 150 | 32.42 | 61.79 | 19.09 | 80.91 |
| 200 | 17.81 | 50.78 | 13.63 | 86.37 |
| 250 | 15.17 | 35.46 | 47.59 | 52.41 |
| 300 | 3.42 | 13.41 | 54.92 | 45.08 |

## 9. Computational Details and Results

To give insight into the phtotophyscial process of **R-1**, density functional theory (DFT) and time-dependent DFT (TDDFT) calculations were performed using the Gaussian 09 software package.[4] At the same time, the Multiwfn 3.8 software packages[5] were further used for wave function analysis. For simulating the UV-vis absorption spectrum and exploring the insight of the emissive state, the dimer models of **R-1** were adopted. The geometry optimizations of ground and the first triplet excited states ($S_0$ and $T_1$ states) were carried out using the PBE0[6,7]-D3[8](BJ)[9] functional together with effective core potential (ECP) of LanL2dz basis set[10,11] was used for Cu atoms, while the 6-31G** basis set[12,13] was used for other atoms. Furthermore, the optimized $S_0$ dimer were also used for the geometry optimizations of excited state ($T_1$), with all atoms except two nine-membered rings were fixed. After geometrical optimization, frequency calculations were conducted to confirm that the optimized geometries are stable structures, as indicated by the absence of imaginary frequency. To obtain the simulated UV-vis spectrum, first 50 spin-allowed transitions were calculated based on optimized $S_0$ dimer. Meanwhile, the 10 spin-forbidden transitions were also obtained with optimized triplet state ($T_1$) structure. For accurately assigning excited state of **R-1**, electron density difference (EDD) maps (isovalue = $5.0\times10^{-4}$ a.u.) were generated. The blue- and purple- regions represent electron transfer from former to latter when excitation.

The colour-filled surfaces of independent gradient model based on the Hirshfeld partition (IGMH) method[14] were drawn by VMD 1.93 program[15] for the selected dimer models based on the optimized dimer model generated by Multiwfn 3.8 software.

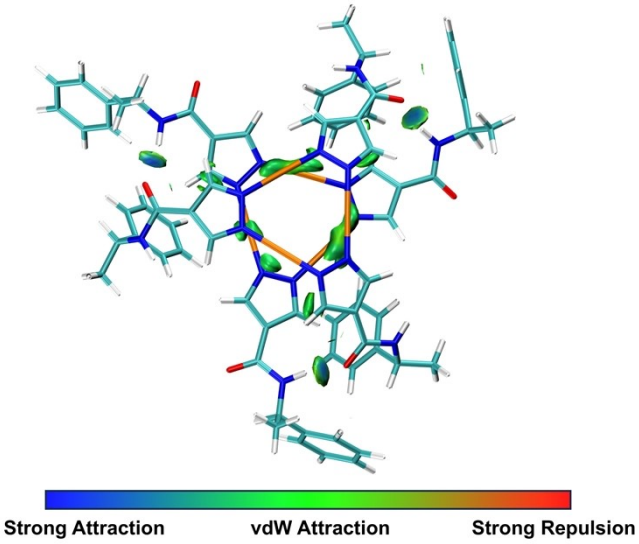


**Fig. S57** IGMH analysis (isovalue = 0.01 a.u.) of two neighboring Cu(I) CTC molecules in **R-1**. The blue IGMH surfaces represents the prospective adaptive weak interaction, the green IGMH surfaces represents the van der Waals interaction. Colour codes: orange, Cu; cyan, C; blue, N; red, O; white, H.

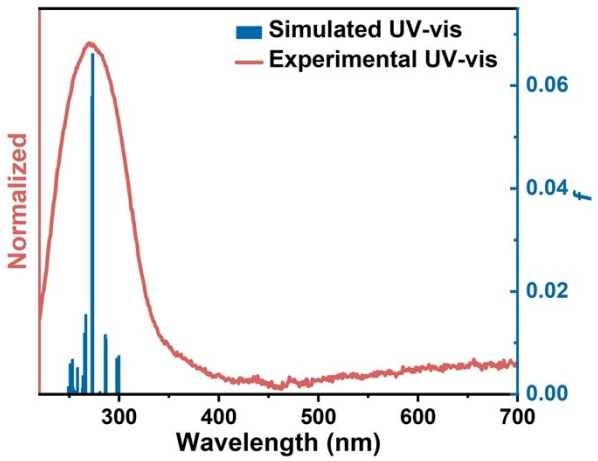


**Fig. S58** The experiment solid-state UV-vis spectrum and the simulated absorption of the dimer of **R-1**. *f*: oscillator strength.

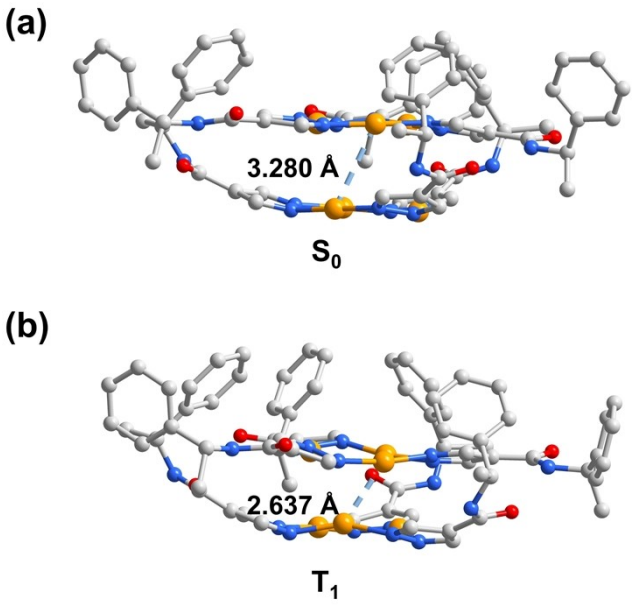


**Fig. S59** Dimer of **R-1** in optimized (a) $S_0$ and (b) $T_1$ structure. Colour codes: orange, Cu; grey, C; blue, N; red, O.

**Table S14** TDDFT result of selected $S_0 \rightarrow S_n$ transition for dimer of **R-1** in $S_0$ geometry

| No. | λ (nm) | E (eV) | *f* | EDD | | Assignment |
|---|---|---|---|---|---|---|
| | | | | Top view | Side view | |
| 1 | 299.8 | 4.14 | 0.01 | 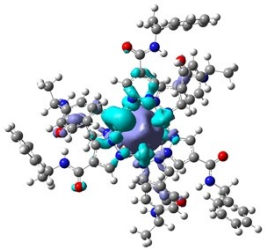 | 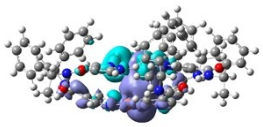 | $^1$LMMCT |
| 6 | 273.5 | 4.53 | 0.07 | 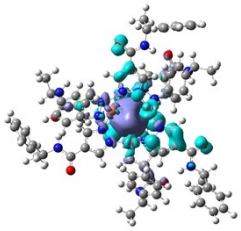 | 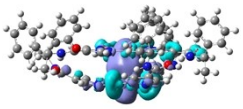 | $^1$LMMCT |
| 7 | 272.8 | 4.55 | 0.06 | 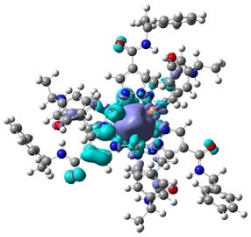 | 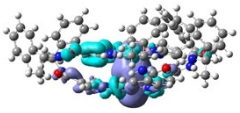 | $^1$LMMCT |

**Table S15** TDDFT result of the $S_0 \rightarrow T_1$ transition for the dimer of **R-1** at the optimized $T_1$ geometry.

| No. | λ (nm) | E (eV) | EDD | | Assignment |
|---|---|---|---|---|---|
| | | | Top view | Side view | |
| 1 | 524.1 | 2.37 | 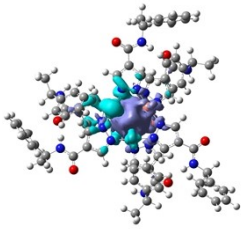 | 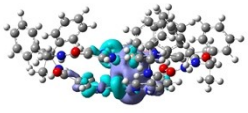 | $^1$LMMCT |

## 10. CD and CPL

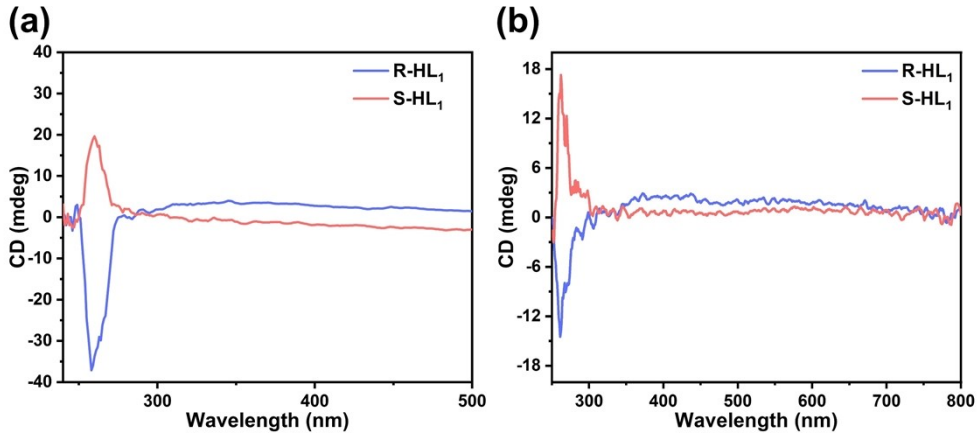


**Fig. S60** CD spectra of R-$HL_1$/S-$HL_1$ in (a) MeOH solution and (b) KBr disk.

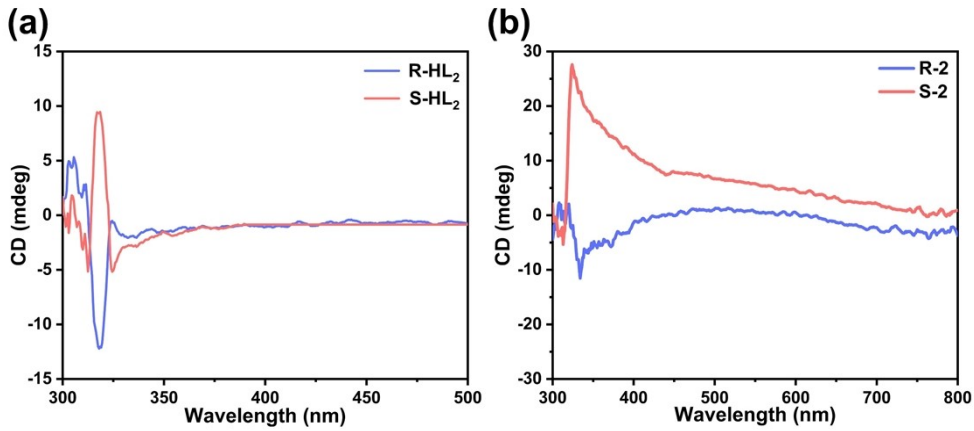


**Fig. S61** (a) CD spectra of R-$HL_2$/S-$HL_2$ in MeOH. (b) CD spectra of **R-2** and **S-2** in solid.

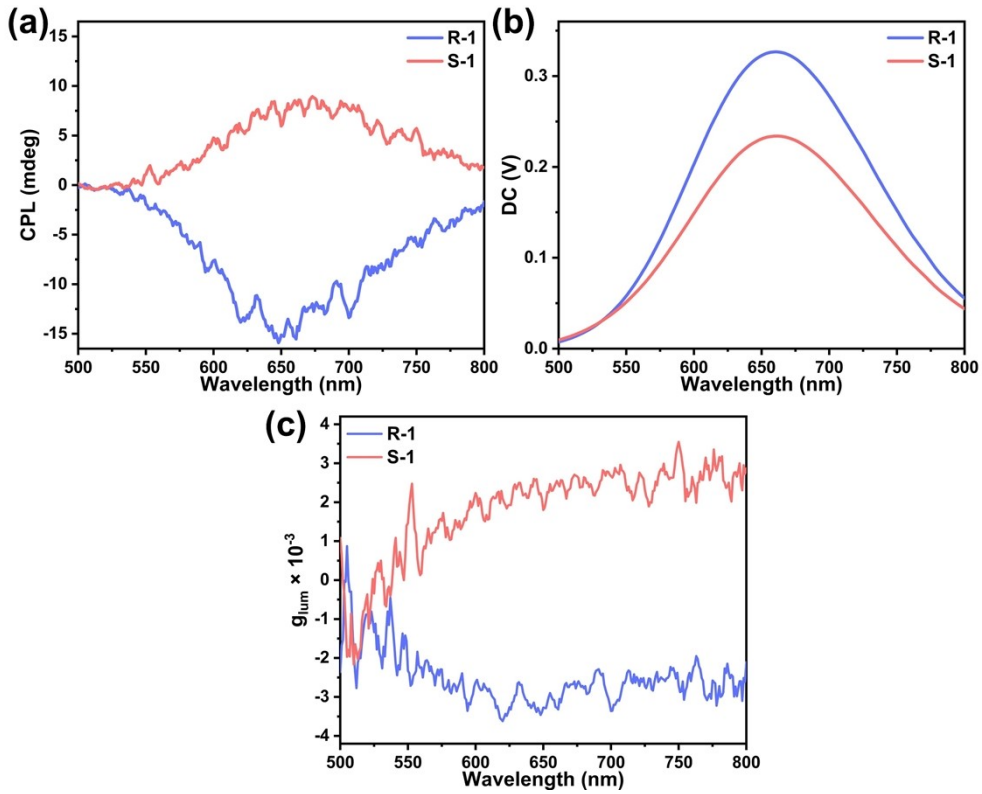


**Fig. S62** The (a) CPL spectra, (b) DC spectra and (c) $g_{lum}$ spectra of **R-1** and **S-1** in powder state with low-crystallinity upon excitation at 305 nm.

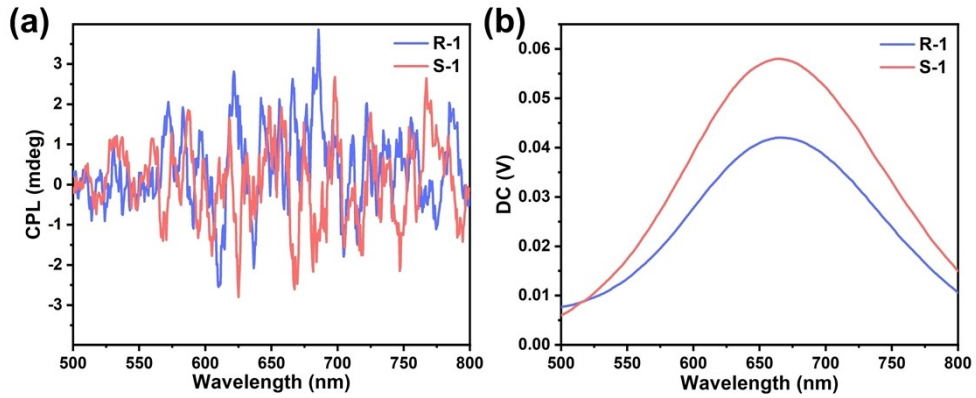


**Fig. S63** The (a) CPL spectra and (b) DC spectra of **R-1** and **S-1** in powder state with non-crystallinity upon excitation at 305 nm.

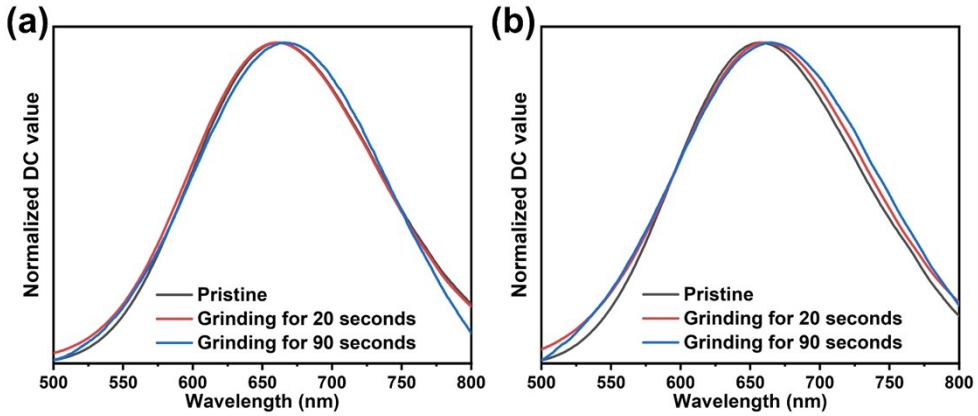


**Fig. S64** The normalized DC spectra of (a) **R-1** and (b) **S-1** before grinding, after grinding for 20 seconds (red line) with low-crystallinity and further grinding for 70 seconds (bule line) with non-crystallinity. These indicate that grinding does not cause changes in the emission wavelength of **R-1**/**S-1**.

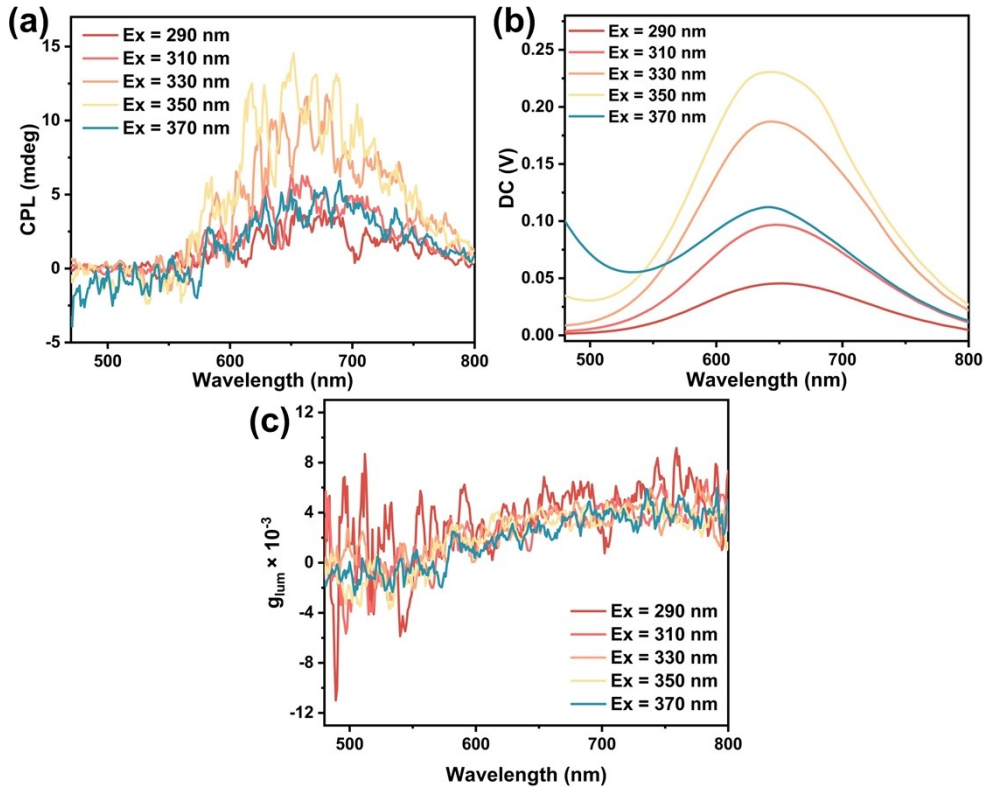


**Fig. S65** (a) CPL emission spectra, (b) DC spectra and (c) $g_{lum}$ spectra of **R-2** in crystal state upon different excitation wavelengths.

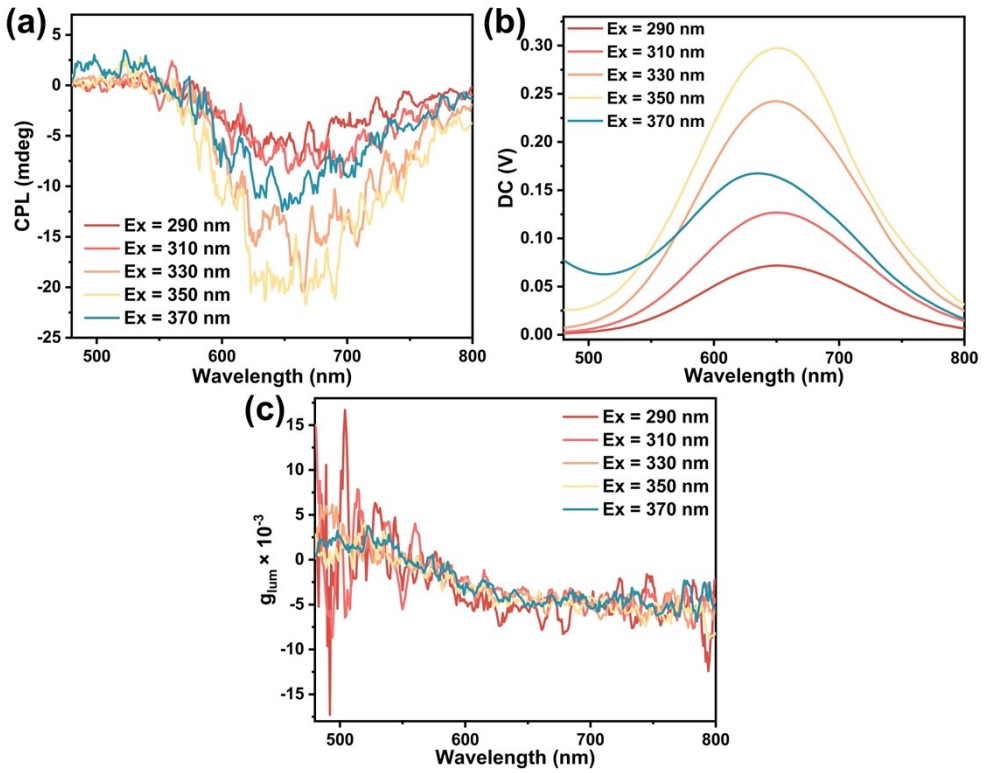


**Fig. S66** (a) CPL emission spectra, (b) DC spectra and (c) $g_{lum}$ spectra of **S-2** in crystal state upon different excitation wavelengths.

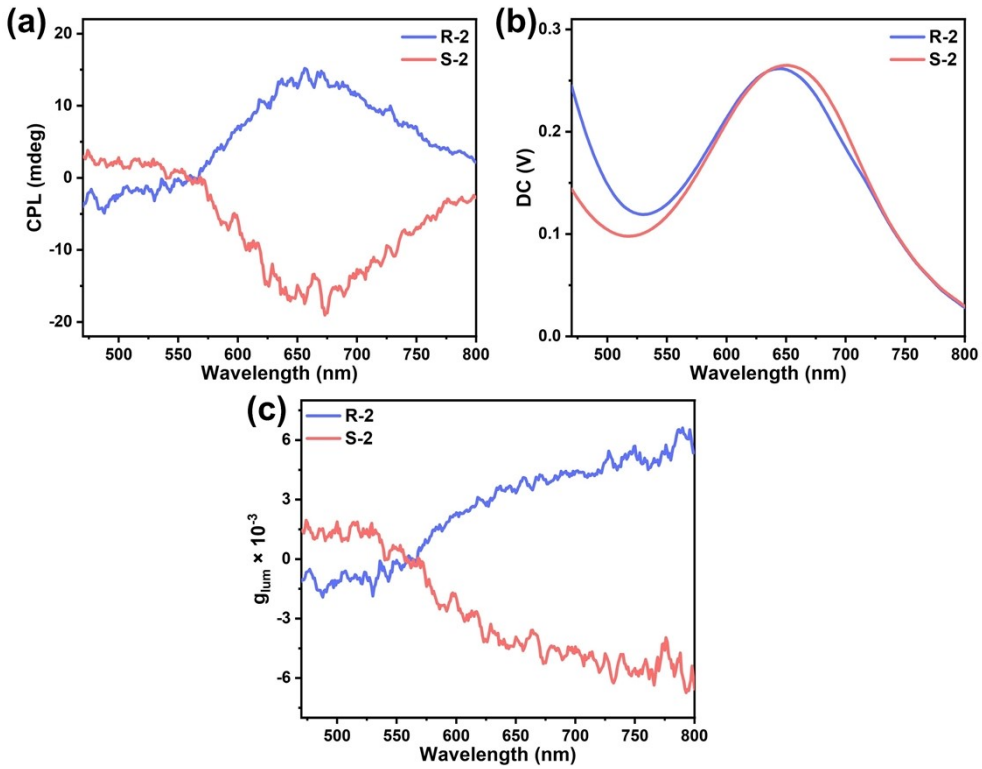


**Fig. S67** (a) CPL spectra, (b) DC value and (c) $g_{lum}$ spectra of **R-2** and **S-2** in crystal state upon excitation at 370 nm. The $|g_{lum}|$ values of **R/S-2** were smaller than those of **R/S-1**, which might be attributed to the poor crystallinity of **R/S-2**.[16]

## 11. Crystal structures modeling of R/S-2

The crystal structures of **R-2/S-2** were analyzed by PXRD experiments combined with theoretical simulations performed in the Materials Studio software package. Simulations of structures similar to **R/S-1**, but with naphthyl groups replacing phenyl groups, were generated. Pawley refinements based on the corresponding stacking mode of **R-2** were performed to give monoclinic space group of $P2_1$ with unit cell parameters of a = 10.6917 Å, b = 20.2477 Å, c = 36.5749 Å, β = 104.4867°, and refinement parameters of $R_p$ = 0.90% and $wR_p$ = 1.50%. Similarly, Pawley refinements based on the corresponding stacking mode of **S-2** were performed to give monoclinic space group of $P2_1$ with unit cell parameters of a = 9.9287 Å, b = 20.9692 Å, c = 35.7146 Å, β = 91.3000°, and refinement parameters of $R_p$ = 1.51% and $wR_p$ = 3.90%. The resulting refined PXRD patterns are in good agreement with the experimental data, as confirmed by the negligible difference curve (Figures S72).

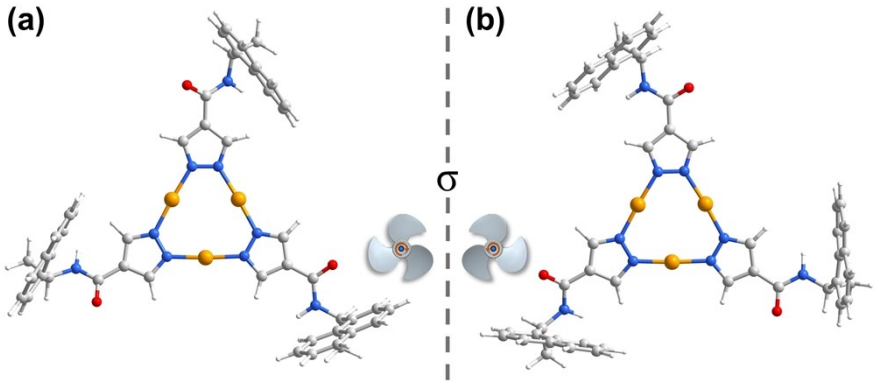


**Fig. S68** Molecular structure models of (a) **R-2** and (b) **S-2**. Colour codes: orange, Cu; grey, C; blue, N; red, O; white, H.

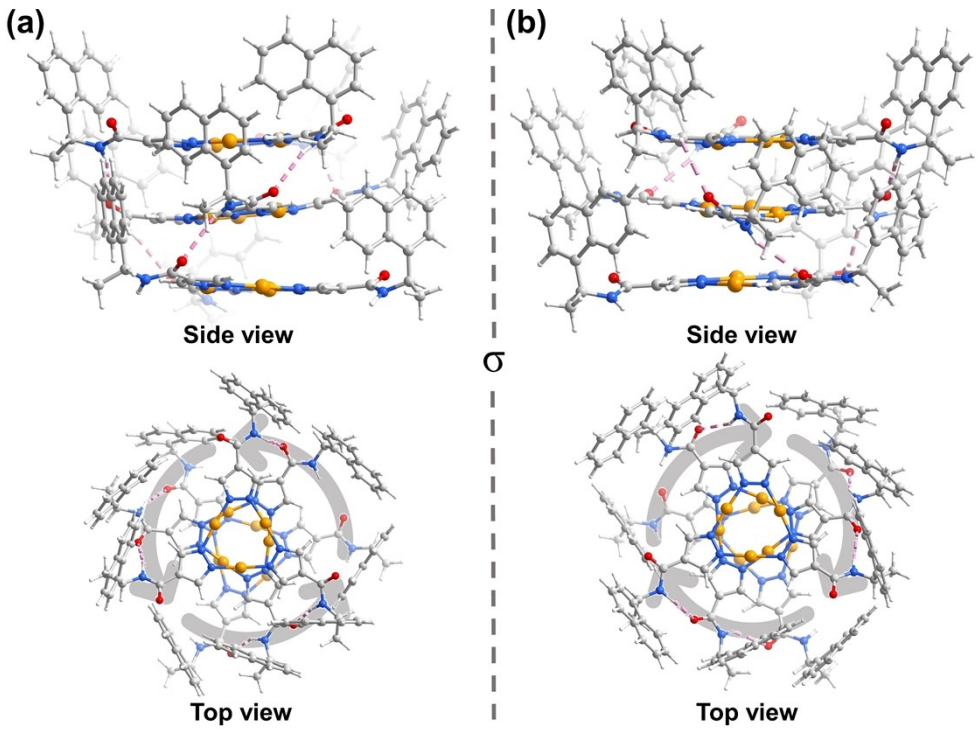


**Fig. S69** Structure of stacking models of (a) **R-2** and (b) **S-2**. The pink dashed lines highlight hydrogen-bonding interactions. Colour codes: orange, Cu; grey, C; blue, N; red, O; white, H.

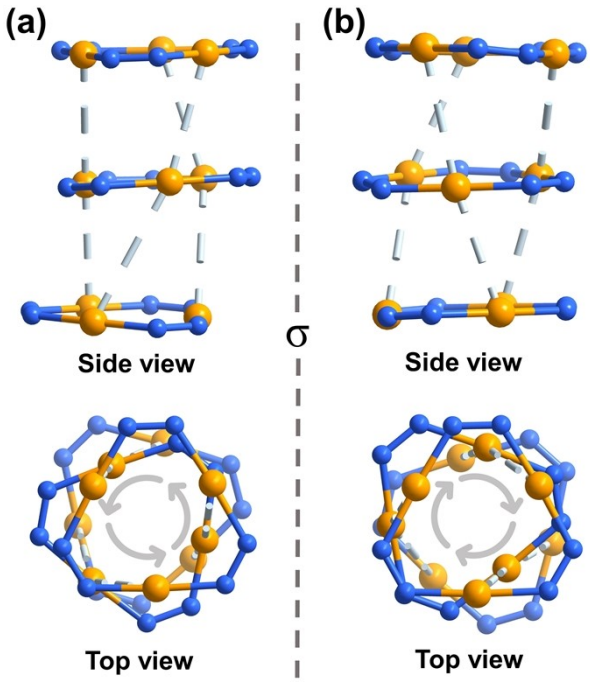


**Fig. S70** Stacking model of $Cu_3$ planes in (a) **R-2** and (b) **S-2**. The blue dashed lines highlight intermolecular Cu···Cu interactions. Colour codes: orange, Cu; blue, N.

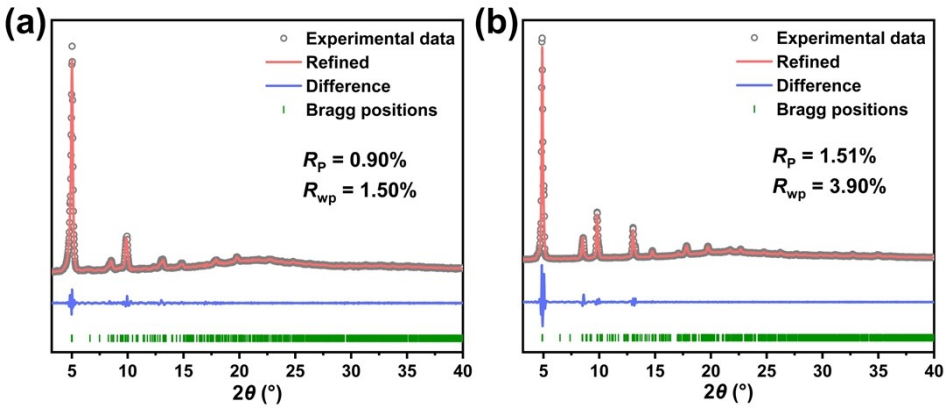


**Fig. S71** PXRD structural analysis of (a) **R-2** and (b) **S-2**.

**Table S16** Parameter of Spiral stacking model for **R-2**.

| Crystal system | | | | monoclinic | | | |
|---|---|---|---|---|---|---|---|
| Space group | | | | $P2_1$ | | | |
| Unit Cell | | | | a = 10.6917 Å, b = 20.2477 Å, c = 36.5749 Å, β = 104.4867° | | | |
| Atom | x | y | z | Atom | x | y | z |
| Cu1 | 0.5227 | 0.28965 | 0.02884 | C159 | 0.35983 | 1.32499 | 0.66103 |
| Cu2 | 0.60831 | 0.58926 | 0.25929 | C160 | 0.23863 | 1.30098 | 0.66158 |
| Cu3 | 1.25187 | 0.56937 | 0.21752 | C161 | 0.175 93 | 1.32402 | 0.68821 |
| Cu4 | 0.87897 | 0.37113 | 0.2556 | C162 | 0.58034 | 1.33565 | 0.82228 |
| Cu5 | 0.85188 | 0.5002 | 0.19594 | C163 | 0.63555 | 1.32747 | 0.79182 |
| Cu6 | 0.58976 | 0.43102 | 0.28434 | C164 | 0.76686 | 1.33842 | 0.79624 |
| Cu7 | 1.28069 | 0.48189 | 0.297 | C165 | 0.84382 | 1.35864 | 0.83105 |
| Cu8 | 0.50863 | 0.4725 | 0.19233 | C166 | 0.22277 | 0.70946 | 0.60692 |
| Cu9 | 1.20037 | 0.40515 | 0.21285 | C167 | 0.32831 | 0.68752 | 0.63493 |
| O10 | 0.96659 | 0.39502 | 0.43327 | C168 | 0.45151 | 0.68842 | 0.62897 |
| O11 | 1.29465 | 0.7931 | 0.32204 | C169 | 0.47134 | 0.713 | 0.59531 |
| O12 | 0.41833 | 0.16802 | 0.22983 | C170 | 1.26146 | 0.59128 | 0.72362 |
| O13 | 1.03008 | 0.46084 | 0.0504 | C171 | 1.25454 | 0.61316 | 0.75917 |
| O14 | 0.41956 | 0.70542 | 0.09203 | C172 | 1.13501 | 0.62269 | 0.76694 |
| O15 | 0.61877 | 0.22477 | 0.12234 | C173 | 1.02121 | 0.61103 | 0.73919 |
| O16 | 0.86849 | 0.78975 | 0.19347 | C174 | 1.1111 | 0.62225 | 0.87365 |
| O17 | 0.66355 | 0.63011 | 0.42227 | C175 | 1.11176 | 0.67735 | 0.89646 |
| O18 | 1.19772 | 0.21996 | 0.35484 | C176 | 0.99603 | 0.70595 | 0.89905 |
| N19 | 1.14183 | 0.55495 | 0.05021 | C177 | 0.87833 | 0.67806 | 0.88012 |
| N20 | 0.98327 | 0.80597 | 0.25319 | C178 | 0.54383 | 0.89045 | 0.99979 |
| N21 | 0.4051 | 0.18135 | 0.16797 | C179 | 0.57523 | 0.94632 | 1.02259 |
| N22 | 0.75562 | 0.53216 | 0.44185 | C180 | 0.7037 | 0.96343 | 1.03788 |
| N23 | 1.40128 | 0.7404 | 0.3748 | C181 | 0.80189 | 0.92465 | 1.03043 |
| N26 | 1.02016 | 0.29265 | 0.41882 | C182 | 0.99818 | 1.17857 | 0.93363 |
| N27 | 1.23489 | 0.16093 | 0.30656 | C183 | 1.03094 | 1.22181 | 0.90779 |
| N28 | 0.56664 | 0.77204 | 0.12914 | C184 | 1.15989 | 1.23325 | 0.90858 |
| N29 | 0.52529 | 0.56495 | 0.17939 | C185 | 1.25723 | 1.20164 | 0.93533 |
| N30 | 1.20831 | 0.52233 | 0.16972 | C186 | 0.70068 | 0.94319 | 0.54179 |
| N32 | 0.49653 | 0.38172 | 0.20888 | C187 | 0.67316 | 0.89571 | 0.56622 |
| N34 | 0.81485 | 0.36064 | 0.20129 | C188 | 0.55063 | 0.89248 | 0.57268 |
| N36 | 0.59346 | 0.3045 | 0.07819 | C189 | 0.45389 | 0.93595 | 0.55441 |
| N40 | 1.18547 | 0.45822 | 0.16768 | H190 | 1.21937 | 0.58367 | 0.06498 |
| N41 | 0.53023 | 0.36561 | 0.24494 | H191 | 1.04746 | 0.78489 | 0.27657 |
| N42 | 0.94761 | 0.59505 | 0.25415 | H192 | 0.41506 | 0.21343 | 0.14655 |
| N43 | 0.97026 | 0.44728 | 0.3229 | H193 | 0.80249 | 0.49107 | 0.43422 |
| N44 | 0.64726 | 0.56281 | 0.3121 | H194 | 1.4541 | 0.69832 | 0.38571 |
| N46 | 1.30959 | 0.57651 | 0.29806 | H195 | 1.05336 | 0.26351 | 0.39962 |

***Table S16 continued***

| Atom | x | y | z | Atom | x | y | z |
|---|---|---|---|---|---|---|---|
| N50 | 1.24873 | 0.38756 | 0.29288 | H196 | 1.26136 | 0.16235 | 0.28093 |
| N55 | 0.80226 | 0.41125 | 0.17793 | H197 | 0.64578 | 0.77396 | 0.15254 |
| N57 | 0.9039 | 0.58685 | 0.21738 | H198 | 0.61158 | 0.35342 | 0.07233 |
| N62 | 0.9417 | 0.38722 | 0.30947 | H199 | 0.66637 | 0.44949 | 0.37445 |
| N65 | 0.56695 | 0.61004 | 0.20564 | H200 | 0.45245 | 0.08205 | 0.17853 |
| N70 | 1.21826 | 0.35726 | 0.25993 | H201 | 1.15886 | 0.05702 | 0.38681 |
| N75 | 0.64576 | 0.50015 | 0.32171 | H202 | 0.67031 | 0.65402 | 0.34354 |
| N95 | 1.29466 | 0.61141 | 0.26683 | H203 | 1.01556 | 0.48919 | 0.3788 |
| C24 | 1.10424 | 0.50198 | 0.06822 | H204 | 0.71367 | 0.4242 | 0.11888 |
| C25 | 0.68488 | 0.5586 | 0.3742 | H205 | 1.1942 | 0.59921 | 0.1285 |
| C31 | 0.63863 | 0.28171 | 0.1145 | H206 | 0.97808 | 0.89771 | 0.22692 |
| C33 | 0.50027 | 0.7136 | 0.12181 | H207 | 0.41871 | 0.32722 | 0.15779 |
| C35 | 0.92607 | 0.7659 | 0.22357 | H208 | 1.27379 | 0.35538 | 0.35031 |
| C37 | 0.6688 | 0.49522 | 0.35936 | H209 | 0.50922 | 0.21279 | 0.05775 |
| C38 | 0.37712 | 0.11138 | 0.15872 | H210 | 1.42378 | 0.8407 | 0.38823 |
| C39 | 0.98898 | 0.35722 | 0.40973 | H211 | 0.53479 | 0.25175 | −0.01194 |
| C45 | 1.3411 | 0.74188 | 0.33706 | H212 | 0.64797 | 0.2035 | 0.02196 |
| C47 | 1.14941 | 0.49587 | 0.10944 | H213 | 0.6752 | 0.28977 | 0.01897 |
| C48 | 1.07491 | 0.06334 | 0.36333 | H214 | 1.06399 | 0.53317 | −0.0067 |
| C49 | 0.66949 | 0.60059 | 0.34335 | H215 | 1.21511 | 0.03465 | 0.27405 |
| C51 | 0.98171 | 0.38143 | 0.37145 | H216 | 1.27995 | −0.00592 | 0.31885 |
| C52 | 0.52403 | 0.66087 | 0.15054 | H217 | 1.37627 | 0.05284 | 0.30123 |
| C53 | 1.22345 | 0.28225 | 0.30389 | H218 | 0.47604 | 0.95389 | 0.25635 |
| C54 | 0.99431 | 0.44621 | 0.36071 | H219 | 0.5306 | 0.82295 | 0.07777 |
| C56 | 0.38594 | 0.29143 | 0.03062 | H220 | 0.75359 | 0.25928 | 0.19492 |
| C58 | 0.74048 | 0.39163 | 0.14301 | H221 | 0.91164 | 0.31738 | 0.50829 |
| C59 | 0.42606 | 0.20503 | 0.20415 | H222 | 1.06501 | 0.29207 | 0.47775 |
| C60 | 0.85193 | 0.08015 | 0.30474 | H223 | 1.25609 | 0.90744 | 0.391 |
| C61 | 1.18749 | 0.54733 | 0.13481 | H224 | 1.11939 | 0.39041 | 0.12148 |
| C63 | 0.71282 | 0.32477 | 0.14474 | H225 | 1.59023 | 0.77963 | 0.43444 |
| C64 | 0.96024 | 0.8773 | 0.25337 | H226 | 1.46931 | 0.74292 | 0.45456 |
| C66 | 0.45366 | 0.32761 | 0.1882 | H227 | 1.49299 | 0.83113 | 0.45636 |
| C67 | 1.2521 | 0.34364 | 0.32056 | H228 | 0.94531 | 0.03734 | 0.39739 |
| C68 | 0.52109 | 0.26319 | 0.04691 | H229 | 1.29314 | 0.09764 | 0.35279 |
| C69 | 1.21684 | 0.21942 | 0.32334 | H230 | 0.34715 | 0.88305 | 0.04958 |
| C71 | 1.39363 | 0.7949 | 0.40055 | H231 | 0.32269 | 0.11994 | 0.09678 |
| C72 | 1.33097 | 0.68124 | 0.3145 | H232 | 0.37958 | 0.03979 | 0.11447 |
| C73 | 0.59856 | 0.25205 | 0.01713 | H233 | 0.49228 | 0.10664 | 0.1173 |
| C74 | 1.07029 | 0.5763 | 0.01246 | H234 | 0.62618 | 0.56414 | −0.03701 |
| C76 | 1.27646 | 0.04117 | 0.30307 | H235 | 0.99575 | 0.67942 | 0.29024 |
| C77 | 0.5719 | 0.9365 | 0.25635 | H236 | 0.84957 | 0.53821 | −0.03613 |

***Table S16 continued***

| Atom | x | y | z | Atom | x | y | z |
|---|---|---|---|---|---|---|---|
| C78 | 0.52796 | 0.83306 | 0.10749 | H237 | 0.45825 | 0.5687 | 0.11871 |
| C79 | 0.93423 | 0.5994 | 0.01246 | H238 | 1.17588 | 0.25639 | 0.24292 |
| C80 | 0.7618 | 0.30684 | 0.18222 | H239 | 1.03965 | 0.92906 | 0.39841 |
| C81 | 0.8224 | 0.89349 | 0.25521 | H240 | 1.01279 | 0.15886 | 0.4363 |
| C82 | 0.83607 | 0.29358 | 0.48721 | H241 | 1.05151 | 0.17228 | 0.48652 |
| C83 | 1.0054 | 0.26264 | 0.45396 | H242 | 1.16604 | 0.19438 | 0.45986 |
| C84 | 0.24386 | 0.09146 | 0.16294 | H243 | 0.29827 | 0.21259 | 0.05583 |
| C85 | 1.20204 | 0.86686 | 0.39883 | H244 | 0.92301 | 0.29333 | 0.33508 |
| C86 | 1.14798 | 0.43991 | 0.13126 | H245 | 0.79415 | 0.58759 | 0.4915 |
| C87 | 0.9751 | 0.09136 | 0.29755 | H246 | 0.74974 | 0.04933 | 0.34599 |
| C88 | 1.49183 | 0.78623 | 0.43881 | H247 | 1.15781 | 0.90197 | 0.28241 |
| C89 | 0.39412 | 0.48888 | 0.47573 | H248 | 1.05279 | 0.89282 | 0.31369 |
| C90 | 1.08882 | 0.08287 | 0.32758 | H249 | 1.04054 | 0.96475 | 0.28427 |
| C91 | 0.95362 | 0.05173 | 0.36959 | H250 | 1.09049 | 0.64145 | −0.03259 |
| C92 | 1.22591 | 0.09654 | 0.32411 | H251 | 1.24061 | 0.60943 | −0.00437 |
| C93 | 0.70069 | 0.57643 | 0.41414 | H252 | 1.15848 | 0.67504 | 0.01351 |
| C94 | 0.31157 | 0.87866 | 0.07471 | H253 | 0.85382 | 0.65411 | 0.1703 |
| C96 | 0.39337 | 0.09378 | 0.11938 | H254 | 0.59514 | 0.93425 | 0.10481 |
| C97 | 0.39256 | 0.85533 | 0.10869 | H255 | 0.72242 | 0.87426 | 0.1187 |
| C98 | 0.8643 | 0.263 | 0.45574 | H256 | 0.63189 | 0.90015 | 0.15166 |
| C99 | 0.70338 | 0.58551 | −0.0154 | H257 | 0.90971 | 0.84132 | 0.41644 |
| C100 | 0.96636 | 0.65939 | 0.26196 | H258 | 0.692 | 0.31917 | 0.51621 |
| C100 | 0.96636 | 0.65939 | 0.26196 | H258 | 0.692 | 0.31917 | 0.51621 |
| C101 | 0.83119 | 0.57148 | −0.01489 | H259 | 0.26924 | 0.53822 | 0.50541 |
| C102 | 0.51987 | 0.48664 | 0.46913 | H260 | 1.34251 | 0.60134 | 0.35676 |
| C103 | 0.49697 | 0.59395 | 0.14519 | H261 | 0.59538 | 0.71489 | 0.2046 |
| C104 | 1.20226 | 0.29258 | 0.26529 | H262 | 0.79268 | 0.95521 | 0.20536 |
| C105 | 1.07857 | 0.87977 | 0.40295 | H263 | 0.12546 | 0.91599 | 0.0462 |
| C106 | 1.06175 | 0.19268 | 0.45924 | H264 | 0.57416 | 0.63656 | 0.0108 |
| C107 | 0.28161 | 0.25616 | 0.03821 | H265 | 0.52808 | 0.27497 | 0.27548 |
| C108 | 0.94784 | 0.34519 | 0.33822 | H266 | 0.0274 | 0.34326 | −0.01234 |
| C109 | 1.25635 | 0.80323 | 0.40509 | H267 | 0.6452 | 0.62129 | 0.52293 |
| C110 | 1.05415 | 0.76544 | 0.41894 | H268 | 0.43037 | 0.62075 | 0.53462 |
| C111 | 0.90541 | 0.64499 | 0.03912 | H269 | 0.9364 | 0.49032 | 0.50333 |
| C112 | 1.18091 | 0.75115 | 0.41525 | H270 | 0.79899 | 0.43642 | 0.49877 |
| C113 | 0.75084 | 0.53897 | 0.48146 | H271 | 0.83779 | 0.49596 | 0.53655 |
| C114 | 0.46142 | 0.27472 | 0.21299 | H272 | 0.07609 | 0.24546 | 0.02771 |
| C115 | 0.63768 | 0.89258 | 0.28407 | H273 | 0.51407 | 0.26671 | 0.46986 |
| C116 | 0.84295 | 0.05899 | 0.34042 | H274 | 1.29305 | 0.71567 | 0.25515 |
| C117 | 0.61283 | 0.53559 | 0.48612 | H275 | 0.0324 | 0.90202 | 0.10096 |
| C118 | 1.05863 | 0.91095 | 0.28558 | H276 | 0.57537 | 0.99004 | 0.20607 |

***Table S16 continued***

| Atom | x | y | z | Atom | x | y | z |
|---|---|---|---|---|---|---|---|
| C119 | 1.14446 | 0.62908 | −0.00345 | H277 | 0.32587 | 0.0148 | 0.20332 |
| C120 | 0.89274 | 0.64608 | 0.20025 | H278 | 0.11957 | −0.02594 | 0.21072 |
| C121 | 0.62526 | 0.88872 | 0.12164 | H279 | −0.08485 | 0.02063 | 0.17359 |
| C122 | 1.00517 | 0.82971 | 0.41308 | H280 | 1.11765 | 1.22627 | 0.56741 |
| C123 | 0.93268 | 0.6937 | 0.22809 | H281 | 1.03276 | 1.11314 | 0.55637 |
| C124 | 0.71109 | 0.29465 | 0.49198 | H282 | 0.8158 | 1.08634 | 0.56372 |
| C125 | 0.36397 | 0.53679 | 0.49973 | H283 | 0.67837 | 1.17095 | 0.57916 |
| C126 | 1.33228 | 0.61712 | 0.3279 | H284 | 0.51701 | 1.38824 | 0.6873 |
| C127 | 0.35871 | 0.34979 | 0.008 | H285 | 0.40527 | 1.30794 | 0.6396 |
| C128 | 0.56825 | 0.66925 | 0.18932 | H286 | 0.19254 | 1.26449 | 0.64103 |
| C129 | 0.75149 | 0.93656 | 0.22747 | H287 | 0.08096 | 1.30475 | 0.68623 |
| C130 | 0.77385 | 0.65769 | 0.03852 | H288 | 0.47736 | 1.32969 | 0.81657 |
| C131 | 0.1844 | 0.89686 | 0.07246 | H289 | 0.57583 | 1.31296 | 0.76454 |
| C132 | 0.34295 | 0.85252 | 0.14151 | H290 | 0.80822 | 1.33225 | 0.77239 |
| C133 | 0.6745 | 0.62712 | 0.01156 | H291 | 0.94545 | 1.36824 | 0.83375 |
| C134 | 0.50997 | 0.30088 | 0.24878 | H292 | 0.12996 | 0.70576 | 0.6131 |
| C135 | 0.76359 | 0.86987 | 0.28376 | H293 | 0.31469 | 0.66985 | 0.66153 |
| C136 | 0.00642 | 0.09482 | 0.14656 | H294 | 0.53133 | 0.67017 | 0.6507 |
| C137 | 0.76036 | 0.23612 | 0.4272 | H295 | 0.56835 | 0.71361 | 0.59128 |
| C138 | 0.12583 | 0.12175 | 0.14296 | H296 | 1.35559 | 0.58347 | 0.71826 |
| C139 | 0.12724 | 0.3302 | −0.00039 | H297 | 1.34194 | 0.62208 | 0.78092 |
| C140 | 0.57718 | 0.58375 | 0.50941 | H298 | 1.1305 | 0.63926 | 0.79469 |
| C141 | 0.45491 | 0.58388 | 0.51629 | H299 | 0.93215 | 0.61765 | 0.74736 |
| C142 | 0.83584 | 0.48702 | 0.50644 | H300 | 1.20245 | 0.6013 | 0.87164 |
| C143 | 0.15436 | 0.27484 | 0.02255 | H301 | 1.20206 | 0.69776 | 0.91251 |
| C144 | 0.61056 | 0.26541 | 0.46543 | H302 | 0.99771 | 0.74957 | 0.91624 |
| C145 | 1.30575 | 0.67596 | 0.27551 | H303 | 0.79256 | 0.7018 | 0.8839 |
| C146 | 0.22762 | 0.36825 | −0.00763 | H304 | 0.44282 | 0.88065 | 0.98853 |
| C147 | 0.21015 | 0.86687 | 0.13794 | H305 | 0.49925 | 0.9763 | 1.02853 |
| C148 | 0.13272 | 0.88953 | 0.10356 | H306 | 0.72726 | 1.00687 | 1.05553 |
| C149 | 0.63298 | 0.23782 | 0.43257 | H307 | 0.90099 | 0.93904 | 1.04236 |
| C150 | 0.62768 | 0.95716 | 0.22785 | H308 | 0.89697 | 1.17295 | 0.93188 |
| C151 | 0.23835 | 0.03842 | 0.18738 | H309 | 0.9557 | 1.24666 | 0.88704 |
| C152 | 0.12082 | 0.01432 | 0.19145 | H310 | 1.18427 | 1.26681 | 0.88845 |
| C153 | 0.00546 | 0.0411 | 0.17054 | H311 | 1.35695 | 1.21167 | 0.93578 |
| C154 | 1.02171 | 1.21555 | 0.57068 | H312 | 0.79641 | 0.94473 | 0.53688 |
| C155 | 0.97435 | 1.15139 | 0.5644 | H313 | 0.74626 | 0.86085 | 0.57998 |
| C156 | 0.85133 | 1.13643 | 0.56823 | H314 | 0.52978 | 0.85534 | 0.59158 |
| C157 | 0.77355 | 1.18563 | 0.57773 | H315 | 0.3597 | 0.92819 | 0.55902 |
| C158 | 0.4219 | 1.37062 | 0.68799 | | | | |

**Table S17** Parameter of Spiral stacking model for **S-2**.

| Crystal system | | | | monoclinic | | | |
|---|---|---|---|---|---|---|---|
| Space group | | | | $P2_1$ | | | |
| Unit Cell | | | | a = 9.9287 Å, b = 20.9692 Å, c = 35.7146 Å, β = 91.3000° | | | |
| Atom | x | y | z | Atom | x | y | z |
| Cu1 | 0.49977 | 0.42224 | 0.27605 | C159 | 0.91135 | −0.45894 | 0.79372 |
| Cu2 | 0.80553 | 0.60497 | 0.24042 | C160 | 0.77769 | −0.43942 | 0.79006 |
| Cu3 | 1.17249 | 0.42041 | 0.22098 | C161 | 0.72303 | −0.39758 | 0.81602 |
| Cu4 | 0.85841 | 0.46311 | 0.28146 | C162 | 0.43488 | −0.27389 | 0.63704 |
| Cu5 | 1.13527 | 0.57895 | 0.21423 | C163 | 0.33168 | −0.23367 | 0.62468 |
| Cu6 | 0.50613 | 0.58047 | 0.29584 | C164 | 0.20399 | −0.23939 | 0.63944 |
| Cu7 | 0.79786 | 0.47064 | 0.1886 | C165 | 0.17874 | −0.28555 | 0.66651 |
| Cu8 | 1.18115 | 0.51128 | 0.29902 | C166 | 1.15998 | −0.17235 | 0.52217 |
| Cu9 | 0.47852 | 0.52972 | 0.20695 | C167 | 1.07066 | −0.12166 | 0.51731 |
| O10 | 1.17436 | 0.20742 | 0.32464 | C168 | 0.93794 | −0.12777 | 0.52846 |
| O11 | 0.37241 | 0.82866 | 0.22274 | C169 | 0.89481 | -0.18355 | 0.5456 |
| O12 | 0.48427 | 0.40098 | 0.44026 | C170 | 0.58122 | 0.09737 | 0.53929 |
| O14 | 0.37841 | 0.31298 | 0.11173 | C171 | 0.66315 | 0.14211 | 0.55754 |
| O15 | 0.75767 | 0.19323 | 0.20781 | C172 | 0.79981 | 0.14525 | 0.55011 |
| O17 | 1.14731 | 0.77848 | 0.35087 | C173 | 0.85579 | 0.104 | 0.5241 |
| O21 | 0.67933 | 0.72827 | 0.09695 | C174 | 0.30709 | 0.29725 | 0.63202 |
| O23 | 0.81321 | 0.61614 | 0.41994 | C175 | 0.39801 | 0.3161 | 0.66008 |
| O41 | 1.07387 | 0.52523 | 0.05347 | C176 | 0.52965 | 0.33134 | 0.6514 |
| N13 | 1.15704 | 0.8259 | 0.29463 | C177 | 0.57273 | 0.32656 | 0.61465 |
| N16 | 0.4641 | 0.80411 | 0.16755 | C178 | 1.33222 | 0.42884 | 0.74367 |
| N18 | 1.2067 | 0.25929 | 0.3792 | C179 | 1.29614 | 0.40797 | 0.77903 |
| N19 | 1.1963 | 0.41837 | 0.30117 | C180 | 1.16548 | 0.38742 | 0.78524 |
| N20 | 1.13029 | 0.52463 | 0.1703 | C181 | 1.06939 | 0.3878 | 0.75614 |
| N22 | 0.47497 | 0.61981 | 0.21953 | C182 | 0.71505 | 0.24651 | 0.89398 |
| N24 | 0.91278 | 0.18463 | 0.25442 | C183 | 0.77704 | 0.19465 | 0.9118 |
| N25 | 1.14717 | 0.46249 | 0.17284 | C184 | 0.91142 | 0.19827 | 0.92356 |
| N26 | 0.8599 | 0.3878 | 0.2498 | C185 | 0.9851 | 0.25347 | 0.91712 |
| N27 | 0.85305 | 0.54118 | 0.31066 | C186 | 0.49442 | 0.0701 | 1.01424 |
| N28 | 0.77042 | 0.55375 | 0.16622 | C187 | 0.56578 | 0.0237 | 1.03462 |
| N29 | 0.77653 | 0.60666 | 0.18614 | C188 | 0.69934 | 0.03381 | 1.0455 |
| N30 | 0.48112 | 0.43873 | 0.19683 | C189 | 0.76384 | 0.08988 | 1.03542 |
| N31 | 1.14351 | 0.62937 | 0.25973 | H190 | 0.5317 | 0.77346 | 0.1546 |
| N32 | 0.43624 | 0.23151 | 0.14975 | H191 | 0.9968 | 0.20639 | 0.26703 |
| N35 | 0.60837 | 0.48838 | 0.45298 | H192 | 0.47113 | 0.21704 | 0.1762 |
| N37 | 0.48526 | 0.64045 | 0.25434 | H193 | 0.67221 | 0.52263 | 0.44173 |
| N38 | 0.51408 | 0.45408 | 0.32709 | H194 | 0.85126 | 0.09118 | 0.2437 |
| N39 | 0.68176 | 0.64242 | 0.05909 | H195 | 0.68468 | 0.59279 | 0.057 |

***Table S17 continued***

| Atom | x | y | z | Atom | x | y | z |
|---|---|---|---|---|---|---|---|
| N40 | 0.90289 | 0.70515 | 0.39598 | H196 | 0.95328 | 0.72358 | 0.37316 |
| N42 | 0.83401 | 0.59716 | 0.29451 | H197 | 0.47545 | 0.9202 | 0.10014 |
| N43 | 1.19631 | 0.38326 | 0.27056 | H198 | 0.4958 | 0.83607 | 0.09187 |
| N49 | 0.52439 | 0.51551 | 0.33474 | H199 | 0.61264 | 0.87763 | 0.12257 |
| N61 | 0.48646 | 0.39606 | 0.22391 | H200 | 0.54618 | 0.56883 | 0.38594 |
| N62 | 0.82836 | 0.39015 | 0.21381 | H201 | 0.7308 | 0.53222 | 0.10837 |
| N69 | 1.16448 | 0.60364 | 0.293 | H202 | 0.42898 | 0.9026 | 0.16578 |
| N73 | 1.1709 | 0.42829 | 0.05424 | H203 | 0.63668 | 0.05954 | 0.25442 |
| C33 | 1.22152 | 0.93917 | 0.28546 | H204 | 1.07784 | 0.09586 | 0.27943 |
| C34 | 1.19367 | 0.2578 | 0.34089 | H205 | 0.95599 | 0.03874 | 0.29432 |
| C36 | 0.86795 | 0.12267 | 0.26843 | H206 | 0.98463 | 0.10925 | 0.32138 |
| C44 | 1.20213 | 0.31707 | 0.31863 | H207 | 0.47091 | 0.73367 | 0.27957 |
| C45 | 0.50537 | 0.87418 | 0.11327 | H208 | 0.74887 | 0.70585 | 0.17247 |
| C46 | 1.1517 | 0.77282 | 0.317 | H209 | 0.43795 | 0.66502 | 0.16638 |
| C47 | 0.53553 | 0.46311 | 0.38838 | H210 | 0.69899 | 0.72911 | 0.02981 |
| C48 | 0.94973 | 0.93368 | 0.34572 | H211 | 0.74967 | 0.73879 | 0.4929 |
| C50 | 1.14108 | 0.89136 | 0.30862 | H212 | 0.59185 | 0.13938 | 0.10594 |
| C51 | 1.15336 | 0.70832 | 0.3004 | H213 | 0.45494 | 0.08374 | 0.10906 |
| C52 | 0.737 | 0.12962 | 0.28978 | H214 | 0.53902 | 0.11461 | 0.15072 |
| C53 | 0.53842 | 0.5232 | 0.37195 | H215 | 0.50612 | 0.36944 | 0.36074 |
| C54 | 0.74203 | 0.56753 | 0.13028 | H216 | 0.42116 | 0.06522 | 0.286 |
| C55 | 0.42654 | 0.78905 | 0.20318 | H217 | 0.71345 | 0.6526 | -0.0333 |
| C56 | 0.72865 | 0.63318 | 0.12743 | H218 | 0.80765 | 0.60819 | 0.00156 |
| C57 | 0.41643 | 0.86073 | 0.14692 | H219 | 0.8512 | 0.68894 | -0.00759 |
| C58 | 0.84929 | 0.28905 | 0.22907 | H220 | 0.46533 | 0.29392 | 0.22546 |
| C59 | 0.83793 | 0.21941 | 0.22911 | H221 | 0.89464 | 0.31173 | 0.28866 |
| C60 | 0.45157 | 0.72423 | 0.21771 | H222 | 0.41591 | 0.20385 | 0.09327 |
| C63 | 0.26855 | 0.85542 | 0.13427 | H223 | 0.38689 | 0.141 | 0.33707 |
| C64 | 0.62692 | 0.09211 | 0.27767 | H224 | 0.19873 | 0.22192 | 0.07624 |
| C65 | 0.76344 | 0.93023 | 0.28585 | H225 | -0.03452 | 0.18738 | 0.07249 |
| C66 | 0.42017 | 0.29541 | 0.14242 | H226 | -0.00924 | 0.95196 | 0.13409 |
| C67 | 0.9928 | 0.91042 | 0.3109 | H227 | 0.49755 | 0.77718 | 0.03317 |
| C68 | 0.25347 | 0.16364 | 0.12439 | H228 | 0.66521 | 0.58439 | 0.50443 |
| C70 | 0.21132 | 0.80222 | 0.11445 | H229 | 0.79047 | 0.52271 | 0.50733 |
| C71 | 0.72568 | 0.9531 | 0.3209 | H230 | 0.67188 | 0.5318 | 0.54438 |
| C72 | 0.97811 | 0.09025 | 0.29248 | H231 | 0.81608 | 0.69284 | 0.31556 |
| C74 | 0.4704 | 0.70435 | 0.25466 | H232 | 0.51624 | 0.76697 | 0.5061 |
| C75 | 0.58863 | 0.1796 | 0.33561 | H233 | 0.61596 | 0.43971 | 0.5041 |
| C76 | 0.45383 | 0.3443 | 0.17069 | H234 | 0.8768 | 0.51018 | 0.36796 |
| C77 | 1.12432 | 0.48187 | 0.07174 | H235 | 0.78772 | 0.31883 | 0.17172 |
| C78 | 0.75218 | 0.65662 | 0.16344 | H236 | 0.062 | 0.52129 | 0.52717 |

***Table S17 continued***

| Atom | x | y | z | Atom | x | y | z |
|---|---|---|---|---|---|---|---|
| C79 | 1.04966 | 0.21163 | 0.42468 | H237 | 0.94896 | 0.8335 | 0.40069 |
| C80 | 0.45389 | 0.66916 | 0.19634 | H238 | 1.08012 | 0.7937 | 0.42733 |
| C81 | 0.85046 | 0.61314 | 0.35563 | H239 | 0.95169 | 0.83785 | 0.45081 |
| C82 | 0.71789 | 0.17412 | 0.31957 | H240 | 0.92315 | 0.71927 | 0.45397 |
| C83 | 0.8538 | 0.64443 | 0.39262 | H241 | −0.12575 | 0.1132 | 0.11854 |
| C84 | 0.66628 | 0.67915 | 0.02426 | H242 | −0.10869 | 0.86142 | 0.10034 |
| C85 | 0.68596 | 0.75656 | 0.47032 | H243 | 0.44813 | 0.43338 | 0.13729 |
| C86 | 0.50149 | 0.12667 | 0.1222 | H244 | 0.19981 | 0.43849 | 0.55792 |
| C87 | 0.51782 | 0.42049 | 0.35906 | H245 | 0.22629 | 0.95024 | 0.15543 |
| C88 | 0.73748 | 0.76377 | 0.43417 | H246 | 0.25798 | 0.78637 | 0.01855 |
| C89 | 0.50317 | 0.09577 | 0.29512 | H247 | 0.36496 | 0.80732 | 0.45625 |
| C90 | 0.54121 | 0.44838 | 0.42868 | H248 | 0.43701 | 0.42525 | 0.54302 |
| C91 | 0.5181 | 0.68097 | 0.01154 | H249 | 0.13539 | 0.70125 | −0.01388 |
| C92 | 0.89777 | 0.90889 | 0.28015 | H250 | 0.94599 | −0.17121 | 0.92803 |
| C93 | 0.76454 | 0.65567 | -0.00551 | H251 | 1.09447 | −0.2193 | 0.88344 |
| C94 | 0.47055 | 0.33738 | 0.20924 | H252 | 1.34017 | −0.21034 | 0.89108 |
| C95 | 1.14742 | 0.43717 | 0.13834 | H253 | 1.44048 | −0.14767 | 0.943 |
| C96 | 0.07366 | 0.80489 | 0.10236 | H254 | 0.5336 | −0.26777 | 0.6257 |
| C97 | 1.19909 | 0.3799 | 0.33132 | H255 | 0.35025 | −0.19844 | 0.60326 |
| C98 | 0.91514 | 0.43807 | -0.0187 | H256 | 0.12364 | −0.20831 | 0.6296 |
| C99 | 0.87431 | 0.32692 | 0.26026 | H257 | 0.0778 | −0.28836 | 0.67616 |
| C100 | 0.69505 | 0.67086 | 0.09368 | H258 | 1.26229 | −0.16711 | 0.51287 |
| C101 | 0.40148 | 0.18283 | 0.12157 | H259 | 1.10332 | −0.07817 | 0.50407 |
| C102 | 0.48395 | 0.13907 | 0.32395 | H260 | 0.86727 | −0.08932 | 0.52384 |
| C103 | 1.13043 | 0.41127 | 0.01575 | H261 | 0.78955 | −0.18641 | 0.55137 |
| C104 | 0.97745 | 0.40567 | 0.01157 | H262 | 0.20524 | 0.29031 | 0.64043 |
| C105 | 0.89457 | 0.37366 | 0.03787 | H263 | 0.36545 | 0.31983 | 0.6887 |
| C106 | 0.44218 | 0.50294 | 0.50304 | H264 | 0.59761 | 0.34693 | 0.67336 |
| C107 | 0.16438 | 0.18782 | 0.09667 | H265 | 0.67517 | 0.33982 | 0.60827 |
| C108 | 0.0304 | 0.16885 | 0.09451 | H266 | 1.43472 | 0.44462 | 0.73948 |
| C109 | 0.0519 | 0.91038 | 0.12882 | H267 | 1.36925 | 0.40813 | 0.80179 |
| C110 | 0.65089 | 0.78831 | 0.40515 | H268 | 1.13828 | 0.37127 | 0.81284 |
| C111 | 1.1187 | 0.54155 | 0.13415 | H269 | 0.97047 | 0.37229 | 0.7632 |
| C112 | 0.44766 | 0.73766 | 0.01916 | H270 | 0.39341 | 0.05842 | 1.00522 |
| C113 | 0.9546 | 0.16193 | 0.42077 | H271 | 0.51789 | −0.02054 | 1.04209 |
| C114 | 0.68448 | 0.53474 | 0.51359 | H272 | 0.75388 | −0.00255 | 1.06112 |
| C115 | 0.832 | 0.64261 | 0.321 | H273 | 0.86953 | 0.09549 | 1.04267 |
| C116 | 1.20025 | 0.32122 | 0.27986 | H274 | 0.17841 | 0.81932 | 0.26651 |
| C117 | 0.81838 | 0.95486 | 0.35053 | H275 | 0.24 | 0.3019 | 0.39105 |
| C118 | 0.55342 | 0.77271 | 0.47808 | H276 | 0.19468 | 0.93661 | 0.25532 |
| C119 | 0.06216 | 0.10468 | 0.15005 | H277 | 0.33096 | 0.92931 | 0.28837 |

***Table S17 continued***

| Atom | x | y | z | Atom | x | y | z |
|---|---|---|---|---|---|---|---|
| C120 | 0.58832 | 0.48807 | 0.4936 | H278 | 0.20386 | 0.98844 | 0.29566 |
| C121 | 1.18185 | 0.20414 | 0.40381 | H279 | 0.01912 | 0.93672 | 0.36948 |
| C122 | 0.19992 | 0.12368 | 0.15279 | H280 | 0.18814 | 0.89383 | 0.33715 |
| C123 | 1.13558 | 0.69291 | 0.26284 | H281 | −0.37632 | 0.9693 | 0.32545 |
| C124 | 0.86253 | 0.54858 | 0.34801 | H282 | 0.23083 | 0.39633 | 0.06966 |
| C125 | 1.30168 | 0.19162 | 0.4307 | H283 | 0.15835 | 0.38688 | 0.13244 |
| C126 | 0.88167 | 0.27132 | 0.46029 | H284 | 0.19395 | 0.39645 | 0.35992 |
| C127 | 1.13126 | 0.48674 | 0.11282 | H285 | −0.02484 | 0.46219 | −0.03935 |
| C128 | 0.81877 | 0.33071 | 0.20003 | H286 | 0.16668 | 0.44985 | −0.00269 |
| C129 | 0.36424 | 0.55286 | 0.48597 | H287 | 0.1038 | 0.58973 | 0.12431 |
| C130 | 0.79113 | 0.22061 | 0.45603 | H288 | −0.0224 | 0.11941 | 0.40494 |
| C131 | 1.01452 | 0.26624 | 0.44635 | H289 | 0.19585 | 0.28225 | 0.26001 |
| C132 | 0.77543 | 0.44073 | -0.02266 | H290 | −0.21173 | 0.97305 | 0.37741 |
| C133 | 0.16756 | 0.51725 | 0.52045 | H291 | 0.17423 | 0.16037 | 0.38627 |
| C134 | 0.22491 | 0.55802 | 0.49415 | H292 | 0.11855 | 0.72493 | 0.23948 |
| C135 | 1.20078 | 0.35023 | 0.00291 | H293 | 0.35399 | 0.23612 | 0.43911 |
| C136 | 1.17098 | 0.65032 | 0.3189 | H294 | 0.37654 | 0.16043 | 0.41708 |
| C137 | 0.75202 | 0.37892 | 0.03408 | H295 | 0.26787 | 0.16648 | 0.4561 |
| C138 | 0.9715 | 0.80633 | 0.42665 | H296 | −0.30892 | 0.22335 | 0.46738 |
| C139 | 0.82784 | 0.16626 | 0.4365 | H297 | −0.2699 | 0.46575 | −0.04626 |
| C140 | 0.88493 | 0.74593 | 0.42897 | H298 | 0.17596 | 0.34113 | −0.02708 |
| C141 | −0.02067 | 0.12706 | 0.12075 | H299 | 0.16983 | 0.3082 | 0.01943 |
| C142 | 0.69426 | 0.41226 | 0.00387 | H300 | 0.31178 | 0.35586 | 0.00596 |
| C143 | −0.00407 | 0.85897 | 0.10956 | H301 | 0.1869 | 0.64285 | 0.34865 |
| C144 | 0.46179 | 0.40927 | 0.1639 | H302 | −0.24378 | 0.12777 | 0.43273 |
| C145 | 0.24535 | 0.47042 | 0.53806 | H303 | −0.41414 | 0.41491 | 0.00056 |
| C146 | 0.51523 | 0.80379 | 0.41354 | H304 | 1.09626 | 0.54893 | 0.82509 |
| C147 | 0.18597 | 0.9087 | 0.14109 | H305 | 0.95389 | 0.50922 | 0.77338 |
| C148 | 0.31132 | 0.74393 | 0.01031 | H306 | 0.71603 | 0.54357 | 0.76688 |
| C149 | 0.46832 | 0.79603 | 0.44988 | H307 | 0.62192 | 0.61852 | 0.81055 |
| C150 | 0.4461 | 0.6296 | −0.00618 | H308 | 0.47579 | 1.09905 | 0.54536 |
| C151 | 0.38035 | 0.46294 | 0.52926 | H309 | 0.62022 | 1.17455 | 0.5776 |
| C152 | 0.24175 | 0.69501 | −0.00764 | H310 | 0.86174 | 1.18018 | 0.56441 |
| C153 | 0.30773 | 0.63829 | −0.01652 | H311 | 0.96212 | 1.108 | 0.51824 |
| C154 | 1.05224 | −0.16309 | 0.9321 | H312 | 0.60942 | 1.24184 | 0.88781 |
| C155 | 1.13698 | −0.19188 | 0.90647 | H313 | 0.71903 | 1.15219 | 0.91768 |
| C156 | 1.276 | −0.18639 | 0.9106 | H314 | 0.95794 | 1.15862 | 0.9383 |
| C157 | 1.3318 | −0.15097 | 0.94006 | H315 | 1.0881 | 1.25608 | 0.92743 |
| C158 | 0.99183 | −0.43625 | 0.82315 | | | | |

## 12. Literature survey

**Table S18** Summary of reported CPL-active coinage metal complexes with orange-red to red emission ($\lambda_{max}$ > 600 nm) in solid state.

| ENTRY | State | $\lambda_{em}$ | QY (%) | $g_{lum}$ ($\times10^{-3}$) | FM[a] ($\times10^{-3}$) | Ref. |
|---|---|---|---|---|---|---|
| Au complex | | | | | | |
| Cl-Au | Crystalline powder | 720 | 70.2 | 3.4 | 2.39 | 17 |
| Br-Au | Crystalline powder | 720 | 72.5 | 2.7 | 1.96 | |
| R-$Au_{13}$-NHC | Solid | 750 | 66 | 2.65 | 1.75 | 18 |
| S-$Au_{13}$-NHC | Solid | 750 | 66 | −2.65 | 1.75 | |
| R-$Au_4$(HMMT)$_4$-red | Solid | 727 | 24.5 | −1.9 | 0.47 | 19 |
| S-$Au_4$(HMMT)$_4$-red | Solid | 727 | 24.5 | 1.3 | 0.32 | |
| Ag complex | | | | | | |
| [$Ag_{17}$(*R*-NYA)$_{12}$]($NO_3$)$_3$ | Solid | 745 | 8 | 1.2 | 0.10 | 20 |
| [$Ag_{17}$(*S*-NYA)$_{12}$]($NO_3$)$_3$ | Solid | 745 | 8 | −1.2 | 0.10 | |
| R-DHLA | Powder | 660 | 7.6 | 2 | 0.15 | 21 |
| S-DHLA | Powder | 660 | 7.6 | −2 | 0.15 | |
| [$Ag_7$(R-DMA)$_2$(dpppy)$_3$]($BF_4$)$_3$ | Solid | 675 | 8.6 | 2 | 0.17 | 22 |
| [$Ag_7$(S-DMA)$_2$(dpppy)$_3$]($BF_4$)$_3$ | Solid | 675 | 9.1 | −2 | 0.18 | |
| {[($Ag_{12}$($S^i$Pr)$_6$(D-CSA)$_6$(An2Py)$_3$)]·($H_2O$)$_2$}$_n$ | Solid | 612 | 50.3 | 12 | 6.04 | 23 |
| {[($Ag_{12}$($S^i$Pr)$_6$(L-CSA)$_6$(An2Py)$_3$)]·($H_2O$)$_2$}$_n$ | Solid | 612 | 50.3 | −12 | 6.04 | |
| [$Ag_{12}$($S^i$Pr)$_6$(D-CSA)$_8$]·($H_2$An2Py)(solvent)$_x$ | Solid | 630 | 7.6 | 1.3 | 0.10 | |
| [$Ag_{12}$($S^i$Pr)$_6$(L-CSA)$_8$]·($H_2$An2Py)(solvent)$_x$ | Solid | 630 | 7.6 | −1.3 | 0.10 | |
| Cu complex | | | | | | |
| (R-MBA)$_4$$Cu_4$$I_4$ | Powder | 630 | 52.8 | 10 | 5.28 | 24 |
| (S-MBA)$_4$$Cu_4$$I_4$ | Powder | 630 | 59.7 | −6 | 3.58 | |
| [$Cu_{14}$(R-DPM)$_8$]($PF_6$)$_6$ | Solid | 726 | 8.2 | 3.0 | 0.25 | 25 |
| [$Cu_{14}$(S-DPM)$_8$]($PF_6$)$_6$ | Solid | 726 | 8.2 | −3.0 | 0.25 | |
| R-2 | Solid | 610 | 5 | +0.8 | 0.04 | 26 |
| S-2 | Solid | 610 | 5 | −0.8 | 0.04 | |
| [D-valinol(18-crown-6)]$^+$[$Cu_5$($S^t$Bu)$_6$]$^-$ | Solid | 660 | 47.4 | 9.77 | 4.63 | 27 |
| [L-valinol(18-crown-6)]$^+$[$Cu_5$($S^t$Bu)$_6$]$^-$ | Solid | 660 | 47.4 | −9.77 | 4.63 | |
| ($Cu_6Br_6$)-R | Crystalline | 637 | 1.12 | 7.0 | 0.08 | 28 |
| ($Cu_6Br_6$)-S | Crystalline | 656 | 1.13 | 7.0 | 0.08 | |
| $Cu_5I_7(L_4)_2$ | Polycrystals | 620 | 6 | 6 | 0.36 | 29 |
| R-$Cu_2I_2$ | Solid | 675 | <1 | 2.2 | <0.02 | 30 |
| S-$Cu_2I_2$ | Solid | 675 | <1 | −2.8 | <0.03 | |
| (S)-$Cu_4I_4$(Hmpy)$_4$·$H_2O$ | Crystal | 610 | 93.2 | −6.7 | 6.24 | 31 |
| (R)-$Cu_4I_4$(Hmpy)$_4$·$H_2O$ | Crystal | 610 | 94.8 | +6.3 | 5.97 | |

| | | | | | | |
|---|---|---|---|---|---|---|
| (S)-$Cu_4I_4$(3Hpy)$_4$ | Crystal | 646 | 83.8 | −3.2 | 2.68 | |
| (R)-$Cu_4I_4$(3Hpy)$_4$ | Crystal | 646 | 78.7 | +2.0 | 1.57 | |
| (S)-$Cu_4I_4$(3AD)$_4$ | Crystal | 609 | 42.3 | −3.4 | 1.44 | |
| (R)-$Cu_4I_4$(3AD)$_4$ | Crystal | 609 | 42.4 | +2.6 | 1.10 | |
| {[(CuI)(Hptdp)]$_4$·$H_2O$}$_n$-M | Single crystals | 501, 605 | 2.4 | −8.0 | 0.19 | 32 |
| {[(CuI)(Hptdp)]$_4$·$H_2O$}$_n$-P | Single crystals | 501, 605 | 2.4 | 8.0 | 0.19 | |
| {Cu(Cbz$^R$)[(***R***)-BINAP]} [R = 3,6-*t*Bu] | Ground | 606 | 53 | 21 | 11.13 | 33 |
| {Cu(Cbz$^R$)[(***S***)-BINAP]} [R = 3,6-*t*Bu] | Ground | 606 | 53 | 21 | 11.13 | |
| R-CS1 | Solid-state | 776 | -- | -- | -- | 34 |
| S-CS1 | Solid-state | 776 | -- | -- | -- | |
| R-CS2 | Solid-state | 858 | -- | -- | -- | |
| S-CS2 | Solid-state | 858 | -- | -- | -- | |
| Mix-metal complex | | | | | | |
| [$Cu_{15}Ag_4$(*R*-PEA)$_{12}$]($BF_4$)$_5$ | Crystal | 626 | 7.02 | 1.0 | 0.07 | 35 |
| [$Cu_{15}Ag_4$(*S*-PEA)$_{12}$]($BF_4$)$_5$ | Crystal | 626 | 7.02 | −1.0 | 0.07 | |
| R-py-Br | Solid | 616 | 57.9 | 1.5 | 0.87 | 36 |
| R-py-I | Solid | 631 | 45.3 | 0.6 | 0.27 | |
| R-py-Cl | Solid | 628 | 5.4 | 0.7 | 0.04 | |
| R-py-Br | Solid | 600 | 62.8 | 1.5 | 0.94 | |
| R-py-I | Solid | 613 | 93 | 1.1 | 1.02 | |
| SCIF-2-Left | Crystal | 652 | 5.49 | 3 | 0.16 | 37 |
| SCIF-2-Right | Crystal | 650 | 5.49 | −3 | 0.16 | |

[a]FM (figure of merit) = PLQY×|$g_{lum}$|

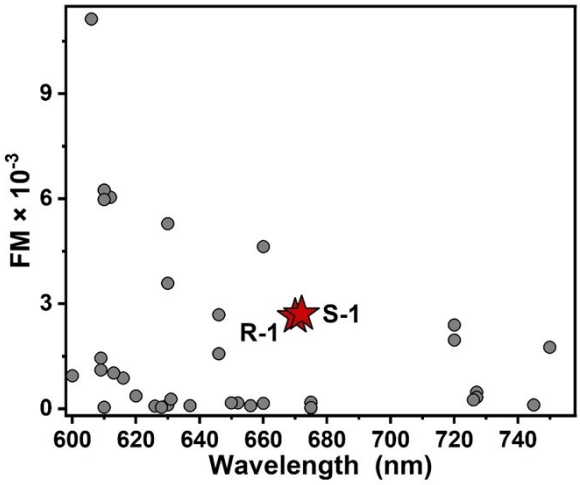


**Fig. S72** Summary of the reported FM values of coinage metal complexes in solid state with emission wavelength exceeding 600 nm.

## 13. Application showcase

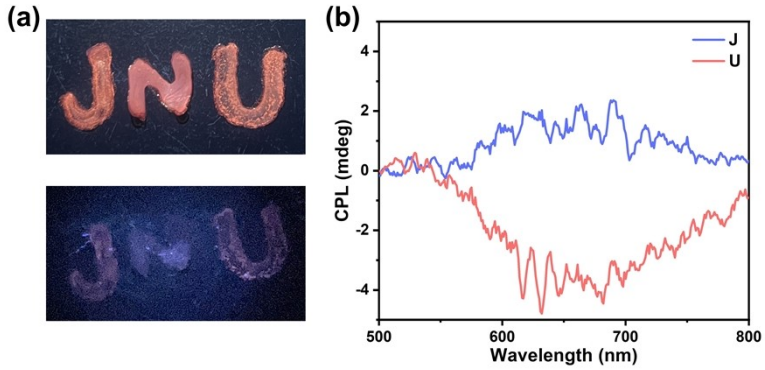


**Fig. S73** (a) The photographs of "**JNU**" pattern under 310 nm (top) and 365 nm (bottom) UV lamp, and. (b) CPL spectrum of "**J**" and "**U**" under 310 nm.

Note: Inspired by the sophisticated and multiplexed photoluminescence characteristics exhibited by **R-2**/**S-2**, their potential as advanced anti-counterfeiting materials were further explored. The synthesized polymeric films of **R-2**@PMMA, **S-1**@PMMA, and **S-2**@PMMA were fabricated into "**J**-", "**N**-", and "**U**-shaped" configurations, respectively. As shown in Figure S72a, the "**JNU**" patterns displayed orange-red emission under 310 nm UV lamp irradiation with uniform chromatic fidelity. Notably, when illuminated by a 365 nm UV lamp, the **S-1**@PMMA film exhibited negligible emission, while the **R-2**@PMMA and **S-2**@PMMA films demonstrated violet emission, revealing encrypted letters "**J**" and "**U**". Moreover, as the "**J**" and "**U**" patterns originated from enantiomeric counterparts **R-2** and **S-2**, respectively, they manifested distinct CPL signals (Figure S72b).

## 14. References


1 Y. Yan, E. J. Carrington, R. Pétuya, G. F. S. Whitehead, A. Verma, R. K. Hylton, C.-C. Tang, N. G. Berry, G. R. Darling, M. S. Dyer, D. Antypov, A. P. Katsoulidis and M. J. Rosseinsky, *J. Am. Chem. Soc.*, 2020, **142**, 14903–14913.

2 G. M. Sheldrick, *Acta Cryst. C*, 2015, **71**, 3–8.

3 C.-Y. Li, H. Xu, P.-M. Cheng, M.-H. Du, L.-S. Long, L.-S. Zheng and X.-J. Kong, *J. Am. Chem. Soc.*, 2023, **145**, 22176–22183

4 M. J. Frisch, G. W. Schlegel, H. B. Trucks, G. E. Scuseria, M. A. Robb, J. R. Cheeseman, G. Scalmani, V. Barone, B. Mennucci, G. A. Petersson, H. Nakatsuji, M. Caricato, X. Li, H. P. Hratchian, A. F. Izmaylov, J. Bloino, G. Zheng, J. L. Sonnenberg, M. Hada, M. Ehara, K. Toyota, R. Fukuda, J. Hasegawa, M. Ishida, T. Nakajima, Y. Honda, O. Kitao, H. Nakai, T. Vreven, J. A. Jr. Montgomery, J. E. Peralta, F. Ogliaro, M. Bearpark, J. J. Heyd, E. Brothers, K. N. Kudin, V. N. Staroverov, T. Keith, R. Kobayashi, J. Normand, K. Raghavachari, A. Rendell, J. C. Burant, S. S. Iyengar, J. Tomasi, M. Cossi, N. Rega, J. M. Millam, M. Klene, J. E. Knox, J. B. Cross, V. Bakken, C. Adamo, J. Jaramillo, R. Gomperts, R. E. Stratmann, O. Yazyev, A. J. Austin, R. Cammi, C. Pomelli, J. W. Ochterski, R. L. Martin, K. Morokuma, V. G. Zakrzewski, G. A. Voth, P. Salvador, J. J. Dannenberg, S. Dapprich, A. D. Daniels, O. Farkas, J. B. Foresman, J. V. Ortiz, J. Cioslowski and D. J. Fox, Gaussian, Inc., Wallingford CT, 2013. Gaussian 09, Revision E.01., 2009.

5 T. Lu and F. Chen, *J. Comput. Chem.*, 2012, **33**, 580–592.

6 J. P. Perdew, K. Burke and M. Ernzerhof, *Phys. Rev. Lett.*, 1996, **77**, 3865−3868.

7 J. P. Perdew, K. Burke and M. Ernzerhof, [Phys. Rev. Lett., **77**, 3865 (1996)]. *Phys. Rev. Lett.*, 1997, **78**, 1396.

8 S. Grimme, J. Antony, S. Ehrlich and H. A. Krieg, *J. Chem. Phys.*, 2010, **132**, 154104.

9 S. Grimme, S. Ehrlich and L. Goerigk, *J. Comput. Chem.*, 2011, **32**, 1456−1465.

10 P. J. Hay and W. R. Wadt, *J. Chem. Phys.*, 1985, **82**, 299–310.

11 W. R. Wadt and P. Hay, J. *Chem. Phys.*, 1985, **82**, 284–298.

12 L. Radom, P. C. Hariharan, J. A. Pople and P. V. R. Schleyer, *J. Am. Chem. Soc.*, 1973, **95**, 6531–6544.

13 M. J. Frisch, J. A. Pople and J. S. Binkley, *J. Chem. Phys.*, 1984, **80**, 3265–3269.

14 T. Lu and Q. Chen, *J. Comput. Chem.*, 2022, **43**, 539–555.

15 W. Humphrey and A. Dalke, K. Schulten, *J. Mol. Graphics*, 1996, **14**, 33–38.

16 C. Zhang, S. Li, X.-Y. Dong and S.-Q. Zang, *Aggregate*, 2021, **2**, e48.

17 H. Yang, S.-K. Peng, J. Zheng, D. Luo, M. Xie, Y.-L. Huang, X. Cai, J. Wang, X.-P. Zhou and D. Li, *Angew. Chem. Int. Ed.*, 2023, **62**, e202310495.

18 P. Luo, X.-J. Zhai, S. Bai, Y.-B. Si, X.-Y. Dong, Y.-F. Han and S.-Q. Zang, *Angew. Chem. Int. Ed.*, 2023, **62**, e202219017.

19 S.-M. Zhai, H. Zhang, Y. Wang, L.-X. Zhang, W.-Y. Jiao, Y.-Q. Zhang, Y. Si, H.-Y. Li, S.-Q. Zang and Z. Han, *Angew. Chem. Int. Ed.*, 2025, e202502168.

20 M.-M. Zhang, X.-Y. Dong, Z.-Y. Wang, X.-M. Luo, J.-H. Huang, S.-Q. Zang and T. C. W. Mak, *J. Am. Chem. Soc.*, 2021, **143**, 6048–6053.

21 J. Kumar, T. Kawai and T. Nakashima, *Chem. Commun.*, 2017, **53**, 1269–1272.

22 W.-M. He, J. Zha, Z. Zhou, Y.-J. Cui, P. Luo, L. Ma, C. Tan and S.-Q. Zang, *Angew. Chem. Int. Ed.*, 2024, **63**, e202407887.

23 J.-Y. Wang, Y. Si, X.-M. Luo, Z.-Y. Wang, X.-Y. Dong, P. Luo, C. Zhang, C. Duan and S.-Q. Zang, *Adv. Sci.*, 2023, **10**, 2207660.

24 L. Yao, G. Niu, J. Li, L. Gao, X. Luo, B. Xia, Y. Liu, P. Du, D. Li, C. Chen, Y. Zheng, Z. Xiao and J. Tang, *J. Phys. Chem. Lett.*, 2020, **11**, 1255–1260.

25 M.-M. Zhang, X.-Y. Dong, Z.-Y. Wang, H.-Y. Li, S.-J. Li, X. Zhao and S.-Q. Zang, *Angew. Chem. Int. Ed.*, 2020, **59**, 10052 –10058.

26 Y. Jin, Q.-C. Peng, J.-W. Xie, K. Li and S.-Q. Zang, *Angew. Chem. Int. Ed.*, 2023, **62**, e202301000.

27 Y. Jin, S. Li, Z. Han, B.-J. Yan, H.-Y. Li, X.-Y. Dong and S.-Q. Zang, *Angew. Chem. Int. Ed.*, 2019, **58**, 12143–12148.

28 J.-J. Fang, Z. Liu, Y.-L. Shen, Z.-Y. Wang, Y.-P. Xie and X. Lu, *ACS Materials Lett.*, 2024, **6**, 1199–1206.

29 L.-Z. Feng, J.-J. Wang, T. Ma, Y.-C. Yin, K.-H. Song, Z.-D. Li, M.-M. Zhou, S. Jin, T. Zhuang, F.-J. Fan, M.-Z. Zhu and H.-B. Yao, *Nat. Commun.*, 2022, **13**, 3339.

30 Z.-Y. Wu, M.-X. Yu, Z.-Q. Zhang, J.-X. Jiang, T. Liu, F.-L. Jiang, L. Chen and M.-C. Hong, *Dalton Trans.*, 2024, **53**, 7315–7320.

31 X. Ji, Y. Liu, R. Li, Z. Zhang, X. Zhang, C. Chen, J. Chen, H. Lu, R. Chen and L.

Mao, *Adv. Opt. Mater.*, 2023, **11**, 2300541.

32 M.-X. Yu, C.-P. Liu, Y.-F. Zhao, S.-C. Li, Y.-L. Yu, J.-Q. Lv, L. Chen, F.-L. Jiang and M.-C. Hong, *Angew. Chem. Int. Ed.*, 2022, **61**, e202201590.

33 A. M. T. Muthig, O. Mrózek, T. Ferschke, M. Rödel, B. Ewald, J. Kuhnt, C. Lenczyk, J. Pflaum and A. Steffen, *J. Am. Chem. Soc.*, 2023, **145**, 4438–4449.

34 Z. Han, Y. Si, X.-Y. Dong, J.-H. Hu, C. Zhang, X.-H. Zhao, J.-W. Yuan, Y. Wang and S.-Q. Zang, *J. Am. Chem. Soc.*, 2023, **145**, 6166–6176.

35 M.-M. Zhang, K.-K. Gao, X.-Y. Dong, Y. Si, T. Jia, Z. Han, S.-Q. Zang and T. C. W. Mak, *J. Am. Chem. Soc.*, 2023, **145**, 22310–22316.

36 X.-H. Ma, J. Li, P. Luo, J.-H. Hu, Z. Han, X.-Y. Dong, G. Xie and S.-Q. Zang, *Nat. Commun.*, 2023, **14**, 4121.

37 S. Chen, W. Du, C. Qin, D. Liu, L. Tang, Y. Liu, S. Wang and M. Zhu, *Angew. Chem. Int. Ed.*, 2020, **59**, 7542–7547.